

Interactive comments on “**Seasonal contrast in size distributions and mixing state of black carbon and its association with PM1.0 chemical composition from the eastern coast of India**”

5 **Response to reviewers**

Observations of the reviewers are in italics, and our response is given below in bold letters.

Reviewer-1: ACP-2019-376-RC1

10 *The size of BC clearly shows seasonal variation and emission sources of BC. They selected a suitable sampling location that gets plumes from both lands as well as from coastal/marine regions on different seasons. They used SP2 and ACMS to characterise the microphysical and chemical properties of BC and other aerosol particles. The research provides useful information on BC mixing with other aerosol components based on a diurnal and seasonal variation on the eastern coast of India. IGP is one of the regional hot spots for BC aerosol concentration in south Asia and the present research provides detail*
15 *information on the mixing scenario of BC aerosol from the IGP and compares with the BC from other parts of India. They quantified the coating of BC in term of ACT and RCT and presented the influence of different coating materials, and they discussed the preferential coating in different seasons. The language used is good but can be polished, especially, long sentences are used, and it makes difficult to communicate the message. I recommend the authors to shorten/split the long sentences. I recommend the*
20 *publication of this article but after addressing the concerns listed below.*

We thank the reviewer for the summary comments and positive recommendation, followed by detailed evaluation, and constructive comments. We have revised the manuscript accordingly, and our responses to the specific comments of the reviewer are given below:

25 *How relevant is the discussion of mineral dust in the introduction section (paragraphs 1 and 2)? I understand that the authors highlight the light-absorbing nature of minerals. But, I did not find any*

further discussion on minerals in the manuscript. In that context, the direct focus on BC mixing state is meaningful.

Complied with. This was originally included since dust constitutes a major fraction of aerosols loading over the IGP during spring and summer. However, we agree that dust is not the theme of this paper, and so we have modified the introduction section to focus mainly on the BC mixing state.

The authors mention the use of 2 kinds of aerosol characterization instruments during the study. But there is no mention of one of the two instruments throughout the introduction section. I had to go through the method section to get information about the second instrument. Please mention a brief introduction on the second instrument used in this study.

Complied with. We have included the relevant details in the introduction section. The following sentences are included in the revised manuscript.

Page 5, Line 14: “Along with this, information on the condensable materials which act as coating substances and constantly alter the physiochemical properties of the BC containing particles, is also essential. Collocated mass spectroscopy-based high-resolution aerosol chemical composition measurements have been employed for this purpose (Liu et al., 2014; Gong et al., 2016).”

Page 5, Line 25: “To meet these objectives, state-of-the-art instruments were installed at Bhubaneswar, which included a single particle soot photometer (SP2) for characterization of refractory BC (rBC) aerosols and an Aerosol Chemical Speciation Monitor (ACSM) for high-resolution measurements of non-refractive submicron aerosol chemical composition for long-term measurements.”

Page 5: Line 31: “The contributions from distinct sources to BC concentrations and the association of coating on BC with possible condensable coating materials are examined, and the implications are discussed.”

*Regarding the use of SP2, a recent finding by Sedlacek III et al. (2018) cautioned about the charring of organic depending on the SP2 laser power (Sedlacek III, Arthur J., et al. "Formation of refractory black carbon by SP2-induced charring of organic aerosol." *Aerosol Science and Technology* 52.12 (2018):*

1345-1350). It is worthy to mention this caveat as the ambient aerosol samples include organics. Clearly mention the power of the laser used during the operation of the SP2.

Thank you, and we agree. We have included this in the revised manuscript. Page 8, Line24.

5 **“Recently, Sedlacek III et al. (2018) have cautioned that rBC may be produced by laser-induced charring of organic substances in the SP2, which depends on the laser power. Such laser-induced charring could result in an overestimate of rBC. During our measurements, the laser power varied in the range 2.1-3.7 V, which is above the threshold to detect rBC with high efficiency (> 2V) (Sedlacek III et al., 2018). Though we cannot rule**
10 **out an additional rBC contribution from charring of organic matter, it is likely this occurs in circumstances when the laser voltage is higher than that used in our study.”**

The following reference has been included in the revised manuscript.

Sedlacek, A. J., III, Onasch, T.B., Nichman, L., Lewis, E.R., Davidovits, P., Freedman, A., and Williams, L.: Formation of refractory black carbon by SP2-induced charring of organic aerosol, *Aerosol Sci. and Technol.*, 52:12, 1345-1350, 2018, DOI:10.1080/02786826.2018.1531107.

15 *Also, it is not always appropriate to assume core-shell structure for coated BC due to the complex mixing state of BC, such as the case when BC is located off-center. Though the study did not utilize single particle off-line analysis to probe the complex internal mixing state of BC, it is useful to mention the effects from*
20 *such BC structures on absorption and scattering signals (e.g., Sedlacek III, Arthur J., et al. "Determination of and evidence for non-core shell structure of particles containing black carbon using the Single Particle Soot Photometer (SP2)." *Geophysical research letters* 39.6 (2012)). The authors should discuss how such noncore- shell particles would affect their results.*

Agree. We have revised the section accordingly by adding the following:

25 **Page 8, Line29.**

“Sedlacek III et al. (2012) examined the structure of rBC containing particles using the ‘lag time’ technique and suggested that the core-shell model does not apply to all rBC – containing particles. A situation with non-core-shell structure (the case when BC is

located off-center) arising due to the complex mixing state of BC may lead to uncertainty in determining the coating thickness of BC. Our study assumes BC to be at the centre and a uniform coating around, in the absence of other measurements to understand the complex coating. A recent study by Liu et al., (2017) demonstrated good agreement between Mie-modelled scattering values using the core-shell approximation and the SP2-measured scattering cross-section for the BC with thicker coatings as is the case for the majority of particles in this study. In addition, further the particle scattering is relatively independent of particle morphology at the SP2 wavelength 1064nm (Moteki et al., 2010).” The following references have been included in the revised manuscript.

Sedlacek, A. J., III, Lewis, E. R., Kleinman, L., Xu, J., and Zhang, Q. : Determination of and evidence for noncore-shell structure of particles containing black carbon using the Single-Particle Soot Photometer (SP2), *Geophys. Res. Lett.*, 39, L06802, 2012, doi:10.1029/2012GL050905.

Moteki, N., Kondo, Y., and Nakamura, S.-i.: Method to measure refractive indices of small nonspherical particles: Application to black carbon particles, *J. Aerosol Sci.*, 41, 513-521, 2010.

For all instruments employed, also mention the model number in addition to the manufacturing company.

Complied with.

Be consistent in the use of units such as for flow rate and BC concentration. The use of different units for the same quantity makes it difficult to infer the values. Minimize the use of numeral values for comparison all the times. It may appear to the authors that these numerals are useful for comparison, but to me, it is a source of distraction. I recommend listing the values in Tables which the authors have already done. Authors can infer Table for values and focus on their findings.

Complied with for the entire manuscript.

General comments:

Page4 line 19: Add some references on the size of monomers for nascent BC.

*Cite (2017): 166, Köylü, Ümit Özgür, et al. "Fractal and projected structure properties of soot aggregates." *Combustion and Flame* 100.4 (1995): 621-633;*

Bhandari, Janarjan, et al. "Effect of thermodenuding on the structure of nascent flame soot aggregates." Atmosphere 8.9.

Complied with. We have added the following references in the revised manuscript.

Köylü, Ü.Ö., Faeth, G.M., Farias, T.L., Carvalho, M.G.: Fractal and projected structure properties of soot aggregates, Combustion and Flame, 100, 621-633, 1995, ISSN 0010-2180, [https://doi.org/10.1016/0010-2180\(94\)00147-K](https://doi.org/10.1016/0010-2180(94)00147-K).

Bhandari, J., China, S., Onasch, T., Wolff, L., Lambe, A., Davidovits, P., Cross, E., Ahern, A., Olfert, J., Dubey, M., and Mazzoleni, C.: Effect of thermodenuding on the structure of nascent flame soot aggregates, Atmos. Meas. Tech. Discuss., <https://doi.org/10.5194/amt-2016-270>, 2016.

Page 4 line19: Also, it is not correct to say that the coated BC is 'spherical' after coating. Rather I would prefer to use the term like 'compact' or 'collapsed' for coated BC core, though the core-shell model treats such coated BC as the spherical core for simplicity.

We agree and have revised the relevant portion (Page 4 , Line 17)

"However, it collapses to a compact BC particle with its cores being coated with other components via coagulation among aggregates and (or) via condensation of atmospheric vapours while aging in the atmosphere."

Page 4, line 27: What are you referring to using "these"? I am not clear.

This sentence is modified in the revised manuscript.

"All the aforementioned processes have implications for direct and indirect radiative forcing of BC".

Page4 line 32: What sources? Do you mean 'aerosol sources'? Be specific.

This is now modified to read 'aerosol sources'.

Page 5, line 24: Only one instrument is revealed. But the authors mention in the abstract that they used 2 instruments. What is the second instrument used? Specify the second instrument as well in the introduction section mentioning why the instrument was selected.

Complied with. The discussion about the ACSM is added here in the revised manuscript.

Page 5, line 25: Do the authors mean to say that the working of SP2 is based on long-term measurements only? Please rephrase the sentence.

The sentence is modified in the revised manuscript as below.

5 **“To meet these objectives, state-of-the-art instruments were installed at Bhubaneswar for long-term measurements. These included a single particle soot photometer (SP2) for characterization of refractory BC (rBC) aerosols and an aerosol chemical speciation monitor (ACSM) for high-resolution chemistry of possible coating materials. The present study provides results from a yearlong database from a combination of these instruments, perhaps for the first time over the Indian region”.**

10 *Page 6, line 12: Do you mean to say ‘above ground level’ by acronym AGL? Please mention the full name for the first time.*

Yes. Complied with.

Page 6, line 28: By ‘Supplementary Figure S1’ are you referring for the figures in an appendix? If so rename the figure as A1.

15 **Complied with. Supplementary figures are now renamed as Figure S1, S2 and so on.**

Page 7, lines 1-8: As the numeral values for meteorological parameters are shown in Table 1, avoid using all these numerals in the text for comparison. Please minimize the use of numeral values in the text. Include only those specific values that are striking to discuss.

Complied with. The sentence is modified in the revised manuscript as below.

20 **“During SMS, the prevailing wind speed and temperature were moderate, and relative humidity (RH) was high (Table 1), while rainfall, associated with the monsoon, was extensive (total rainfall ~ 878 mm). Compared to the SMS, lower temperatures, winds and RH prevailed during the PoMS, with lower total rainfall (~ 201 mm). The lowest temperatures and RH of the year were seen during winter when calm wind conditions**
25 **prevailed with almost no rainfall. The PMS witnessed the highest temperatures of the year (as high as 41 °C), moderately humid atmosphere and relatively higher wind speed compared to winter. During this season the region received a total rainfall of ~149 mm**

associated with thundershower events that led to high-velocity local winds. Details are given in Table 1”

Page 7 lines 15-17: Include the model number and company name for each instrument

Complied with. The sentence is modified in the revised manuscript as below.

5 “In the present study data was collected using a single-particle soot photometer (SP2) (Model: SP2-D; Droplet Measurement Technologies, Boulder, USA) and an Aerosol Chemical Speciation Monitor (ACSM) (Model: 140; Aerodyne Research Inc., USA).”

Page8 line2: It is mentioned that the RI of 2.26 – 1.26i is used for BC. Is this RI representative for ambient BC aerosol in the region? I am aware of the use of the above-mentioned RI value for BC. However, the
10 *RI of 2.26 – 1.26i looks higher than usually used value for the RI of BC.*

The RI 2.26-1.26i has been widely used in the SP2 community to derive the scattering properties of rBC at the specified SP2 wavelength 1064nm (Moteki et al., 2010; Taylor et al., 2015; Laborde et al., 2012). The other RI, as commonly seen in the literature, are used for the other wavelengths, mainly for the optical properties in the visible range. We do
15 not have a region-specific RI value for BC.

References:

Laborde, M., Schnaiter, M., Linke, C., Saathoff, H., Naumann, K. H., Möhler, O., Berlenz, S., Wagner, U., Taylor, J. W., Liu, D., Flynn, M., Allan, J. D., Coe, H., Heimerl, K., Dahlkötter, F., Weinzierl, B., Wollny, A. G., Zanatta, M., Cozic, J., Laj, P.,
20 Hitzenberger, R., Schwarz, J. P., and Gysel, M.: Single Particle Soot Photometer intercomparison at the AIDA chamber, Atmos. Meas. Tech., 5, 3077-3097, 10.5194/amt-5-3077-2012, 2012.

Liu, D., Whitehead, J., Alfarra, M. R., Reyes-Villegas, E., Spracklen, Dominick V., Reddington, Carly L., Kong, S., Williams, Paul I., Ting, Y.-C., Haslett, S., Taylor, Jonathan W., Flynn, Michael J., Morgan, William T., McFiggans, G., Coe, H., and
25 Allan, James D.: Black-carbon absorption enhancement in the atmosphere determined by particle mixing state, Nat. Geosci., 10, 184-188, 10.1038/ngeo2901, 2017.

Moteki, N., Kondo, Y., and Nakamura, S.-i.: Method to measure refractive indices of small nonspherical particles: Application to black carbon particles, *J. Aerosol Sci.*, **41**, 513-521, 2010.

5 Taylor, J., Allan, J., Liu, D., Flynn, M., Weber, R., Zhang, X., Lefer, B., Grossberg, N., Flynn, J., and Coe, H.: Assessment of the sensitivity of core/shell parameters derived using the single-particle soot photometer to density and refractive index, *Atmos. Meas. Tech.*, **8**, 1701-1718, 2015.

Page 8 line 9: As mentioned earlier, be consistent in picking unit for a given quantity. Here for flow rate, you used cm³/min while in line 21 you used liters/minute.

10 **Complied with.**

Page 8, line 15: For the 40-100 nm range, mention clearly that the size is ‘aerodynamic diameter’.

Complied with.

Page 8, line 26: The sub-heading 3.1 can be made more specific. By ‘Mass and number concentration’ only it is not clear what is being measured.

15 **Complied with. The sub-heading 3.1 is modified as “BC mass and number concentrations” in the revised manuscript.**

Pages 8-9 section 3.1: As mentioned earlier, use as least numeral values as possible in the discussion. All the numerals can be summarized in the table. Also, use the same units for particle concentration. In some cases, ng/m³ is used in some instance, µg/m³ is used for particle concentration.

20 **Complied with. Particle concentration is expressed in µg m⁻³ throughout the revised manuscript (relevant text is modified in abstract, discussion and conclusions). Units in figure 3(a) also are now modified.**

Page 10, line 27: I am not clear about this ‘...reported for reported from...’. Please clarify this sentence.

Sorry; the repeated word is deleted.

25 *Page 11, line 2: Is ‘Figure S1’ the same labelled as ‘Figure A1’ in the appendix?*

In the revised manuscript, all the supplementary figures are labelled as Figure S1, S2, and so on. All these figures, corresponding text and labels are available as supplementary information in the revised manuscript.

Add label for each season in the map. In fig. A1 (a) and (b), it will be useful to mention the location of the distinct data points below south India as a note.

Complied with. Now labels are added in Figure S1.

5 **“During SMS (and PoMS as well), a considerable amount of fire events are noticeable below south of India (over Srilankan region)”**

Page 11, line 10: It is mentioned that the BC mass loading was lowest during PMS, but fire events were maximum during PMS throughout the Indian region, as shown in Fig. A (d). Is not it reasonable to expect a high concentration of BC?

10 **The PMS is characterised by intense solar heating of the landmass and very little precipitation. As such, this season exhibits very high surface temperatures (going as high as 47-49 °C). Strong thermal convection resulting from intense solar heating of the dry land lifts the planetary boundary layer to higher altitudes, and with winds gaining speed, there is greater dispersion of the aerosols (Nair et al., 2007; Kompalli et al., 2014) leading to a substantial reduction in the surface concentrations. This stronger particle**
15 **dispersion resulted in lower concentrations at the surface level, despite any increased contribution from fire events. Several studies have previously highlighted the presence of elevated aerosol layers over the Indian region during the pre-monsoon season (Satheesh et al., 2008; Babu et al., 2011).**

20 **Babu, S.S., Moorthy, K. K., Manchanda, R. K., Sinha, P. R., Satheesh, S. K., Vajja, D. P., Srinivasan, S., Kumar, V. H. A.: Free tropospheric black carbon aerosol measurements using high altitude balloon: Do BC layers build 'their own homes' up in the atmosphere?, Geophys. Res. Lett. 38, L08803, 2011, doi:10.1029/2011GL046654.**

25 **Satheesh, S. K., Moorthy, K.K., Babu, S.S., Vinoj, V., Dutt, C. B. S.: Climate implications of large warming by elevated aerosol over India. Geophys. Res. Lett. 35, L19809, 2008, doi:10.1029/2008GL034944.**

Nair V. S., Moorthy K.K., Alappattu, D. P., Kunhikrishnan, P. K., George, S., Nair, P. R., Babu, S. S., Abish, B., Satheesh, S. K., Tripathi, S. N., Niranjana. K., Madhavan, B.

L., Srikanth, V., Dutt, C.B.S., Badarinath, K. V. S., Reddy, R. R.: Wintertime aerosol characteristics over the Indo-Gangetic Plain (IGP): Impacts of local boundary layer processes and long-range transport; *J. Geophys. Res.* 112 D13205, 2007, doi: 10.1029/2006 JD008099.

5 *Page 14 lines7-9: The sentence “The figure reveals. . .” is not clear to me. Please rewrite the sentence*
Complied with. The sentence is modified in the revised manuscript as below.

“In addition to the typical double-humped diurnal variation of BC mass concentration, which arises due to the combined effects of atmospheric boundary layer dynamics (Kompalli et al., 2014) and diurnal variation of the anthropogenic activities, very
10 **interesting links between BC core and relative coating thickness are noticeable from the**
Figure”.

Page 14 line11, line 13: Do you mean to say that the RCT of BC is contributed by the day-night temperature difference in different seasons? I am not clear.

The sentence is modified in the revised manuscript as below for better clarity.

15 **“and the amplitude of the BC variation has a marked seasonality. It is caused by the**
seasonal change in the diurnal variation of the ABL driven by seasonal changes in
surface heating and resulting thermal convection. The highest amplitude occurs in winter
since the diurnal variation of the ABL is greatest due to the high variation in surface
temperature; with ΔT (i.e. $T_{\max} - T_{\min}$) ~ 12 °C over a 24 hour period. Conversely, the lowest
20 **amplitude occurs during the monsoon season, when thermal convection is highly**
suppressed due to the overcast sky, low surface heating and the surface energy balance
being dominated by latent heat (the average diurnal amplitude of temperature variation,
 $\Delta T \sim 4.9$ °C).”

Page 15 lines6-9: The sentence ‘Interestingly. . .occurring’ is a long sentence.

25 **The sentence is split into two sentences in the revised manuscript as below.**

“Interestingly, during the morning period when the BC mass concentration peaks due to
the combined effect of the boundary layer dynamics (fumigation effect) and sources
(rush hour traffic contribution), RCT was at a minimum. This suggests that fresh

emissions from rush hour traffic, which would push up the BC concentration and lower the RCT, outweigh the fumigation effect; though both may be occurring around the same period.”

Page 15, lines 13-16: The sentence ‘Not. . .role’ is again a long sentence and is not clear. Simplify your statement.

The sentence is split into simpler sentences as below:

“The diurnal variations in RCT are suppressed in the SMS and PMS compared to the winter and PoMS due to the seasonality of the boundary layer dynamics that modulates the concentrations of BC and the other condensing species. In addition to this, the wet scavenging by intense rains during the SMS ensures that a greater proportion of the remaining BC in the atmosphere is likely to be freshly emitted. Such extensive precipitation also leads to a reduction in concentrations of the coating substances. During the PMS, BC particles generally have larger core sizes, and the relative coating thickness is reduced in magnitude. These effects also play a role in shaping up the diurnal pattern.”

Page 16, line 28: Chlorine is shown to be present in very low concentration even when air mass arrived from marine region to the sampling site during PMS. Is this concentration normal during the PMS as well?

Since the ACSM measures only NR-PM₁ and does not detect refractory materials (sublimation temperature > 600 °C), which includes sea salt chloride, chloride measured by the ACSM is mainly from the sources other than of marine origin.

Page 17 lines 10-13: The sentence ‘Further. . . mixed’ is not clear. In “absorption condensable species”, do you mean ‘absorption of condensable species’ and the part “which already more internally mixed” is not clear.

The sentence is modified in the revised manuscript as below.

“The concentrations of freshly produced particles with little or no coating) arising from primary as well as secondary sources are, in general, greater during day. It enables more efficient adsorption of condensable species on these particles, compared to relatively

aged particles during the night which are already coated or internally mixed due to aging. A greater fractional change can occur more quickly on fresh BC particles compared to particles which are already thickly coated since a much smaller amount of condensable material is required.”

5 **Technical comments:**

Page4 line 16: Correct the year for ‘China et al., 2012’ to make it ‘2013’.

Complied with.

Page4 line 27: A sentence starts with a pronoun at the beginning of a paragraph. It makes it difficult to know what you are referring to using a pronoun in the very beginning of a paragraph.

10 **The sentence is modified in the revised manuscript as below.**

“All the aforementioned processes have implications for direct and indirect radiative forcing of BC.”

Page 10 line3: What is represented by ‘A’ in equation (1)? Mention it.

Complied with.

15 *Page 11 line1: add ‘of’ before ‘larger-sized BC particles. . .’.*

Complied with.

Page 20, line 2: Stronger is already a comparative adjective. Remove ‘more’ before stronger.

Complied with.

20

25

Reviewer-2: ACP-2019-376-RC2

This paper describes measurements of black carbon (BC) containing particles and of non-refractory PM1 over 9-10 months at an urban site on the east coast of India. The data show some interesting seasonal trends and are worth publishing.

5 **We thank the reviewer and appreciate the summary evaluation of the merit of our work.**

However, the paper itself needs significant work. There are many missing words, misused words, confusing sentences and repetitive sections. It should not be such hard work to figure out what the authors are trying to say. Since the paper has several UK co-authors, I am surprised that it was not carefully edited by a native English speaker before submission. This paper needs major revisions before it is

10 *accepted for publication.*

We are sorry. Now we have revised the manuscript thoroughly, considering all the suggestions of the reviewer, including those on the language.

Specific comments:

15 *1- The introduction is rather repetitive and does not mention the second instrument, the ACSM. Please tighten up the language.*

Complied with. Also commented by reviewer 1. We have removed the reduntant statements and also added the details of the second instrument. The following sentences are included in the revised manuscript.

20 **Page5, Line 14: “Along with this, information on the condensable materials which act as coating substances and constantly alter the physiochemical properties of the BC containing particles, is also essential. Collocated mass spectroscopy-based high-resolution aerosol chemical composition measurements have been employed for this purpose (Liu et al., 2014; Gong et al., 2016).”**

25 **Page5, Line 25: “To meet these objectives, state-of-the the-art instruments were installed at Bhubaneswar, which included a single particle soot photometer (SP2) for characterization characterisation of refractory BC (rBC) aerosols and an Aerosol Chemical Speciation Monitor (ACSM) for high-resolution measurements of non-refractive submicron aerosol chemical composition for long-term measurements.”**

Page5: Line 31: “The contributions from distinct sources to BC concentrations and the association of coating on BC with possible condensable coating materials are examined, and the implications are discussed.”

2- page 2, lines 17 -25. It would be helpful to mention which months are included in each season.

5 **Complied with.**

3- page 2, lines 28 - 33: The statement “The diurnal pattern of sulphate resembled that of the RCT” and the statement “the coating on BC showed a negative association with sulphate” contradict each other. The association plot in Figure 11 is an interesting way to present the data, but the conclusions are tenuous and don’t belong in the abstract. I would delete the sentence starting “Though the pre-monsoon: : :” and ending “: : :mixing state of BC.”

10

Complied with. The sentence is deleted.

The following sentence is added in the revised manuscript (Page 2, Line29)

“Seasonally, the coating on BC showed a negative association with the mass concentration of sulphate during the pre-monsoon season and with organics during the post-monsoon season.”

15

4- page 4, line 6: VOCs are not an aerosol species.

Agreed. We have rewritten the sentence.

“...phosphates, and secondary organic aerosols (SOA) originating from volatile organic compounds (VOC)”.

20

5- page 4, line 19: A diameter of a few tens of nanometers is more likely for the primary spherules than for the chain agglomerates. Please cite a reference or correct the text.

Complied with. We have included the following references in the revised manuscript. (Page 4, Line 17)

References:

25

Bhandari, J., China, S., Onasch, T., Wolff, L., Lambe, A., Davidovits, P., Cross, E., Ahern, A., Olfert, J., Dubey, M., and Mazzoleni, C.: Effect of thermodenuding on the structure of nascent flame soot aggregates, Atmos. Meas. Tech. Discuss., <https://doi.org/10.5194/amt-2016-270>, 2016.

5 Bond, T. C., Doherty, S. J., Fahey, D. W., Forster, P. M., Berntsen, T., DeAngelo, B. J.,
Flanner, M. G., Ghan, S., Karcher, B., Koch, D., Kinne, S., Kondo, Y., Quinn, P. K.,
Sarofim, M. C., Schultz, M. G., Schulz, M., Venkataraman, C., Zhang, H., Zhang, S.,
Bellouin, N., Guttikunda, S. K., Hopke, P. K., Jacobson, M. Z., Kaiser, J. W., Klimont,
Z., Lohmann, U., Schwarz, J. P., Shindell, D., Storelvmo, T., Warren, S. G., and
Zender, C. S.: Bounding the role of black carbon in the climate system: A scientific
assessment, *J. Geophys. Res. Atmos.*, 118, 5380–5552, doi:10.1002/jgrd.50171,
2013.

10 Köylü, Ü.Ö., Faeth, G.M., Farias, T.L., Carvalho, M.G.: Fractal and projected structure
properties of soot aggregates, *Combustion and Flame*, 100, 621-633, 1995, ISSN
0010-2180, [https://doi.org/10.1016/0010-2180\(94\)00147-K](https://doi.org/10.1016/0010-2180(94)00147-K).

6- page 4, line 27: Paragraph starts with the word “These,” but it is not clear what “these” is referring
to.

This sentence is modified in the revised manuscript as below:

15 **“All the aforementioned processes have implications for direct and indirect radiative
forcing of BC”.**

7- page 6, line 9: Figure 1b can be removed. No-one needs to see a picture of a shipping container.

Complied with. Revised figure 1 is shown below:

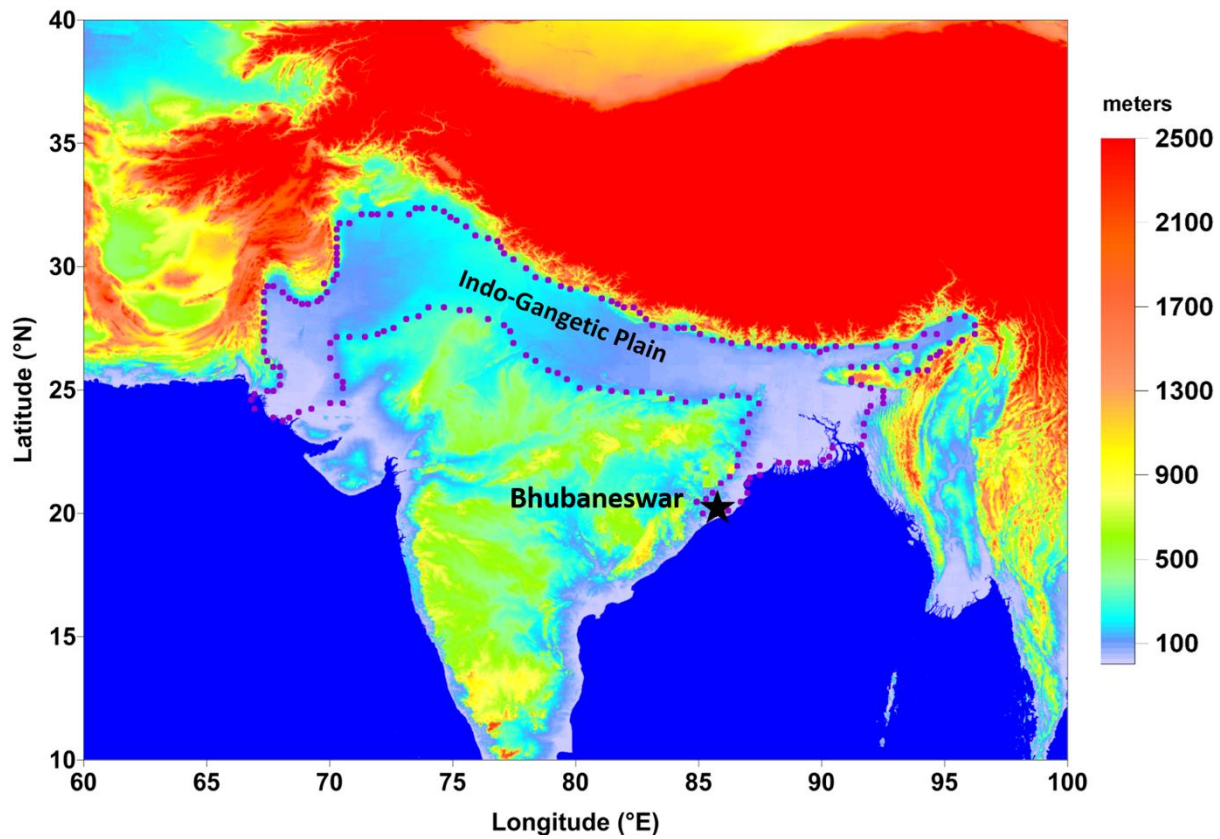


Figure 1: Geographic location of Bhubaneswar marked by a star symbol on the topographic map; the boundary of the Indo-Gangetic Plains (IGP) region is indicated with dotted lines.

5 8- page 6, line 11: Example of poor English usage “away from the proximity of.” Just say “not near.”
Complied with.

9- page 6, line 25: You refer to Figure S1, but the extra figures are in an appendix. Please label extra material consistently.

10 **Complied with. Supplementary figures are renamed as Figure S1, S2 and so on in the revised manuscript.**

10- page 6, line 30: I don’t understand what the words in parentheses are conveying. If you mean that there are more fire events in those regions, please rephrase the sentence.

Complied with. The sentence is now rephrased and split into simpler sentences as below: (Page 6, Line 30)

5 **“Figure S1 depicts the seasonal variation in the distribution of fires. The greatest number of fire events across the Indian region occur during the PMS. However, during other seasons, less intense fires are noticeable at the sub-regional scale, which are confined mostly to the northwest IGP during the PoMS, and to western, northeastern regions during winter”.**

11- page 7, lines 10-14: What about the 6-week gap in November-December? That is more than a brief gap and needs some explanation.

10 **It has been explained in the revised manuscript as below:**

“Only major gap in the data occurred during 11-November to 27-December, 2016, when measurements were paused due to logistical issues at the experimental site.”

12- page 7, lines 17-18: Why mention instruments that are not relevant to this study?

Complied with. These sentences have been removed in the revised manuscript.

15 *13- page 7, lines 31 – page 8, line 4: What do you mean by scattering enhancement? I think you are deriving the optical diameter of the coated particle from the scattering signal using a Mie Scattering model, but this description is garbled. Please phrase this more clearly.*

Complied with. This discussion is rephrased in the revised manuscript as below:

20 **“This signal is reconstructed using the leading edge only (LEO) fitting technique, which uses the leading edge of the unperturbed scattering signal before volatilization of the coating material becomes significant. This is used to reconstruct the full scattering signal (Liu et al., 2014). The reconstructed scattering signal and the BC core size (D_c) are used to derive the optical diameter of the BC particle or the coated BC size (D_p) by employing Mie calculations, where the whole particle is idealized as a two-component**
25 **sphere with a concentric core-shell morphology”.**

14- page 8, line 15: Specify that this size range is vacuum aerodynamic diameter. The range is really more like 80 nm – 800 nm.

Complied with.

15- page 8, lines 19-20: *It really doesn't seem necessary to discuss the pumps on the ACSM.*

Complied with.

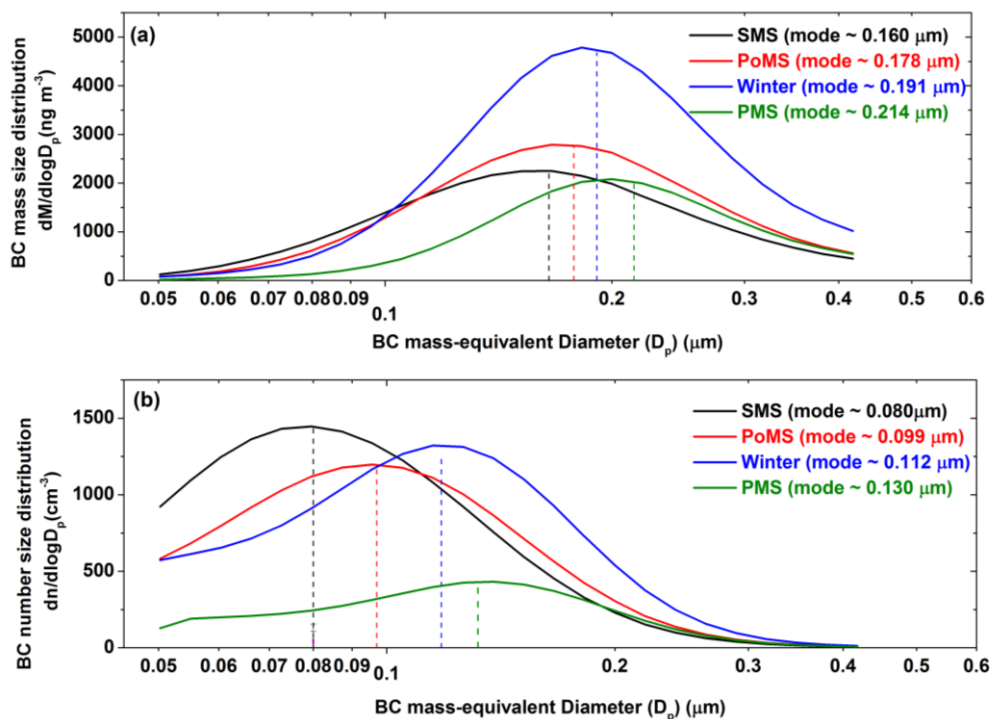
16 – page 10, lines 6-7 and elsewhere: *Please pick one term, either counts or number and use it consistently throughout the paper including the figures.*

5 **Complied with. We have used 'number' instead of 'count' and count median diameter (CMD) is modified to number median diameter (NMD) throughout the manuscript, including figures.**

17- page 10, first paragraph: *Why is there a distinct jog at 40 nm in the number size distributions?*

10 **Thanks to the reviewer for this observation. In the present data analysis, the sum of the masses of all the single particle rBC detected formed the total rBC mass loading. A certain amount of rBC mass exists at core sizes, too small to be detected by the SP2, or too large, thus saturating the detector. In the present analysis, masses of such BC particles are predicted based on the extrapolation of a log-normal fit on the D_c mass distribution (Liu et al., 2014). The values below 50 nm are obtained from such**

15 **extrapolation and in the revised manuscript, the particles with $D_c < 50$ nm are omitted, and the figure is modified (Supplementary figure S2).**



18- page 16, line 16: What does “evolving least-squares fitting” mean?

This sentence has been modified in the revised manuscript as below:

5 “These size distributions were parameterized by least-squares fitting to an analytical monomodal log-normal distribution”.

19- pages 10-11: I find this discussion extremely confusing and repetitive. The most important data is displayed in Figures 3 and 4 (and Table 4). I do not understand the point of averaging the size and number distributions over a season, taking the mode and getting a slightly different number than the average of the mode for individual data points. This does not add any new information and leads to repetitive discussion of the results. I would remove Figure 5, Table 2 and the associated discussion. Similarly, with the peak of the seasonal number size distributions – what new information does this give you beyond what you already know from the BC mass loading?

10

We partly agree. The idea of averaging over seasons is to provide inputs into models being developed in our own group and elsewhere, where the seasonal averages are needed. However, the repetitive discussions are avoided, and Figure 5 (and Table 2) is

15

moved to supplementary section as supplementary figure S2 (and supplementary table-1) in the revised manuscript.

The discussion about previous work is split between page 10, lines 18-22 and page 11, line 29 – page 12, line 4. Please consolidate.

5 **Complied with.**

Finally, if you think you can tell the difference between local emissions during SMS with a smaller size and continental outflow with a larger size, why not make two entries in Table 3 for this study?

Complied with. These entries are made in the Table (Table-2 in the revised manuscript).

10 *20- Pages 12-13: The discussion of RCT and ACT is confusing and repetitive. You are making a major assumption of core-shell morphology in order to calculate D_p and therefore RCT and ACT. Really all you can say is that you have a ratio that represents the amount of non-BC material associated with BC – you don't know the morphology of the particles nor how it changes with season. Morphology is likely to be quite different between fresh emissions during SMS and aged emissions during other seasons. I would not interpret RCT and ACT as literal diameters and coating thicknesses. In fact, I do not think ACT adds*
15 *to the discussion. I would rewrite this section to present only the RCT data and include enough caveats that it is clear RCT is a representation, not an actual ratio of diameters.*

We agree with the reviewer. It is correct that both RCT and ACT are used to represent the amount of non-BC material associated with BC and not an actual ratio of diameters. The information on the morphology of the BC, which may vary seasonally, is not available
20 **during our study period. The morphology would also be different for fresh and aged emissions. The coating thickness for individual particles is dependent on core sizes. However, the coating parameters estimated here are the bulk coating thicknesses in a given time window. It is calculated as the total volume of coated BC particles divided by the total volume of the rBC cores following Liu et al., (2014), which was used by**
25 **subsequent studies (Liu et al., 2019, Brooks et al., 2019). As described by Liu et al., (2019), as the contribution from smaller particles to the integrated volume is very less, the bulk coating thickness values are generally independent of the uncertainties arising due to the presence of smaller particles. Some of the studies reported coating on rBC in terms**

of absolute coating thickness (ACT) in nm (Gong et al., 2016; Li et al., 2019; Cheng et al., 2018; Zanatta et al., 2019). Thus we used both these parameters for comparison of our values with the other regions. The RCT and ACT come from derived parameters that require Mie calculations based on a core-shell model that may not bear relation to reality. The caveat is that we assume the morphology of the particles ; they are spherical and coating is uniform (coated particle also is spherical). We agree that this is an oversimplification and the true morphology could be different. The RCT (and ACT) parameter provides a qualitative measures of the amount of condensed material that is present on the same particle as the rBC core. We are using this to examine the extent of rBC mixing with other components in different seasons and compared to different regions. Further, using correlations with the bulk NR-PM1 composition, we can obtain some insights into the coating material associated with rBC in different periods. Thus, we have used both the volume-weighted bulk RCT (D_p/D_c) and ACT ($(D_p-D_c)/2$) in this study as representative diagnostics for the overall mixing state of the whole population of BC particles. We have modified the text in the revised manuscript to reflect the above discussion.

Page 8; Line 7

“These are calculated as the total volume of coated BC particles divided by the total volume of the rBC cores in a given time window (5 minutes) following Liu et al., (2014), which has been used by subsequent studies (Liu et al., 2019, Brooks et al., 2019a). It may be noted that the RCT and ACT used in this study come from derived parameters that require Mie calculations based on a core-shell model that may not bear relation to reality, and the RCT (and ACT) is not an actual ratio of diameters. The coating thickness for individual particles is dependent on core sizes. However, we have used the volume-weighted bulk RCT and ACT as representative diagnostics for the overall mixing state of the whole population of BC particles (Gong et al., 2016; Cheng et al., 2018; Liu et al., 2019). As described by Liu et al., (2019), since the contribution from smaller particles to the integrated volume is very less, the bulk coating thickness values are generally independent of the uncertainties arising due to the presence of smaller particles. Further,

the information on the morphology of the BC, which would be different for fresh and aged emissions, is not available in this study.. The important caveat here is that we assume the morphology of the particles; they are spherical and coating is uniform (coated particle also is spherical). The RCT (and ACT) parameter provides a qualitative measure of the amount of condensed material that is present on the same particle as the rBC core. We are using this to examine the extent of rBC mixing with other components in different seasons and compared to different regions. Further, using correlations with the bulk NR-PM1.0 composition, we intend obtain some insights into the coating material associated with rBC in different periods”.

References:

Brooks, J., Liu, D., Allan, J. D., Williams, P. I., Haywood, J., Highwood, E. J., Kompalli, S. K., Babu, S. S., Satheesh, S. K., Turner, A. G., and Coe, H.: Black carbon physical and optical properties across northern India during pre-monsoon and monsoon seasons, *Atmos. Chem. Phys.*, 19, 13079–13096, <https://doi.org/10.5194/acp-19-13079-2019>, 2019.

Cheng, Y., Li, S.M., Gordon, M., and Liu, P.: Size distribution and coating thickness of black carbon from the Canadian oil sands operations. *Atmos. Chem. Phys.*, 18, 2653–2667, 2018.

Li, K., Ye, X., Pang, H., Lu, X., Chen, H., Wang, X., Yang, X., Chen, J., and Chen, Y.: Temporal variations in the hygroscopicity and mixing state of black carbon aerosols in a polluted megacity area, *Atmos. Chem. Phys.*, 18, 15201–15218, <https://doi.org/10.5194/acp-18-15201-2018>, 2018.

Liu, D., Joshi, R., Wang, J., Yu, C., Allan, J. D., Coe, H., Flynn, M. J., Xie, C., Lee, J., Squires, F., Kotthaus, S., Grimmond, S., Ge, X., Sun, Y., and Fu, P.: Contrasting physical properties of black carbon in urban Beijing between winter and summer, *Atmos. Chem. Phys.*, 19, 6749–6769, <https://doi.org/10.5194/acp-19-6749-2019>, 2019.

Zanatta, M., Laj, P., Gysel, M., Baltensperger, U., Vratolis, S., Eleftheriadis, K., Kondo, Y., Dubuisson, P., Winiarek, V., Kazadzis, S., Tunved, P., and Jacobi, H.-W.: Effects of mixing state on optical and radiative properties of black carbon in the European Arctic, *Atmos. Chem. Phys.*, 18, 14037–14057, <https://doi.org/10.5194/acp-18-14037-2018>, 2018.

I also don't understand the point of Figure 7. You already have the information about the width of the distributions in Table 4. You mention multiple maxima, but have no interpretation. The discussion of Figure 7 on page 13 repeats the same information about sources and processing as on page 12, making this section very repetitive. I would remove Figure 7 and the associated discussion.

We have complied with the reviewer's suggestion. Figure 7 has been moved to supplementary information in the revised manuscript (Supplementary Figure S3) and the repetitive discussion is removed.

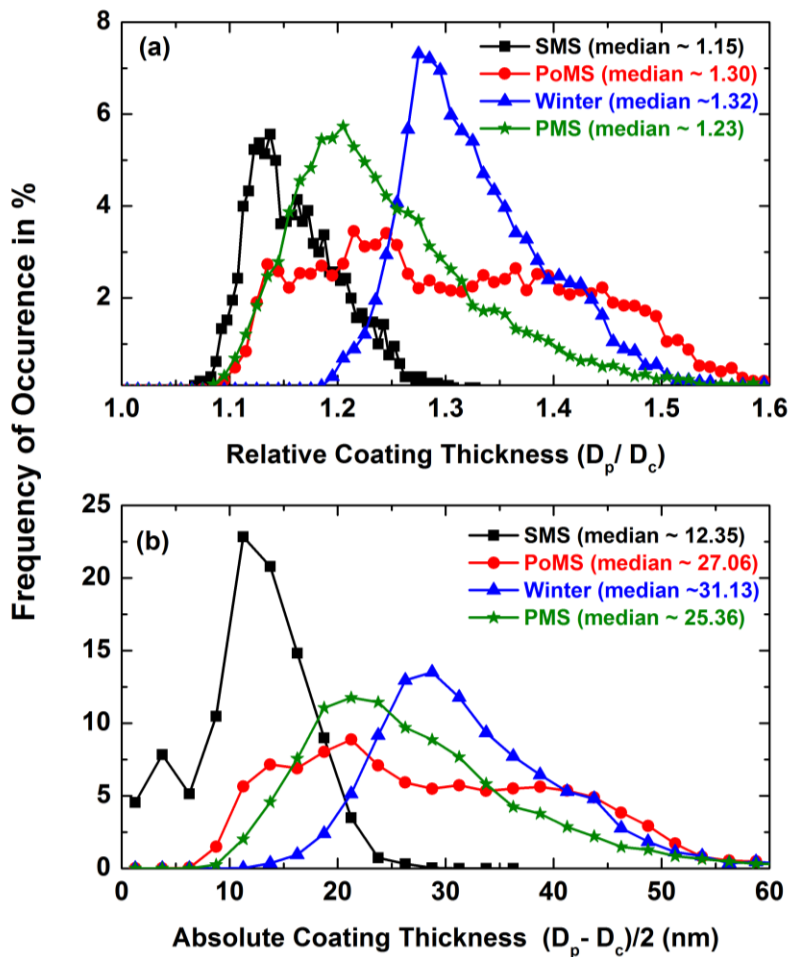
21- Page 12, lines 12-14: "Both of these parameters: : :mixing state of the particles." I do not understand this sentence. Does "both" refer to RCT and ACT or to Dp and Dc? Either way, how can Dp not depend on the mixing state?

Yes. Both refer to RCT and ACT. We have modified the sentence in the revised manuscript accordingly.

22- Page 13, lines 1-2: "Intra-seasonal variability: : :Figure 6) is also higher during PoMS." I do not understand this sentence. Figure 6 shows daily values, not seasonal values. By eye, the variation in the daily points and the spread of the error bars looks very similar across PoMS, Winter and PMS. There are very few points during SMS, so it is hard to draw conclusions for that season.

The sentence is modified in the revised manuscript.

"Intra-seasonal variability (as highlighted by the wide range of frequency of occurrence of RCT and ACT values during the PoMS seen in the supplementary figure S3) is also higher during the PoMS".



23- Pages 15-17, Section 3.5: I have several questions about the ACSM data analysis. Why is ammonia
 5 so low? Was the aerosol not neutralized and do you have corroborating evidence? Or was the RIE_{NH_4}
 incorrect for this instrument? Why not estimate OOA and HOA using the parameterization in Ng et al.
 (EST 2011)? This would give you additional information about local and regional sources.

**We agree with the reviewer that the estimation of OOA and HOA provides information on
 the nature of sources. Detailed factorization of organics forms the scope for the future
 10 study, and is not attempted here. Periodic ionization efficiency calibrations were
 performed using ammonium nitrate, ammonium sulphate, and corresponding RIE_{NH_4}
 values were updated in the DAQ of the ACSM. The reviewer made a good observation**

about the concentration of ammonium. We have estimated the aerosol neutralization ratio (ANR) (this information is not available in the present manuscript) in terms of the ACSM measured (m) NH_4^+ to predict (p) NH_4^+ ratio for different seasons and found a seasonal variability in the ANR values indicating ammonium deficit to fully neutralized aerosol system. A detailed analysis on this is being carried out. Earlier, Mahapatra et al., (2013) estimated chemical composition of total suspended particulate (TSP) matter at Bhubaneswar using year-round filter-based sampling and have reported that both the acidic and basic components have significant seasonal variability. From the recent filter-based offline chemistry data there is evidence for seasonally varying ANR which indicated dominance of acidic (NO_3^- and SO_4^-) over basic (NH_4^+ , Mg^{2+} and Ca^{2+}) atmospheres in different seasons at Bhubaneswar (unpublished data). One of the reasons for ammonium deficiency is possible heterogeneous reactions during the presence of a high number of pre-existing large particles and very high concentrations of acidic species (Pathak et al., 2009; Hsu et al., 2014). Collocated measurements of number size distributions of ultrafine and fine particles during the present study period at the site have also revealed the absence of new particle events due to high condensation sink (unpublished data) corroborating the above. The consolidated analysis of the aerosol chemistry from a combination of the size segregated off-line and online data methods is in progress to understand these aspects in detail.

References:

- Mahapatra, P.S., Ray, S., Das, N., Mohanty, A., Ramulu, T.S., Das, T., Chaudhury, G.R., Das, S. N.: Urban air-quality assessment and source apportionment studies for Bhubaneshwar, Odisha, *Theor. Appl. Clim.*, 112, 243-25, 2013.
- Hsu, S.-C., C. S. L. Lee, C.A. Huh, R. Shaheen, F.-J. Lin, S. C. Liu, M.-C. Liang, Tao, J.: Ammonium deficiency caused by heterogeneous reactions during a super Asian dust episode, *J. Geophys. Res. Atmos.*, 119, 2014, 6803–6817, doi:10.1002/2013JD021096.

Pathak, R.K., Wu, W.S., Wang, T.: Summertime PM_{2.5} ionic species in four major cities of China: nitrate formation in an ammonia-deficient atmosphere, *Atmos. Chem. Phys.*, 9, 1711–1722, 2009. DOI: 10.5194/acp-9-1711-2009.

24- Page 17, lines 1-7: “Even though: : :coating.” I do not understand this sentence, partly because it is too long and convoluted, but also because the two parts contradict each other. You say in part a that concurrent peaks in RCT and sulphate suggest that sulphate is mixed with BC, but in part b, you say the opposite. You can’t have it both ways. Or are you saying that the ACSM detects sulphate when it is mixed with BC, but not organic? That does not make sense.

This confusion has been cleared. We have rewritten this in the revised manuscript as below: (Page17, Line1)

“It is challenging to determine the exact coating material on the atmospheric BC particles in a multi-component system containing organic and inorganic aerosols, and gaseous vapours. The association between the diurnal variations of organics and sulphates and BC mixing state as represented by RCT presents two possibilities of having different coating material on BC during a day. Similar diurnal variations in RCT (as seen in Figure 6) and sulphate suggest the possibility of sulphate serving as the most probable material. However, organic matter can also contribute to the BC coating material due to its huge abundance in particles of submicron sizes. This is particularly true during the late evening periods, when concurrent peaks in the mass fraction of organics and rBC mass loading occur, a significant fraction of which could be secondary in nature. The extent of contribution of each species depends on processes such as gas-phase chemistry and production of condensable vapours and strength of the condensation sink”.

25- Pages 17-18, Section3.7: Figure 11 is another way of comparing the diurnals for RCT and MF. While it is a nice visualization, I don’t think it needs a new section repeating much of the discussion as in Section 3.6. I would combine the discussion in Sections 3.6 and 3.7.

Complied with. We have combined the sections 3.6 and 3.7, which describe the association between rBC relative coating thickness and NR-PM₁ chemical species in diurnal and seasonal scales.

I also wonder if you have thought about the fraction of particles containing BC (i.e., $BC \text{ number conc.} / (BC \text{ num conc.} + \text{scatt num conc.})$)? This fraction is much higher in SMS than in PoMS or Winter and is lowest in PMS. The low value in PMS might be part of the reason that the association in Figure 11d and h is so poor since there is less overlap between the particle population detected with the ACSM and the population detected with the SP2.

Agreed with thanks. We have modified the text in the revised manuscript to include this possibility. (Page18, Line 28)

“It may be noted that it is difficult to decipher the exact coating on BC with the present approach, since the SP2 retrieves black carbon mass and provides a measure of co-existing material within the same particles (as measured by RCT) whereas the ACSM measures the mass of refractory material in the total submicron population. An examination of coating material can only be directly achieved by employing the instruments such as the soot particle aerosol mass spectrometer (Aerodyne SP-AMS) (Liu et al., 2018). However, the SP2 can determine both the rBC content of single particles and the optical size by light scattering for diameters between 200 and 400 nm. The coating thickness estimated within this range represents most of the particles which contribute significantly to the light extinction. A comparison of the proportion of rBC containing particles within the total population as a function of season sheds some light on interpreting variation throughout the year. In our study, the fraction of particles containing BC, i.e., the ratio of BC number concentration and total number concentration (BC number concentration + scattering number concentration) showed a clear seasonal variation. The fraction of BC containing particles was highest during the SMS (mean $\sim 0.69 \pm 0.11$) and decreased through winter ($\sim 0.44 \pm 0.16$), PoMS ($\sim 0.36 \pm 0.11$) to reach the lowest value ($\sim 0.25 \pm 0.10$) during the PMS. This shows a gradual decrease in the overlap between the particle population detected with the ACSM and the population detected with the SP2 with changing seasons from SMS to PMS. This should be borne in mind while examining the association between the ACSM detected particle mass concentrations and the SP2 derived coating parameters.”

Reference:

Liu, D., Taylor, J. W., Crosier, J., Marsden, N., Bower, K. N., Lloyd, G., Ryder, C. L., Brooke, J. K., Cotton, R., Marenco, F., Blyth, A., Cui, Z., Estelles, V., Gallagher, M., Coe, H., and Choularton, T. W.: Aircraft and ground measurements of dust aerosols over the west African coast in summer 2015 during ICE-D and AER-D, *Atmos. Chem. Phys.*, **18, 3817–3838, <https://doi.org/10.5194/acp-18-3817-2018>, 2018.**

5

26- Figure 1: It is very hard to see the circle indicating the IGP in panel (a). I would delete panel (b). There is no need for a picture of a shipping container.

Complied with. Panel (b) has been deleted, and Figure 1 has been modified in the revised manuscript.

10

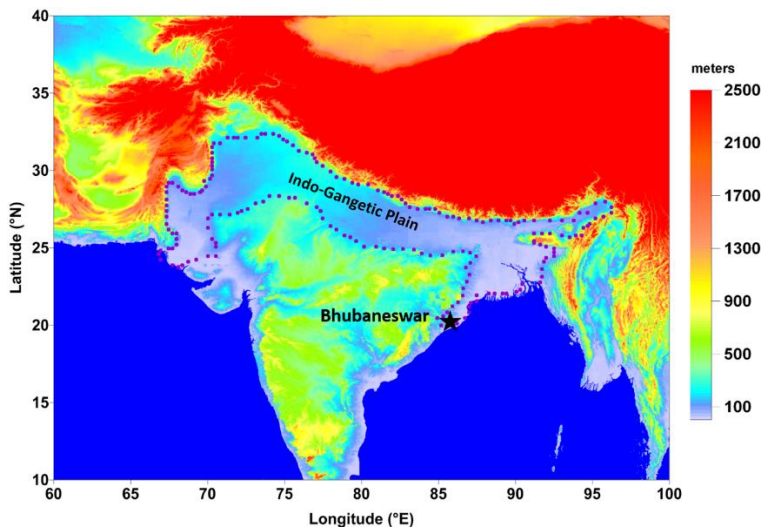
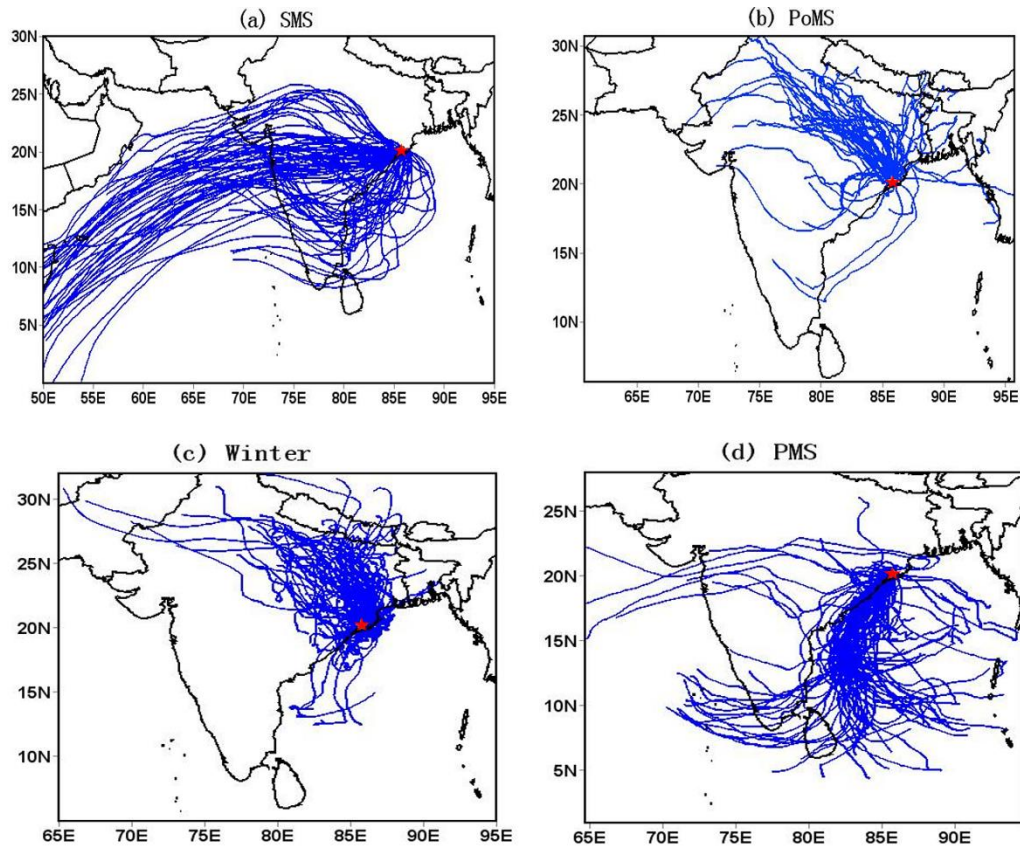


Figure 1: Geographic location of Bhubaneswar marked by a star symbol on the topographic map; the boundary of the Indo-Gangetic Plains (IGP) region is indicated with dotted lines.

27- Figure 2: The star symbol is not visible.

15

Figure 2 has been updated in the revised manuscript.



28- Figure 3: Indicate the seasons in panels (a) and (b).

Figure 3 has been updated in the revised manuscript as per the suggestion.

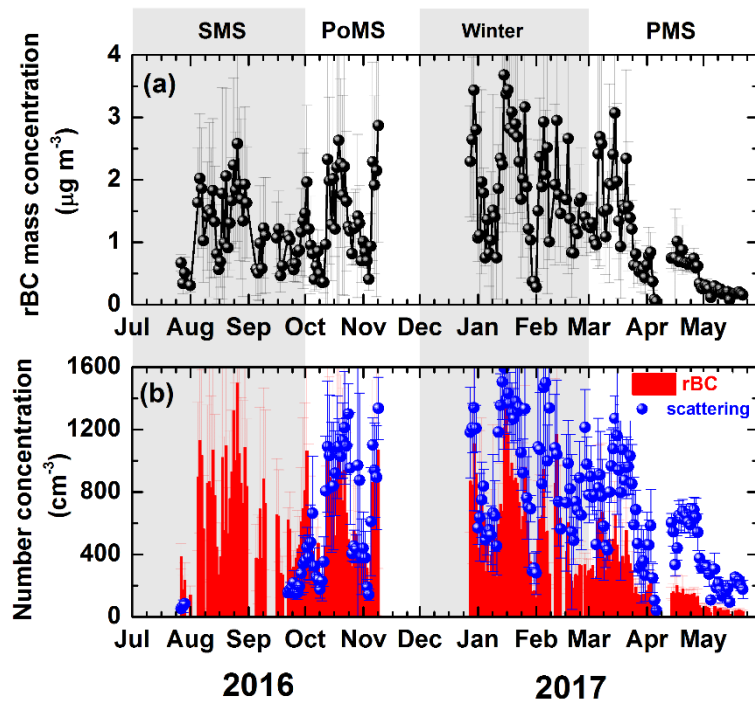
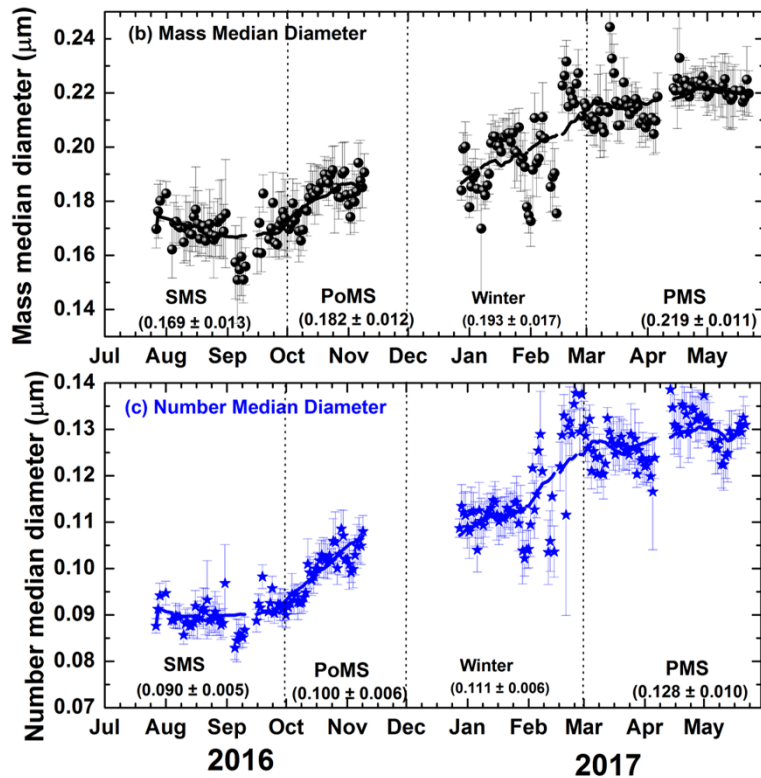
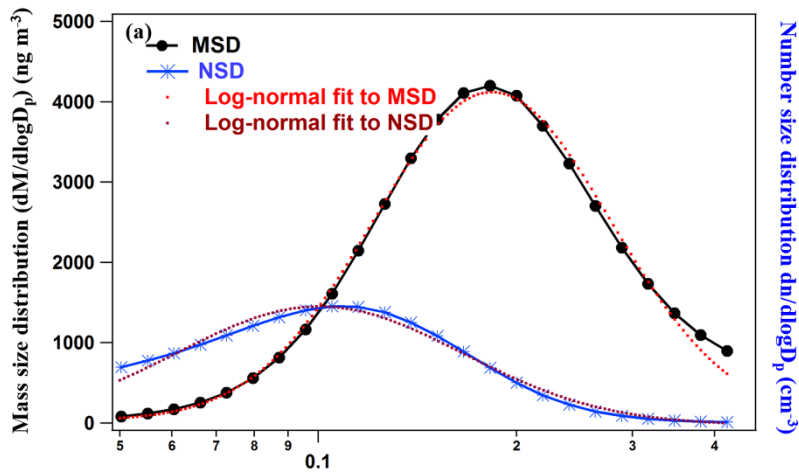


Figure 3: Temporal variation of daily mean (a) r_{BC} mass concentration; and (b) number concentration of BC (bars) and non-BC scattering particles (filled circle). The vertical line passing through them is the standard deviation. The shaded portions demarcate the seasons.

5 29- Figure 4: Include the dashed lines in the legend. Panel (b) has circles not triangles. Please use either number or count, but not both.

Complied with. Figure 4 is modified in the revised manuscript.



Do you have any data covering the gap between end of May and August? Do the MMD and CMD really drop from PMS to SMS values over 6 weeks? Or could you have some kind of instrumental drift that causes both to increase over the displayed 10 months of data?

Unfortunately, no data is available covering the gap between the end of May and August during the present study period due to technical issues with the SP2 optics (a drop in the SP2 laser power due to contamination of the optics owing to heavy particle loading). We rule out any instrumental drift as it has been periodically calibrated to account for any variation in the laser power and detector response. Notably, the present MMD values during the PMS are consistent with the values reported by Brooks et al., (2019) based on the aircraft experiments over the same region. They have reported that core MMD values which were 0.22 μm during the PMS (flights on 11–12 June 2018) dropped down to 0.20 μm with the onset of monsoon (flights on 30 June–11 July 2018; which were temporally just 2-4 weeks away from the pre-monsoon flights). They attributed it to change in the nature of air masses. The large scale changes in the air mass characteristics combined with the widespread precipitation across the Indian region associated with monsoon circulation contributes to changes in both the nature and strength of BC sources.

Reference:

Brooks, J., Liu, D., Allan, J. D., Williams, P. I., Haywood, J., Highwood, E. J., Kompalli, S. K., Babu, S. S., Satheesh, S. K., Turner, A. G., and Coe, H.: Black carbon physical and optical properties across northern India during pre-monsoon and monsoon seasons, *Atmos. Chem. Phys.*, **19**, 13079–13096, <https://doi.org/10.5194/acp-19-13079-2019>, 2019.

30- Figure 11: “Speices” is mis-spelled in the x-axis label.

It has been corrected in the revised manuscript.

31- Table 1: “metrological” should be “meteorological”

It has been corrected in the revised manuscript

32- Table 3: “Shangai” is mis-spelled.

25 **It has been corrected in the revised manuscript**

33- Table 4: Are these averages of the daily values shown in the figures, or averages of all the underlying data? Please specify. Also, somewhere in the text you should state the time-base of the SP2 data.

The values tabulated are averages of all the underlying data. Table-4 Table-3 in the revised manuscript) has been slightly modified as per the suggestion from reviewer-1. Time-base of the processed SP2 data is 5 minutes, and it is specified in the revised manuscript.

5 34- Figure A1 (or S1?): Please decide if this section is an appendix or supplemental information.

In the revised manuscript, Figure S1, S2, S3 and S4 are available as supplementary figures, and the corresponding discussion is available as supplementary information.

Please label the panels with the season. It's not clear what the words in parentheses in the last sentence are supposed to mean.

10 **Complied with. Now labels are added in Figure S1. Figure caption has been revised.**

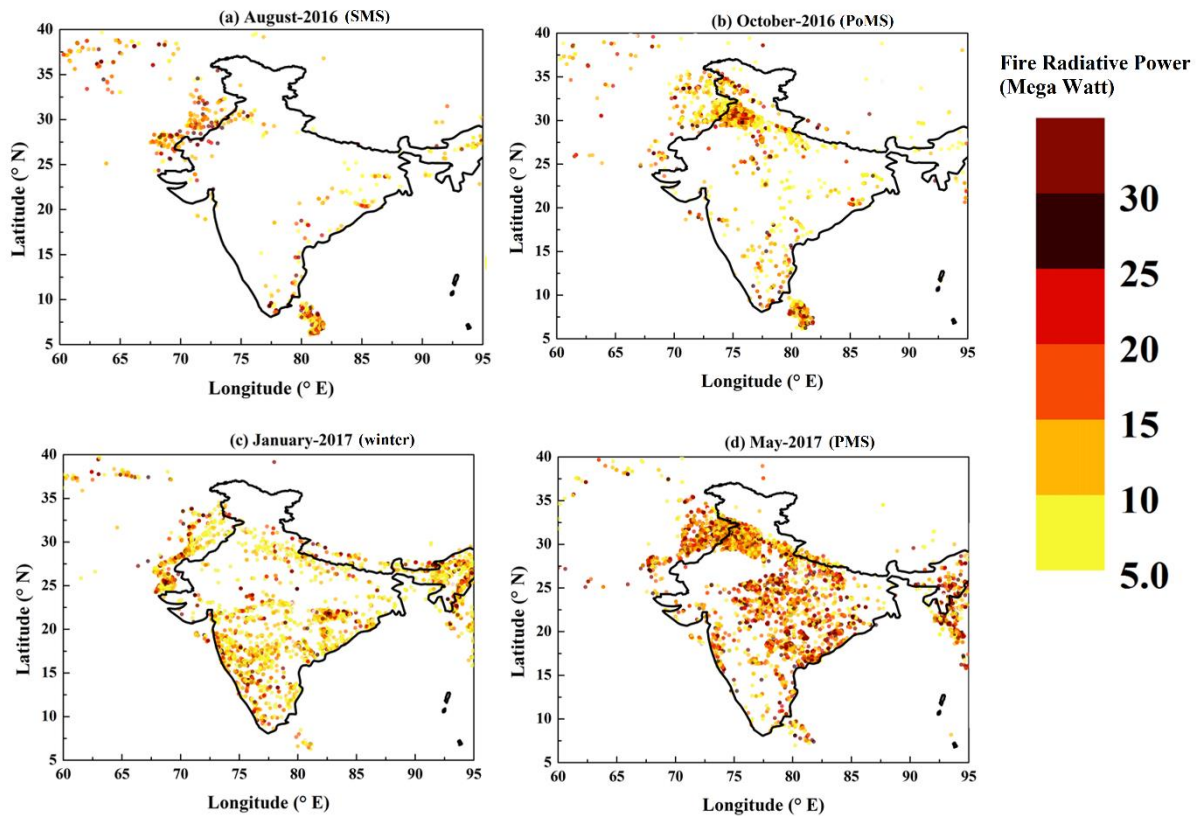


Figure S1: Spatial distribution of Moderate Resolution Imaging Spectroradiometer (MODIS) fire radiative power (MODIS Thermal Anomalies / Fire locations Collection 6 product obtained from <https://earthdata.nasa.gov/firms>) for the

representative months of different seasons; (a) August -2016 (SMS), (b) October -2016 (PoMS), (c) January -2017 (winter) and (d) May -2017 (PMS). A significant amount of fire events during PMS are seen over the Indian region. During the PoMS (fire events to confined to northwest IGP) and winter (fire events to confined to western, northeastern regions of India) less intense regional fire events are noticeable. During SMS (and PoMS as well), a considerable amount of fire events are noticeable below south of India (over Srilankan region).

5

10

15

Seasonal contrast in size distributions and mixing state of black carbon and its association with PM1.0 chemical composition from the eastern coast of India

Sobhan Kumar Kompalli¹, Surendran Nair Suresh Babu¹, Sreedharan Krishnakumari Satheesh^{2,3},
5 Krishnaswamy Krishnamoorthy², Trupti Das⁴, Ramasamy Boopathy⁴, Dantong Liu^{5,6}, Eoghan
Darbyshire⁵, James Allan^{5,7}, James Brooks⁵, Michael Flynn⁵, Hugh Coe⁵

¹Space Physics Laboratory, Vikram Sarabhai Space Centre, India.

²Centre for Atmospheric & Oceanic Sciences, Indian Institute of Science, India.

10 ³Divecha Centre for Climate Change, Indian Institute of Science, Bangalore, India

⁴Institute of Minerals and Materials Technology, CSIR, Bhubaneswar.

⁵Centre for Atmospheric Science, School of Earth and Environmental Sciences, University of Manchester, Manchester, UK.

⁶Department of Atmospheric Sciences, School of Earth Sciences, Zhejiang University, Hangzhou, Zhejiang, China.

⁷National Centre for Atmospheric Science, UK.

15

Correspondence to: S. Suresh Babu (sureshsplvssc@gmail.com), Sobhan K. Kompalli (sobhanspl@gmail.com)

Abstract

Over the Indian region, aerosol absorption is considered to have a potential impact on regional climate, monsoon and hydrological cycle. Black carbon (BC) is the dominant absorbing aerosol, whose absorption potential is ~~largely determined~~determined mainly by its microphysical properties, including its concentration, size, and mixing state with other aerosol components. The Indo-Gangetic Plains (IGP) is one of the regional aerosol hot spots with diverse sources, both natural and anthropogenic, but still the information on the mixing state of the IGP aerosols, especially BC, is limited and a ~~major-significant~~ source of uncertainty in understanding their climatic implications. In this context, we present the results from intensive measurements of refractory BC (rBC) carried out over Bhubaneswar, an urban site in the eastern coast of India, which experiences contrasting airmasses (the IGP outflow or coastal/marine airmasses) in different seasons. This study helps to elucidate the microphysical characteristics of BC over this region and delineates the IGP outflow from the other airmasses. The observations were carried out as part of “South West Asian Aerosol Monsoon Interactions (SWAAMI)” collaborative field experiment during July 2016-May 2017, using a single particle soot photometer (SP2) that uses a laser-induced incandescence technique to measure the mass and mixing state of individual BC particles and an aerosol chemical speciation monitor (ACSM) to infer possible coating material. Results highlighted the distinctiveness in aerosol microphysical properties in the IGP airmasses. BC mass concentration was highest during winter (December-February) ($\sim 1.94 \pm 1.58 \mu\text{g m}^{-3}$), when the prevailing air masses were mostly of IGP origin, followed by post-monsoon (October-November) (mean $\sim 1.34 \pm 1.40 \mu\text{g m}^{-3}$). Mass median diameter (MMD) of the BC mass size distributions were in the range 0.190-0.195 μm suggesting mixed sources of BC, and further, higher values (~ 1.3 - 1.8) of bulk relative coating thickness (RCT) (ratio of optical and core diameters) were seen indicating a large-significant fraction of highly coated BC aerosols in the IGP outflow. During the pre-monsoon (March-May), when marine/coastal airmasses prevailed, BC mass concentration was lowest ($\sim 0.82 \pm 0.84 \mu\text{g m}^{-3}$) and larger BC cores (MMD $> 0.210 \mu\text{m}$) were seen suggesting distinct source processes, while RCT was ~ 1.2 - 1.3 , which may translate into higher extent of absolute coating on BC cores which may have important crucial regional climate implications. During the summer monsoon (July-September), BC size distributions were dominated by smaller cores (MMD $\leq 0.185 \mu\text{m}$) with the lowest coating, indicating fresher BC, likely from fossil fuel sources. A clear diurnal variation pattern of BC and RCT was noticed in all the seasons, and day time peak in RCT suggested enhanced coating on BC due to the condensable coating material originated from photochemistry. Examination of sub-micron aerosol chemical composition highlighted that the IGP outflow was dominated by organics (47-49%) and marine/coastal airmasses contained greater-higher amounts of sulphate (41-47%), while ammonium and nitrate were seen in minor amounts with significant concentrations only during the IGP airmass periods. The diurnal pattern of sulphate resembled that of the RCT of rBC particles, whereas organic mass showed a pattern similar to that of the rBC mass concentration. Seasonally, the coating on BC showed a negative association with the mass concentration of sulphate during the pre-monsoon season and with organics during the post-monsoon season. ~~the~~ Though the pre-monsoon is sulphate dominated, the coating on BC showed a negative association with sulphate and same is true for organic mass during the post-monsoon, suggesting preferential

Formatted: Indent: First line: 0 cm, Right: 0 cm

Formatted: Not Highlight

Formatted: Not Highlight

Formatted: Not Highlight

Formatted: Not Highlight

Formatted: Not Highlight

Formatted: Not Highlight

~~coating and importance of source processes (and co-emitted species) on the mixing state of BC.~~ This is the first experimental data on the mixing state of BC from a long time series over the Indian region, and includes new information on black carbon in the IGP outflow region. This data helps in improving the understanding of regional BC microphysical characteristics and their climate implications.

5

Keywords: Refractory black carbon, size distribution, mixing state, Indo-Gangetic Plain outflow

1. Introduction

The state of mixing of aerosols, especially that of absorbing aerosols, remains poorly quantified, despite its important role in determining the regional and global radiative impacts of aerosols and aerosol-cloud interactions (Bond et al., 2013; Liu et al., 2013; IPCC 2013). The importance of the Southwest Asian region need not be over-emphasized in this context; where the two most-absorbing aerosol species, Black carbon (BC) from a wide variety of sources in the locale and dust co-exist along with a ~~large-broad~~ spectrum of other aerosol species such as sulphates, nitrates, phosphates, ~~volatile organic compounds (VOC)~~, and secondary organic aerosols (SOA) ~~originating from volatile organic compounds (VOC)~~ (Lee et al., 2002; Shiraiwa et al., 2007; Moteki et al., 2007; Moffet and Prather, 2009; Zhang et al., 2015). ~~The dust is emitted from both local arid regions as well as advected from far off regions such as the Middle East and Eastern Africa, and these different sources are known to have distinctly differing absorption properties (Moorthy et al. 2007). Large-Significant~~ seasonal changes in synoptic meteorology occur in this region throughout the year associated with the Asian monsoon system and the associated changes in atmospheric humidity and thermal convection, which is modulated by the local (meso-scale) meteorology and the regional orography. This interplay confines the aerosol between the Bihar Plateau to the South and the high Himalayan ranges to the north. Such strong variation is therefore likely to lead to significant changes in the aerosol characteristics, especially the state of mixing (Lawrence and Lelieveld 2010; Srivastava and Ramachandran, 2013; Srinivas and Sarin 2014; Moorthy et al., 2016; Raatikainen et al., 2017).

~~Both BC and dust are~~ highly porous in nature (Adachi et al., 2010, 2014; China et al., ~~2012~~2013; Bond et al., 2013; Scarnato et al., 2015), and provide surface area for adhesion of other particulate and gaseous species, paving the way for ~~surface-surface~~-based chemical reactions. ~~In this regard, BC has some special significance.~~ Nascent BC is hydrophobic, and is comprised of chain ~~aggregates~~agglomerates with diameters of the order of few tens of nanometers (~~Köylü et al., 1995; Bond et al., 2013; Bhandari et al., 2016 and references therein~~)-. ~~However, it collapses to a compact BC particle with its cores being coated with other components via coagulation among aggregates and (or) via condensation of atmospheric vapours while aging in the atmosphere.~~However, it collapses to spherical BC cores coated with other components via ~~coagulation among aggregates and (or) condensation of atmospheric vapours while aging in the atmosphere~~ (Weingartner et al., 1997; Zuberi et al., 2005). Coatings of non-absorbing components on the core BC, alter the morphology of the BC and enhance the absorption potential of the resultant ~~mixed-mixed~~-phase particle to varying magnitudes through ~~so-so~~-called 'lensing effect' (e.g. Shiraiwa et al., 2010; Cappa et al., 2012; Peng et al., 2016; Ueda et al., 2016; Wang et al., 2016). In addition, the coating of other soluble species on BC affects its hygroscopic properties (Weingartner et al., 1997; McMeeking et al., 2011; Liu et al., 2013; Laborde et al., 2013), atmospheric life-time and makes it more cloud condensation nuclei (CCN) active (Liu et al., 2013; IPCC 2013).

~~All the aforementioned processes have implications for direct and indirect radiative forcing of BC. These have implications for direct and indirect radiative forcing of BC. In the last few decades~~ Due to the rapid growth in the human population, ~~across the region and the large-substantial~~ increase in vehicle use, large scale industrialization and ~~increased~~-anthropogenic

Formatted: Not Highlight

Formatted: Not Highlight

Formatted: Not Highlight

activities ~~have taken place over the Indian region in the last few decades.~~ These factors resulted in a significant increasing trend in the overall regional aerosol burden ~~over the Indian region has increased~~ amplified significantly and displays an increasing trend (Babu et al., 2013; Moorthy 2016). The Indo-Gangetic Plain (IGP) region is one of the aerosol hot spots with potential implications to regional radiative forcing (Nair et al., 2017) and circulation (Lawrence and Lelieveld 2010; Gautam et al., 2009) and has attracted wide attention. Large heterogeneity in the nature of aerosol sources over the IGP (industrial and vehicular emissions, crop residue and residential fuel burning) results in BC particles with varying microphysical properties (size, concentrations and mixing state) which determine its absorption potential and radiative effects (Jacobson 2001; Cappa et al., 2012; Petzold et al., 2013; Bond et al., 2013). Hence it is essential to gather information on BC microphysical properties including its mixing state to understand its effect on absorption enhancement and further BC climatic implications (both direct and indirect effects).

Detailed characterization of the state of mixing of aerosols over the Indo-Gangetic Plains (IGP), which is recognized as one of the most complex regions as far as aerosols are concerned (Moorthy et al. 2016), remains virtually non-existent. There have been a few limited and isolated studies (Thamban et al., 2017 and references therein) that have been mainly based on chemical composition and theoretical/model calculations (Dey et al., 2008; Srivastava and Ramachandran, 2013) and did not explore BC mixing state due to inherent limitations of the methodologies employed. While characterization of BC spectral absorption properties and its mass loading over India are numerous (e.g. Beegum et al., 2009; Kompalli et al., 2014; Prasad et al., 2018 and references therein), reports on the size distribution of BC and its mixing state are extremely limited and site/season-specific (Raatikainen et al., 2017; Thamban et al., 2017). The non-availability of state-of-art instruments for near-real-time estimating of coating of BC core with other species has been one of the main reasons for such limited exploration. In this context, the single particle soot photometer (SP2), a laser-induced incandescence technique, offers a powerful tool for long-term measurements at single particle level (Moteki and Kondo, 2007; Schwarz et al., 2008, 2013; Laborde et al., 2012; Liu et al., 2014). Along with this, information on the condensable materials which act as coating substances and constantly alter the physiochemical properties of the BC containing particles, is also essential. Collocated mass spectroscopy-based high-resolution aerosol chemical composition measurements have been employed for this purpose (Liu et al., 2014; Gong et al., 2016).

Recognizing the need for the above information for better understanding aerosol-radiation-cloud-monsoon interactions over the South Asian region, a super site (first of three) was established in July-2016 at Bhubaneswar located in the eastern IGP, as part of the joint Indo-UK experiment, "South West Asian Aerosol Monsoon Interactions (SWAAMI)" executed by the Space Physics Laboratory of Indian Space Research Organisation (ISRO), the Indian Institute of Science (IISc), Bengaluru and the University of Manchester, United Kingdom. The key objectives have been (a) assessment of the impact of BC and co-emitted organic/inorganic species on the radiation budget via the direct, semi-direct and indirect effects, and (b) assessment/evaluation of the impact/effects of the aerosol radiative forcing on the local energy budget, atmospheric dynamics and hydrological cycle over India. Under this, state-of-the-art instruments were installed at Bhubaneswar, which included a single particle soot photometer (SP2) for characterization of refractory BC (rBC) aerosols and the Aerosol Chemical

Formatted: Not Highlight

~~Speciation monitor (ACSM) for high-resolution measurements of non-refractive submicron aerosol chemical composition for long-term measurements. To meet these objectives, state-of-the-art instruments were installed at Bhubaneswar, which included a single particle soot photometer (SP2) for characterization of refractory BC (rBC) aerosols and an Aerosol Chemical Speciation Monitor (ACSM) for high-resolution measurements of non-refractive submicron aerosol chemical composition for long-term measurements. The present study provides results from a yearlong database from a combination of these instruments, perhaps for the first time over the Indian region based on long-term measurements, perhaps for the first time over the Indian region. This paper provides~~ includes the details of the measurement and analysis, presents the results on the concentrations (mass and number), size distribution, mixing state in terms of coating thickness of BC, the seasonality and responses to contrasting air mass types. The contributions from distinct sources ~~to BC concentrations, the association of coating on BC with possible condensable coating material~~ are also examined, and implications are discussed.

Formatted: Not Highlight

2. Experimental details

2.1 Observational site, general meteorology and data period

The measurements were carried out from Bhubaneswar, the capital city of Odisha state, in the eastern part of India (denoted by the star symbol in Figure 1a), and is an aerial distance of 53 km from the western coastline of the Bay of Bengal. It is a moderately industrialized city, typically urbanized and with the consequent anthropogenic emissions (industrial, traffic and household). It receives outflow from the Indo-Gangetic Plain (IGP, indicated by ~~an oval symbol~~ dotted lines in the figure), lying to its west, through advection by the synoptic westerlies for ~~the most part~~ of the year. The urban area is surrounded by rural regions along a radius of 70 km that host a variety of anthropogenic activities involving burning of solid fuel (wood, dung cake etc.) for household cooking and small-scale industries such as brick kilns, and ~~coal~~ coal-fired thermal power plants. It also comprises of a major shipping harbour (Mahapatra et al., 2013a; Venkatraman et al., 2005; Verma et al., 2012).

Formatted: Not Highlight

Formatted: Not Highlight

Aerosol measurements are carried out at this supersite from a custom-built container (~~Figure 1b~~) installed in the premises of the Institute of Minerals and Materials Technology (IMMT), Bhubaneswar (20.20°N, 85.80 °E, 78 above mean sea level) which is ~~away from the proximity of~~ not near to any major industrial and urban activities. ~~The~~ Sampling of ambient aerosols is done by drawing air at 16.67 litres min⁻¹ from a height ~3 meters ~~above ground level~~ (AGL) through a stainless-steel tube fitted with a PM10 inlet. Another stainless tube, with ~~an~~ inner diameter of ~0.635 cm and 30 cm length, was used for isokinetic subsampling from this main flow inside the stack. ~~In order to~~ To keep the relative humidity of the sample flow < 50 %, a ~~naafion~~ Nafion membrane dryer was installed downstream the sample flow and further, using isokinetic flow splitters this flow was distributed among the various aerosol instruments. Data collection commenced from July 2016, and the data collected until May 2017 are used in this work.

Formatted: Not Highlight

Bhubaneswar experiences contrasting seasonal air masses linked with the Asian monsoon system (Asnani, 1993). In Figure 2, isentropic five-day air mass back trajectories arriving at 100 meters AGL at the sampling site are shown, which

were computed for all the individual days during: (a) summer monsoon (SMS) (June–September), (b) post-monsoon (PoMS) (October–November), (c) winter (December–February), (d) pre-monsoon (PMS) (March–May). It clearly reveals the dominance of the IGP outflow during the PoMS and winter season, while mixed (continental and marine/coastal) airmasses prevailed during the SMS; and predominantly coastal transit/marine air masses during the PMS. Thus, the examination of the seasonal characteristics will help in delineating the distinctiveness of the IGP airmasses and characterising various source, sink and transformation (aging) processes. While the contribution from fossil fuel sources will be less variant, the contribution from biomass burning sources varies seasonally. In supplementary Figure S1, spatial distribution of Moderate Resolution Imaging Spectroradiometer (MODIS) fire radiative power (MODIS Thermal Anomalies / Fire locations, Collection 6 product obtained from <https://earthdata.nasa.gov/firms>) for the representative months of different seasons; (a) August -2016 (SMS), (b) October -2016 (PoMS), (c) January -2017 (winter) and (d) May -2017 (PMS). ~~that were Figure S1, clearly depicts seasonally varying source contributions with the highest amount of fire events occurring all over the Indian region during the PMS, whereas during the PoMS (northwest IGP) and winter (western, north eastern regions of India) less intense regional fire events are noticeable. Figure S1 depicts the seasonal variation in the distribution of fires. The greatest number of fire events across the Indian region occur during the PMS. However, during other seasons, less intense fires are noticeable at the sub-regional scale, which are confined mostly to the northwest IGP during the PoMS, and to western, north-eastern regions during winter.~~

Table-1 depicts the seasonal average of several important meteorological parameters: temperature (T), relative humidity (RH), pressure (P) and wind speed (WS) along with maximum and minimum values recorded in that season measured using a collocated automatic weather station. ~~During SMS, the prevailing wind speed and temperature were moderate, and relative humidity (RH) was high (Table 1), while rainfall, associated with the monsoon, was extensive (total rainfall ~ 878 mm). Compared to the SMS, lower temperatures, winds and RH prevailed during the PoMS, with lower total rainfall (~ 201 mm). The lowest temperatures and RH of the year were seen during winter when calm wind conditions prevailed with almost no rainfall. The PMS witnessed the highest temperatures of the year (as high as 41 °C), moderately humid atmosphere and relatively higher wind speed compared to winter. During this season the region received a total rainfall of ~149 mm associated with thundershower events that led to high-velocity local winds. Details are given in Table 1. During SMS, high RH ($\sim 77.1 \pm 17.5\%$), moderate temperatures ($\sim 30.1 \pm 3.8\text{ }^\circ\text{C}$) and moderate wind speeds (up to max. 5.2 m s^{-1}) prevailed. Also, this season witnessed heavy rainfall (total rainfall ~ 878 mm) associated with the monsoon. Compared to the SMS, lower temperature ($\sim 28.3 \pm 6.3\text{ }^\circ\text{C}$), RH ($\sim 71.0 \pm 21.2\%$) and mean wind speeds ($\sim 1.07 \pm 0.67\text{ m s}^{-1}$) prevailed during the PoMS, with total rainfall (~ 201 mm) also being lower than during the SMS and temperature ranging from a minimum of $21\text{ }^\circ\text{C}$ to a maximum of $34\text{ }^\circ\text{C}$. During winter, lower temperatures (from a minimum of $18\text{ }^\circ\text{C}$ to a maximum of $36\text{ }^\circ\text{C}$) and dry weather (mean RH $57.4 \pm 22.9\%$) with calm wind conditions (mean wind speed $\sim 0.95 \pm 0.53\text{ m s}^{-1}$) prevailed with almost nil rainfall, whereas the PMS witnessed the highest temperature of the year (mean $\sim 33 \pm 7.5\text{ }^\circ\text{C}$ and range: $18.9\text{--}41\text{ }^\circ\text{C}$) with average wind speed $\sim 1.97 \pm 0.92\text{ m s}^{-1}$ and a moderately humid atmosphere (mean RH $\sim 67.1 \pm 28.2\%$),~~

Formatted: Not Highlight

Formatted: Not Highlight

Formatted: Not Highlight

Formatted: Not Highlight

Formatted: Font: (Default) +Headings (Times New Roman), 10 pt, Not Bold, Font color: Custom Color(19,20,19)

Formatted: Font: (Default) +Headings (Times New Roman), 10 pt, Not Bold, Font color: Custom Color(19,20,19)

Formatted: Not Highlight

~~During this season the region received a total rainfall of ~149 mm associated with thunder shower events that led to high high-velocity local winds.~~

The sampling period spanned from 27-July, 2016 to 22-May, 2017, representing all the seasons of the year, atmospheric conditions and distinct prevailing airmasses. The data has been collected continuously, except for brief gaps during calibration, system checks (flow rate, chamber temperatures, etc.) and preventive maintenance of the instruments or minor technical issues. ~~Only major gap in the data occurred during 11-November to 27-December, 2016, when measurements were paused due to logistical issues at the experimental site.~~

2.2 Instrumentation

In the present study, data ~~was/were~~ collected using a single-particle soot photometer (SP2) (~~Model: SP2-D; Make: Droplet~~ Measurement Technologies, Boulder, USA) and an Aerosol Chemical Speciation Monitor (ACSM) (~~Model: 140; Make: Aerodyne Research Inc., USA~~). ~~A scanning-mobility-particle-sizer (SMPS) (to measure particle-number-size-distributions) and a 7-channel Aethalometer were also operated, but they are not relevant to the present study.~~

The SP2 allows the characterization of the mixing state of refractive BC (rBC) of single particles by employing a laser-induced incandescence technique and obtaining the scattering properties based on excitation by a 1064 nm Nd:YAG intracavity laser (Moteki and Kondo, 2007; Schwarz 2013, 2008; Laborde et al., 2012; Liu et al., 2014; Shiraiwa 2007). It also provides information about the number/mass concentrations and size distribution of rBC. While the amplitude of the scattering signal provides the information about the optical size (D_p) of the particle, the amplitude of the incandescence signal is proportional to the mass of the rBC. The mass equivalent diameter, or BC core diameter (D_c), is defined as the diameter of a sphere containing the same mass of rBC as measured in the particle using a density, $\rho \sim 1.8 \text{ g cm}^{-3}$ for atmospheric BC (Bond and Bergstrom, 2006; Moteki and Kondo, 2010; Moteki et al., 2010; McMeeking et al., 2011). Additionally, the scattering signal from the BC containing particles provides information about the scattering cross-section of the particle. However, since the particle is subjected to intense thermal heating and evaporation of the coating while passing through the laser beam, the scattering signal gets perturbed. ~~This signal is reconstructed using the leading edge only (LEO) fitting technique which uses the leading edge of the unperturbed scattering signal before its volatilization (Liu et al., 2014) from which the full scattering signal is reconstructed. This signal is reconstructed using the leading edge only (LEO) fitting technique, which uses the leading edge of the unperturbed scattering signal before volatilization of the coating material becomes significant. This is used to reconstruct the full scattering signal (Liu et al., 2014). The reconstructed scattering signal and the BC core size (D_c) are used to derive the optical diameter of the BC particle or the coated BC size (D_p) by employing Mie calculations, where the whole particle is idealized as a two-component sphere with a concentric core-shell morphology. The scattering enhancement can be determine by using the BC core size (D_c) to derive the optical diameter of the BC core of the particle and the coated BC size (D_p) and employing Mie calculations where the whole particle is idealized as a two-component sphere with a concentric core-shell morphology.~~ In the present study, we have used a core (rBC)

Formatted: Not Highlight

Formatted: Not Highlight

Formatted: Not Highlight

Formatted: Subscript

Formatted: Subscript

refractive index value of $2.26 - 1.26i$ (Moteki et al., 2010; Liu et al., 2014; Taylor et al., 2014) and a coating refractive index of $1.5+0i$, which is representative of the corresponding values determined for inorganic salts (e.g., ammonium sulphate) and secondary organic aerosol (Schnaiter et al., 2005; Lambe et al., 2013). To quantify the extent of coating on the BC particle, relative coating thickness (RCT) and absolute coating thickness (ACT), defined as D_p/D_c and $(D_p-D_c)/2$ respectively, were used. These are calculated as the total volume of coated BC particles divided by the total volume of the rBC cores in a given time window (5 minutes) following Liu et al., (2014), which has been used by subsequent studies (Liu et al., 2019, Brooks et al., 2019a). It may be noted that the RCT and ACT used in this study come from derived parameters that require Mie calculations based on a core-shell model that may not bear relation to reality, and the RCT (and ACT) is not an actual ratio of diameters. The coating thickness for individual particles is dependent on core sizes. However, we have used the volume-weighted bulk RCT and ACT as representative diagnostics for the overall mixing state of the whole population of BC particles (Gong et al., 2016; Cheng et al., 2018; Liu et al., 2019). As described by Liu et al., (2019), since the contribution from smaller particles to the integrated volume is very less, the bulk coating thickness values are generally independent of the uncertainties arising due to the presence of smaller particles. Further, the information on the morphology of the BC, which would be different for fresh and aged emissions, is not available in this study. The important caveat here is that we assume the morphology of the particles; they are spherical and coating is uniform (coated particle also is spherical). The RCT (and ACT) parameter provides a qualitative measure of the amount of condensed material that is present on the same particle as the rBC core. We are using this to examine the extent of rBC mixing with other components in different seasons and compared to different regions. Further, using correlations with the bulk NR-PM1.0 composition, we intend obtain some insights into the coating material associated with rBC in different periods. Liu et al., (2010, 2014) have described the configuration, operation, data interpretation procedures and uncertainties of this specific instrument in detail. Taylor et al. (2014) described the methodology to determine the D_p/D_c in detail and examined the sensitivity of the derived parameters to the density and refractive index values. The SP2 was operated at a flow rate of $80 \text{ cm}^3 \text{ min}^{-1}$ ($0.08 \text{ litres min}^{-1}$) and was periodically calibrated. Aquadag® black carbon particle standards (Aqueous Deflocculated Acheson Graphite, manufactured by Acheson Inc., USA) were used for the calibration of the SP2. However, as Aquadag®-generated particle standards do not represent ambient BC, a correction factor of 0.75 is incorporated (e.g., Moteki and Kondo 2010; Laborde et al., 2012). Recently, Sedlacek III et al. (2018) have cautioned that rBC may be produced by laser-induced charring of organic substances in the SP2, which depends on the laser power. Such laser-induced charring could result in an overestimate of rBC. During our measurements, the laser power varied in the range 2.1-3.7 V, which is above the threshold to detect rBC with high efficiency ($> 2V$) (Sedlacek III et al., 2018). Though we cannot rule out an additional rBC contribution from charring of organic matter, it is likely this occurs in circumstances when the laser voltage is higher than that used in our study. Further, Sedlacek III et al. (2012) examined the structure of rBC containing particles using the 'lag time' technique and suggested that the core-shell model does not apply to all rBC -containing particles. A situation with non-core-shell structure (the case when BC is located off-center) arising due to the complex mixing state of BC may lead to uncertainty in determining the coating thickness of BC. Our study assumes BC to be at the centre and a uniform coating around, in the absence of other

Formatted: Not Highlight

Formatted: Not Highlight

5 measurements to understand the complex coating. A recent study by Liu et al., (2017) demonstrated good agreement between Mie-modelled scattering values using the core-shell approximation and the SP2-measured scattering cross-section for the BC with thicker coatings as is the case for the majority of particles in this study. In addition, further the particle scattering is relatively independent of particle morphology at the SP2 wavelength 1064nm (Moteki et al., 2010). The SP2 was operated at a flow rate of $80 \text{ cm}^3 \text{ min}^{-1}$ ($0.08 \text{ litres min}^{-1}$) and was periodically calibrated. Aquadag® black carbon particle standards (Aqueous Deflocculated Acheson Graphite, manufactured by Acheson Inc., USA) were used for the calibration of the SP2. However, as Aquadag®-generated particle standards do not represent ambient BC, a correction factor of 0.75 is incorporated (e.g., Moteki and Kondo 2010; Laborde et al., 2012).

10 Real-time characterization of the non-refractory PM1.0 aerosol mass and composition was carried out using an the ACSM (Ng et al., 2011). The ACSM was operated with 30 minutes sampling interval alongside the SP2. The ACSM uses quadrupole mass spectrometry to chemically characterize the submicron (vacuum aerodynamic diameter ~ 40-1000 nm range) particulate composition of the organic, sulphate, nitrate, ammonium and chloride components. Initially, the particles are focused on to a resistively heated thermal vaporizer operating at 600 °C using an aerodynamic particle focusing lens in a high vacuum environment. The evaporated gas stream from the particle evaporation is detected after ionization via electron impact by the mass spectrometer. The mass spectra are used to extract chemical composition information. ~~The differential pumping required for the separation of gas from the particle beams is achieved by employing three turbo molecular pumps along with a main diaphragm pump.~~ From a the main flow rate of 3 litres min^{-1} , the ACSM draws a sample flow of 0.1 litres min^{-1} using a 100 μm diameter critical aperture. The instrument is periodically calibrated, and all the corrections described in Ng et al., (2011) were applied during the data post-processing. A real-time and ~~composition-composition~~-dependent collection efficiency (CE) correction based on Middlebrook et al. (2012) was applied to account for the uncertainties arising due to the usage of a standard vaporizer.

3. Results and Discussion

3.1 BC mass and number concentrations

25 Temporal variation of daily mean mass concentration of BC, and number concentrations of BC and non-BC scattering particles (individual data points are available with 5 min time resolution) are shown respectively in Figure 3(a) and Figure 3(b). Number concentrations of BC and scattering particles peak in winter, while they are the lowest in PMS with moderate values through PoMS. The overall annual mean number concentrations (and their standard deviation) of rBC and non-BC particles (that are in the detection range of the SP2 (200-400 nm) only) are $\sim 496 (\pm 536) \text{ cm}^{-3}$ and $702 (\pm 458) \text{ cm}^{-3}$ respectively, suggesting a large variability (and a skewed distribution) and the median values of rBC and non-BC particles are 333 cm^{-3} and 595 cm^{-3} respectively.

Formatted: Not Highlight

Formatted: Not Highlight

Formatted: Font: (Default) +Body (Times New Roman), English (United States)

Formatted: Indent: First line: 1.27 cm

Formatted: Font: 10 pt

Formatted: Not Highlight

Formatted: Not Highlight

Formatted: Font: (Default) +Headings (Times New Roman), 10 pt

Similarly, the BC mass concentration also showed significant temporal variation with high values during winter and low values during PMS. During SMS the daily mean mass concentration ranged between $0.3071-0.2581-26 \mu\text{g m}^{-3}$ with a seasonal mean $\sim 1.23 \pm 1.03 \mu\text{g m}^{-3}$, and during PoMS the seasonal mean was $\sim 1.338-34 \pm 1.40396 \mu\text{g m}^{-3}$ with daily mean values varying between $0.36357-2.8769 \mu\text{g m}^{-3}$. Winter witnessed enhanced BC mass concentrations with daily mean values ranging between $0.281-3.680 \mu\text{g m}^{-3}$ and a seasonal mean of $\sim 1.9354 \pm 1.578 \mu\text{g m}^{-3}$, whereas the lowest concentrations were found during PMS with daily mean values varying between $0.052-3.074 \mu\text{g m}^{-3}$ and a seasonal mean of $\sim 0.93 \pm 0.99 \mu\text{g m}^{-3}$. Lower values during SMS may be attributed to wide-spread precipitation across the region and decreased source strength during rainy periods. Conversely, the decrease in rainfall, prevailing calm wind conditions, coupled with ~~decreased-reduced~~ ventilation due to the shallow boundary layer as a result of prevailing lower temperatures, contributed to the build-up of aerosols during PoMS, which continued and was further enhanced during winter. During PMS, strong thermal convection resulting from ~~enhanced-increased~~ solar heating of the dry land lifts the boundary layer to higher altitudes, and with winds gaining speed, there is greater dispersion of the aerosols (Kompalli et al., 2014) leading to a substantial reduction in the surface concentrations. The annual mean rBC mass concentration is $1.340 \pm 1.322 \mu\text{g m}^{-3}$. In an earlier experiment during winter at Kanpur, a polluted urban area in the central IGP, Thamban et al., (2017) have reported rBC mass concentration in the range ~ 0.73 to $17.05 \mu\text{g m}^{-3}$ with a mean (\pm standard deviation) $\sim 4.06 \pm 2.46 \mu\text{g m}^{-3}$ which is about twice as high as we have seen at Bhubaneswar at the eastern fringe of the IGP. In a short experimental campaign during pre-monsoon season 2014, Raatikainen et al., (2017) have reported average rBC mass concentrations of $11 \pm 11 \mu\text{g m}^{-3}$ for Gual Pahari (an IGP site close to Delhi) and $1.0 \pm 0.6 \mu\text{g m}^{-3}$ for the high-altitude site Mukteshwar, in the foot-hills of the central Himalayas. The significantly higher values seen over the central IGP stations ~~awere~~ attributed to the proximity of local emissions. However, our values at Bhubaneswar are comparable to the mean rBC values reported by Liu et al., (2014) over London ($\sim 1.3 \mu\text{g m}^{-3}$) and higher than the values over Paris city ($\sim 0.9 \mu\text{g m}^{-3}$, Laborde et al., 2013); but are significantly lower than those reported over ~~several~~ Chinese cities, Beijing ($\sim 5.5 \mu\text{g m}^{-3}$, Wu et al., 2016), Shanghai ($\sim 3.2 \mu\text{g m}^{-3}$, Gong et al., 2016), Shenzhen ($\sim 4.1 \mu\text{g m}^{-3}$, Huang et al., 2012), Kaiping ($\sim 3.3 \mu\text{g m}^{-3}$, Huang et al., 2011). Our values are higher than the values reported by Wang et al., (2018) over a remote site in the southern Tibetan Plateau ($\sim 0.31 \pm 0.35 \mu\text{g m}^{-3}$).

3.2 Seasonal distinctiveness of BC size distribution and modal parameters

The size distribution of BC cores is one of the ~~important-critical~~ factors while determining light absorption characteristics of the aerosols and direct radiative forcing (Reddington et al., 2013). Knowing BC size distribution (in addition to its coating information) is also ~~important-vital~~ to understand BC life cycle, as BC from different sources would have different sizes and different scavenging mechanisms display different size and ~~composition-composition~~-dependent efficiencies which can ~~effect~~ ~~affect~~ BC aging process. In the present study, modal parameters (mass median diameter (MMD) and ~~count-number~~ median

Formatted: Not Highlight

Formatted: Not Highlight

Formatted: Not Highlight

Formatted: Not Highlight

Formatted: Not Highlight

Formatted: Not Highlight

Formatted: Not Highlight

Formatted: Not Highlight

Formatted: Not Highlight

Formatted: Not Highlight

Formatted: Not Highlight

diameter (~~CMD-NMD~~) were determined for each of the BC size distributions by representing them using mono-modal ~~log~~ ~~log-normal~~ fit (e.g., Shiraiwa et al., 2007; Schwarz et al., 2008; Liu et al., 2010; Wang et al., 2016) of the following form:

$$\frac{dA}{d \ln D_p} = \sum \frac{A_0}{\sqrt{2\pi} \ln \sigma_m} \exp \left[-\frac{(\ln D_p - \ln D_m)^2}{2 \ln \sigma_m} \right] \quad (1)$$

Here A_0 corresponds to mass/number concentration of the mode, D_m is the mass/~~count-number~~ median diameter, D_p is particle diameter, ~~A is mass/number concentrations,~~ and σ_m is the geometric standard deviation. A typical mass and number size distribution and corresponding modal fit are shown in Figure 4(a), and the temporal variations of daily mean MMD (~~CMD-NMD~~) values derived from individual size distributions are shown in Figure 4(b) and Figure 4(c). Here each symbol represents the mean value for the day and the vertical line passing through it is the corresponding standard deviation. The solid continuous line shows the 30-day smoothed variation and the dotted vertical lines separate different seasons. Both, MMD and ~~CMD-NMD~~, gradually increase from their respective minimum values during the summer monsoon season (SMS) through ~~post-post~~-monsoon and winter season to reach the highest values during the pre-monsoon season, indicating the progressively dominating share of larger particles in the size distribution. Further, the seasonal mean mass and number size distributions ~~are~~-shown in ~~supplementary Figure-figure 5-S2 (along with the relevant discussion) highlighting-highlighteds~~ the changes in the BC microphysical properties (abundance and sizes) with changes in the source processes along with seasonal transformation.

~~These size distributions were parameterized by using least-squares fitting to an analytical mono-modal log-normal distribution. These size distributions were parameterized by evolving least-squares fitting to mono-modal log-normal distribution.~~ These modal parameters estimated for different seasons were tabulated in ~~Supplementary Table-21~~.

Previous studies suggested that different sources emit BC particles with ~~different core diameters~~varying diameters of core, where smaller modes indicate urban outflow with dominance of fossil fuel sources, and larger modes ($>0.20 \mu\text{m}$) are more likely to be associated with solid-fuel sources including biomass/coal burning (Schwarz et al., 2008; Liu et al., 2010, 2014; Sahu et al., 2012; Reddington et al., 2013).

Viewed in the light of the above, the lowest seasonal mean MMD $\sim 0.169 \pm 0.013 \mu\text{m}$ (~~CMD-NMD~~ $\sim 0.090 \pm 0.005 \mu\text{m}$), occurring during SMS, highlights the possible dominance of fresh emissions containing smaller sized particles (and/or externally mixed particles), when washout also is quite significant. As the season advances, MMD and ~~CMD-NMD~~ increase, due to ~~aging~~ processes (including ~~the~~ coagulation of the agglomerates), as the removal mechanism is weakened (significantly low precipitation) during these seasons. The modal values during the ~~post-post~~-monsoon and winter seasons (MMD $\sim 0.182 \pm 0.012$; $\sim 0.193 \pm 0.017 \mu\text{m}$ and ~~CMD-NMD~~ $\sim 0.100 \pm 0.006$; $\sim 0.111 \pm 0.006 \mu\text{m}$ respectively) are comparable with those ~~reported for~~-reported from the continental outflows (McMeeking et al., 2010, 2011; Ueda et al., 2016) suggesting mixed sources and/or aged BC. By the pre-monsoon season, the MMD values reached beyond $0.20 \mu\text{m}$ and

Formatted: Right: 0 cm

continued to remain so throughout PMS highlighting the dominance of larger core BC particles (likely solid fuel, e.g., coal/biomass burning emissions). These seasonally changing size distributions (and MMD values) reflect the combined effect of the nature of sources, the efficiency of sink and role of transport. It is difficult-challenging to delineate local sources from those in far-far-field regions that transport BC to the receptor sites. While the smaller MMD during the SMS suggests the effective wet removal of larger sized BC particles, while-whereas weaker wet removal in the other seasons led to larger MMD values. As evident from the supplementary figure S1, intense-extreme fire events that occur over the Indian region, and this combined with enhanced boundary layer heights (due to increased temperatures) enabling effective dispersion of pollutants, both horizontally and vertically, is responsible for larger BC cores observed during the PMS.

Table 2 and Figure 5(a) also suggested similar conclusions. The modal diameters changed from lowest values (~0.165 μm) during SMS to the highest value (~0.214 μm) in the PMS through the seasons PoMS (~0.178 μm) and winter (~0.191 μm), signifying the changing source and atmospheric dynamical processes and that size distributions progressively developed towards larger sized BC particle dominance from SMS to PMS. The peak concentrations suggested the highest mass loading in winter ($M_0 \sim 4679 \text{ ng m}^{-3}$), followed by PoMS ($M_0 \sim 2752 \text{ ng m}^{-3}$) and SMS ($M_0 \sim 2225 \text{ ng m}^{-3}$), whereas the lowest loading was seen PMS ($M_0 \sim 2031 \text{ ng m}^{-3}$).

The size distribution during SMS is slightly skewed towards lower size regime and resulted in a broad width (standard deviation (σ_w) ~1.99), and as the seasons progress towards PMS such skewness (or lack of it as indicated by decreased σ_w values) progressively shifted towards larger size ranges in addition, in addition to drop in smaller sized particle concentrations due to the changes in the nature of sources. These values also indicate the other atmospheric dynamical processes that control the BC life cycle apart from the source and sink as described above. Extended rainfall reduces the overall mass loading due to wet scavenging in SMS and partly in PoMS, smaller BC particles prevailed while larger particles are more prone to being scavenged. Lack of wet removal mechanism in dry seasons (winter and PMS) resulted in an extended life time of BC, resulting in a greater higher atmospheric life time. Also, seasonally varying boundary layer dynamics determines the extent of the near near-surface aerosol loading (this aspect is discussed in a later section).

Similar to the mass size distributions, examination of the modes of the number size distribution in different seasons suggested smaller size particles (mode ~0.080 μm) during SMS which progressively increased towards larger core BC particles with season from PMS (~0.130 μm) through PoMS (~0.099 μm) and winter (~0.112 μm) with broader widths, highlighting seasonal changes in the nature of dominant sources. But mean BC number size distributions showed a slightly different picture when mode peak values were considered. The largest modal number concentration is seen during SMS ($N_0 \sim 1502 \text{ cm}^{-3}$) (albeit lower mode diameter suggesting the smaller particle dominance possibly of regional origin due to the extended precipitation causing below cloud scavenging restricting the abundance and life time of larger particles), followed by winter ($N_0 \sim 1270 \text{ cm}^{-3}$) and PoMS ($N_0 \sim 1219 \text{ cm}^{-3}$). PMS showed the lowest peak number abundance ($N_0 \sim 407 \text{ cm}^{-3}$).

A summary of MMD values reported in the literature with different emission sources and atmospheric conditions along with the present values is made in Table-32. Several earlier publications reported a range of MMD values (0.100-0.170 μm) for urban regions with near-near-source fossil fuel emissions (McMeeking et al., 2010; Liu et al., 2014; Laborde et al., 2013;

Formatted: Not Highlight

Cappa et al., 2012; Kondo et al., 2011; Cheng et al., 2018), whereas, urban/continental outflows depict MMDs in the range of 0.140–0.180 μm (Shiraiwa et al., 2007; Wang et al., 2018). The MMD values are $\sim 0.211 \pm 0.014 \mu\text{m}$ for fresh biofuel/crop residue sources (Raatikainen et al., 2017), and in the range $\sim 0.220\text{--}0.240 \mu\text{m}$ for aged BC from biomass burning sources (Liu et al., 2010) or high urban pollution episodes with high biomass burning (Gong et al., 2016). Table-3-2 highlights that MMD values depend strongly on the nature of BC sources-processes and reiterate that present values depict seasonally changing sources, from fossil fuel dominance in SMS to solid fuel (biomass or coal burning) dominance in PMS through mixed sources typical for outflow during PoMS and winter.

3.3 Seasonal changes in mixing state of BC

The mixing state of BC depends on several parameters such as concentration of condensable species that adsorb or condense on to the BC core, atmospheric humidity, the atmospheric lifetime of BC cores (including photochemical aging) and the size distributions (Liu et al., 2013; Ueda et al., 2016; Cheng et al., 2018). As the source strengths of condensable species are likely to vary with season (due to seasonality of local emissions, prevailing meteorology and long-range transport) the mixing state of BC would respond to such changes. With a view to examining this, we have quantified the mixing state of BC in terms of (a) the volume weighted bulk relative coating thickness ($\text{RCT} \sim D_p/D_c$) and (b) absolute coating thickness ($\text{ACT} \sim (D_p - D_c)/2$), where D_p and D_c respectively represent the particle diameter and the core diameter. Both these parameters (RCT and ACT) have been determined from BC mass equivalent diameters which that depend only on the emission source characteristics and not on the morphology or mixing state of the particles (Liu et al., 2014; 2019; Brooks et al., 2019a). They help to evaluate the changes in physiochemical properties of BC during its atmospheric transit life-time. While RCT quantifies the extent of coating on a BC core, ACT provides the magnitude of coating in nm. The temporal variation of daily mean values of RCT (half circles) and ACT (star symbol) are shown in Figure 6, where the solid line represents the 30-day running-mean smoothed variation revealing the seasonality.

The figure shows strong seasonality in the coating on BC owing to the effects of the multiple processes discussed above. Both relative and absolute coating thicknesses are very low during the monsoon season; and increase gradually towards winter through the post-post-monsoon (though the increase is not fully-entirely depicted due to a gap in the data). Further, the values slightly dropped during February-March (seasonal transformation from winter to PMS) and further-also increased again towards summer. The low values of RCT and ACT during SMS (seasonal mean $\text{RCT} \sim 1.16 \pm 0.04$ and $\text{ACT} \sim 12.12 \pm 4.98 \text{ nm}$) indicate thin coating on freshly emitted small BC cores. This is attributed to (a) the short life-time of BC in this season due to their efficient washout by the wide-spread monsoon rainfall, (b) and the lower concentration of condensable gas-gas-phase precursors caused by this wet removal, and (c) South-westerly/westerly air masses prevailed during this period which advect cleaner marine air. Thus, so that the the cores are basically of nascent BC particles, which emanated from fossil fuel emissions, and have (as indicated by the least-lower mass/ number median diameters seen in supplementary Figure 5S2, black line) with lesser coated cores prevailed during the SMS. As the season advances to PoMS, the monsoon

activity is subdued leading to an increased lifetime of BC, and a change in air mass (Figure 2b) results in the advection of different types of aerosols and gaseous species from the more polluted north-western IGP (rather than the predominantly oceanic nature of the air mass in SMS). The air mass is drier than during monsoon. The particle size distribution shows the increased presence of larger particles, and consequently higher median diameters (Figure S2, red lines) indicating a change in the nature of sources. All these resulted in an increase in the overall coating during PoMS with seasonal mean values of 1.32 ± 0.14 for RCT and 28.74 ± 12.31 nm for ACT highlighting an enhancement of $\sim 32\%$ of the particle sizes due to thick coating of condensable vapours on BC cores during this season. Intra-seasonal variability (as highlighted by the wide range of frequency of occurrence of RCT and ACT values during the PoMS seen in the supplementary figure S3) is also higher during the PoMS~~intra-seasonal variability (highlighted by the standard deviation of the seasonal mean values of RCT and ACT noted in Figure 65) is also higher during PoMS.~~ During winter, in general, the RCT values are higher (mean RCT $\sim 1.34 \pm 0.12$) the extent of absolute coating on the cores is also highest (mean ACT $\sim 33.51 \pm 11.76$ nm) suggesting thickly coated BC particles. This~~It~~ is attributed to the availability of condensable vapours advected by the continental air masses (Figure 2c) and the longer residence time of BC and the larger mode diameters (Figure 4 and blue line in supplementary figure S2, blue line). In winter, the air mass pathways originated from the highly polluted IGP region prevail over Bhubaneswar with an abundance of condensable species. The combination of prevailing calm weather conditions and absence of precipitation enhanced the life of aerosols and thus resulted in thickly coated BC aerosols. As the season changes to summer/ pre-monsoon, the RCT decreased (mean RCT $\sim 1.26 \pm 0.10$) because of the larger BC cores (highest MMD values, Figure 4 and green line in Figure S2) while the absolute coating thickness ~~remains~~remained high (mean $\sim 27.41 \pm 10.72$ nm). This ~~occurred~~is as a result of the relative increase in larger particles, which for the same RCT would lead to higher ACT.

The seasonality of the coating characteristics; ~~discussed above,~~ is further demonstrated in the supplementary Figure S3 and described in relevant discussion in the supplementary information, Figure 7, which shows the frequency distribution of the RCT and ACT values for each season (median values for each season are also shown in the figure). The monsoon season was characterised by a narrow distribution, with the lowest median values for both RCT and ACT. Such thin coatings were seen due to the reduced life-time and absence of multiple processes which include: (a) decreased atmospheric life-time, leading to not having enough time to get thickly coated (as coating thickness depends on the particle life-time also), (b) lowered concentration of advected anthropogenic precursor species, making lesser availability of coating material, and (c) fast wet-removal (of the core and the coating material) by extensive rainfall. South westerly/westerly air masses prevailed during this period which advect cleaner marine air to the site, while wash-out due to large-scale precipitation removed aged aerosols. During other seasons, the distributions are quite broad, and showed multiple maxima (especially during PoMS and winter). During these seasons, BC particles in the IGP outflow are characterised by extensive coating resulting from the enormous shift in the air mass from marine to continental at the end of the monsoon season bringing air from the most polluted central IGP, added with the associated change in the size distribution and residence time. Based on their study during a heavy air pollution episode in Shanghai, Gong et al., (2016) have reported instantaneous ACT values ranging between 50-300 nm in

different number size regimes with distinct sources and aging process of BC. Such high magnitudes of ACT are possible in the extremely polluted airmasses in the near the immediate vicinity of sources. ~~Coating. The coating~~ on BC particles enlarges the available absorption cross-section and results in absorption enhancement. Moffet and Prather (2009) have examined the sensitivity of optical properties to the microphysical properties of BC; and found absorption enhancement in the ranges from 1 (for no coating) to 3.4 (for largest particle sizes). ~~They reported and further, larger more substantial~~ absorption enhancements (1.6) for larger shell/core ratios (RCT ~1.75) obtained for the aged BC, ~~which~~ compared to ~~those for~~ fresh BC (absorption enhancement of 1.4 and RCT ~1.07). Direct comparison of the coating parameters (RCT and ACT) in the present study with other studies is not possible. This is because of the difficulties in comparison across studies as detailed by Cheng et al., (2018), which include different system configurations, ~~the~~ difference in techniques used in ~~the~~ fitting of scattering amplitudes and the range of mass equivalent diameters.

3.4 Diurnal variations of rBC mass concentration and RCT

At the shorter times scales (within a day), the mesoscale processes and atmospheric boundary layer (ABL) dynamics would be influential in modulating the mixing characteristics of BC (for example, Liu et al., 2014; Laborde et al., 2013). ~~To examine this, the~~ seasonal mean diurnal variations of BC mass concentration (red-star symbol) and relative coating thickness (RCT) (blue-filled circle) ~~are~~ shown in Figure 8-6 ~~reflect these processes~~. The vertical lines in each panel ~~in the figure~~ mark the local sunrise and sunset times for the season.

~~The figure reveals, in addition to the typical double-humped diurnal variation of BC mass concentration due to the well-known combined effects of boundary layer dynamics (Kompalli et al., 2014) and diurnal variation of the anthropogenic activities, very interesting links between BC core and relative coating thickness. In addition to the typical double-humped diurnal variation of BC mass concentration, which arises due to the combined effects of atmospheric boundary layer (ABL) dynamics (Kompalli et al., 2014) and diurnal variation of the anthropogenic activities, very interesting links between BC core and relative coating thickness are noticeable from the figure. While BC and RCT depict the double-humped diurnal variation, they are were almost in the opposite sense, and the amplitude of the variation has showed a marked seasonality. The amplitude of the BC variation has a marked seasonality. It is caused by the seasonal change in the diurnal variation of the ABL driven by seasonal changes in surface heating and resulting thermal convection. The highest amplitude occurs in winter since the diurnal variation of the ABL is greatest due to the high variation in surface temperature; with ΔT (i.e. $T_{\max} - T_{\min}$) ~ 12 °C over a 24 hour period (here where T_{\max} and T_{\min} are maximum and minimum temperatures). Conversely, the lowest amplitude occurs during the monsoon season, when thermal convection is highly suppressed due to the overcast sky, low surface heating and the surface energy balance being dominated by latent heat (the average diurnal amplitude of temperature variation, $\Delta T \sim 4.9$ °C), with The highest amplitude was seen in winter (when the day-night temperature variation is the highest; with ΔT (i.e. $T_{\max} - T_{\min}$) ~ 12 °C where T_{\max} and T_{\min} are maximum and minimum temperatures over the 24-hour period) and lowest amplitude was noticed during the monsoon (when the temperature variation is the least; $\Delta T \sim 4.9$ °C). The~~

Formatted: Font: (Default) +Headings (Times New Roman), 10 pt, Not Bold

Formatted: Font: (Default) +Headings (Times New Roman), 10 pt, Not Bold

diurnal variation in BC mass concentrations and the factors determining it over the Indian region have been widely reported (e.g., Beegum et al., 2009; Mahapatra et al., 2013a; Kompalli et al., 2014), the diurnal pattern of the BC mixing state has not been previously observed. More intriguing is the sense of variation opposite to that of BC; with peaks occurring around 02:00 to 04:00 hrs and 12:00 to 15:00 hrs local time with troughs in between.

5 As previously discussed, the increased RCT values are associated with aging of BC cores and availability of condensable vapours (which are generally co-emitted with BC or produced photochemically from species that are co-emitted). As a result, the peak in RCT during daytime can be attributed to the abundance of condensable material originating due to photochemistry and thus gas-phase photochemical processing leading to enhancement in the extent of coating (Liu et al., 2014; Chakraborty et al., 2018; Brooks et al., 2018, 2019b). The second peak occurring during late night- early morning
10 periods is more likely to be linked to the increased aging of BC, (lack of fresh emissions on the one hand and reduced condensation sink due to decrease in concentration of pre-existing foreign particles that compete with BC to adsorb condensable vapours (e.g., Babu et al., 2016 and references therein) on the other). The amplitude of the day time peak in RCT is greater than or equal to the early morning (dawn) peak due to two factors: (a) enhanced dispersion during day time due to increased convective mixing results in reduced particle abundance, thus increasing the probability of enhanced vapour adsorption on individual particles, (b) day time build-up of possible coating material due to photochemistry (which is a stronger factor than the first one), and both these conducive conditions are not available during early morning. ACT also showed a similar pattern to RCT but much a more pronounced diurnal variation, whereas there is no discernible variation in the diurnal pattern of MMD (supplementary Figure S2S4).

The morning peak in BC mass concentration, occurring shortly after sunrise is due to the well-known ‘fumigation effect’, i.e., when the thermals generated after the sunrise break the inversion and bring down the pollutants from the residual layer, as has been discussed in several papers (Beegum et al., 2009; Kompalli et al., 2014; Babu et al., 2016). Also, rush hour concentration due to the build-up of vehicular traffic ~~also~~ contributes to this. The succeeding trough is due to enhanced convective mixing and deepening of the ABL. After the sunset as the thermals subside, the shallow nocturnal boundary layer sets in and the resulting stable conditions lead to the second peak due to confinement of the aerosols near to the surface.
25 Further, lower temperatures and wind speeds coupled with reduced emissions result in a gradual decrease in BC mass concentration leading to a night time minimum.

~~Interestingly, during the morning period when the BC mass concentration peaks due to the combined effect of the boundary layer dynamics (fumigation effect) and sources (rush hour traffic contribution), RCT was at a minimum. This suggests that fresh emissions from rush hour traffic, which would push up the BC concentration and lower the RCT, outweigh the fumigation effect; though both may be occurring around the same period. Interestingly when the morning peak in BC mass concentration was observed due to the combined effect of the boundary layer dynamics (fumigation effect) and sources (rush hour traffic contribution), RCT showed a minimum. It suggests that the rush hour traffic source which would push up the BC concentration and lower the RCT outweighs the fumigation effect though both the processes may be occurring go occurring.~~ The diurnal variation is more pronounced during the PoMS and winter (Fig. S6b,c) and subdued

Formatted: Not Highlight

Formatted: Not Highlight

Formatted: Not Highlight

Formatted: Not Highlight

Formatted: Not Highlight

Formatted: Not Highlight

during the SMS and the PMS (Fig 8a-6a and 8d6d) owing to varying strength of ventilation of aerosols due to changes in the atmospheric boundary layer dynamics in different seasons (Kompalli et al., 2014). Similarly, the amplitude in the diurnal variation of RCT is highest in the PoMS (RCT changing from 1.42 to 1.25), followed by winter and largely-mostly subdued during the SMS and PMS. The diurnal variations in RCT are suppressed in the SMS and PMS compared to the winter and PoMS due to the seasonality of the boundary layer dynamics that modulates the concentrations of BC and the other condensing species. In addition to this, the wet scavenging by intense rains during the SMS ensures that a greater proportion of the remaining BC in the atmosphere is likely to be freshly emitted. Such extensive precipitation also leads to a reduction in concentrations of the coating substances. During the PMS, BC particles generally have larger core sizes, and the relative coating thickness is reduced in magnitude. These effects also play a role in shaping up the diurnal pattern. Not only are diurnal variations in RCT suppressed in the SMS and PMS compared to the winter and PoMS due to differences in boundary layer dynamics, in SMS less aged BC and enhanced precipitation removing coating substances and in the PMS the prevailing larger BC core sizes reducing the relative coating thickness may also play a role.

3.5 Non-refractive PM1.0 mass concentrations

To examine-identify the likely coating material on BC cores, mass concentration and chemical composition of non-refractive PM1.0 (NR-PM1) aerosols obtained from the measurements of the ACSM are examined.

The seasonal mean mass concentrations and fractional contribution of different species (organics, sulphate, nitrate, ammonium, and chloride), as deduced from the ACSM measurements are shown in Figure 97. There are-is a clear seasonal changes in chemical composition associated with distinct airmasses and a wide variety of sources. While-as expectedExpectedly, the mass concentration was highest during winter ($20.45 \pm 22.55 \mu\text{g m}^{-3}$) followed by PoMS ($13.90 \pm 10.62 \mu\text{g m}^{-3}$) (due to the combined effects of reduced removal, confinement of aerosols near surface due to shallow boundary layer and change in characteristics of long-range transport.), Examination of the mass fraction (MF) values revealed that organics (0.39-0.49), were showed a dominant contribution of species, -organics (0.39-0.49), with the highest fraction in winter (0.49). Sulphate, the next major contributor (MF varied in the range 0.27 to 0.47) showed strong seasonality, being highest in the PMS (0.47) followed by the SMS (0.41), and lowest in winter (0.27) and PoMS (0.28). If This is further corroborated by the airborne Aerosol Mass Spectrometer (AMS) measurements during SWAAMI (Brooks et al., 20182019b), which have shown significant presence of sulphate in the Central IGP extending to higher altitudes even during the monsoon season. Ammonium, nitrate and chloride are only minor components of the NR-PM1 mass loading. The significant presence of nitrate during the PoMS and winter (14%) suggest advection of anthropogenic emissions from the central IGP likely as a result of enhanced ammonia emissions during the growing season and cooler-colder temperatures, favouring NH_4NO_3 formation.

It is clear that when the IGP air masses prevailed (PoMS and winter) organics dominated the NR-PM1 mass concentration, while during mixed/coastal air masses (SMS and PMS) sulphate also equally or prominently contributed to

NR-PM1 mass concentration, clearly depicting seasonal contrast in the mass concentrations with the changing nature of sources in distinct airmasses.

Earlier studies (e.g. Kumar et al., 2016; Thamban et al., 2017; Chakraborty et al., 2018 and references therein) have examined the NR-PM1 chemical composition over Kanpur, an urban location in the central IGP, using an aerosol mass spectrometer (AMS) and reported the dominance of organics during PoMS and winter. Pandey et al. (2014) developed a multi-pollutant emission inventory for different sectors of India and reported that residential biomass burning (cooking stoves) is the ~~largest-most significant~~ contributor for PM2.5 and organic carbon aerosols. Recently from the molecular analysis of the PM2.5 emissions over a village in the IGP, Fleming et al., (2018) have ~~eharacterized-characterised~~ a wide range of ~~partiele-particle~~-phase compounds produced by traditional cook-stoves and pointed out various organic compounds originate from these sources. Viewed in this context, ~~the~~ dominance of organics in the IGP outflow is not surprising. From their filter based chemical composition measurements over Bhubaneswar, Mahapatra et al., (2013b) have suggested that the sources of SO₄²⁻ were anthropogenic, crustal and marine, with the major contributor being the anthropogenic sources. So sulphate is possibly of mixed origin and present in significant proportions, more so during non-IGP airmass periods (SMS and PMS).

3.6 ~~Association between rBC relative coating thickness and NR-PM1 chemical species~~ ~~Diurnal variations of NR-PM1 species and association with BC mixing state~~

~~In this section we examine the association between BC mixing state and NR-PM1 chemical species in diurnal and seasonal scales.~~ It is worthwhile to examine the diurnal pattern of NR-PM1 species which will act as coating substances and understand any possible association with that of RCT. ~~In order-t~~To evaluate this in terms of the relative magnitude of each species, hourly averaged mass fractions of organics, sulphate, nitrate, ammonium and chloride aerosols are considered, and the seasonal mean diurnal variation of these ~~species-arejs~~ shown in Figure ~~408~~. It is ~~clearly-seen that~~; sulphate dominated during the daytime in the PoMS, winter and the PMS, with a diurnal variation that resembled that of the RCT (Figure ~~86~~) during these seasons. The diurnal variation indicates strong photo-chemical production of sulphate from gas-phase chemistry. The weak nature of the day time peak in sulphate during the PMS may be attributed to enhanced dispersion resulting in lower ~~near-near~~-surface concentrations which overcomes photochemical production. The organics dominated during the night, which is due to a combination of factors including source processes and photochemistry, and its diurnal variation is almost opposite to that of the RCT. The diurnal variations of organics depict two pronounced peaks occurring during ~~the~~ morning (06:00-08:00 hrs) and late evening (20:00-22:00 hrs), similar to the rBC mass loading.

The diurnal pattern of other species (nitrate, ammonium and chloride, whose concentrations were lower except in winter) followed a pattern similar to organics, but with less variation. Absence of day time enhancement of nitrate and ammonium indicated that photochemical production ~~may-might~~ not be significant or possibly destruction (evaporative loss, i.e., gas-particle partitioning of NH₄NO₃) dominated.

It is challenging to determine the exact coating material on the atmospheric BC particles in a multi-component system containing organic and inorganic aerosols, and gaseous vapours. The association between the diurnal variations of organics and sulphates and BC mixing state as represented by RCT presents two possibilities of having different coating material on BC during a day. Similar diurnal variations in RCT (as seen in Figure 6) and sulphate suggest the possibility of sulphate serving as the most probable material. However, organic matter can also contribute to the BC coating material due to its huge abundance in particles of submicron sizes. This is particularly true during the late evening periods, when concurrent peaks in the mass fraction of organics and rBC mass loading occur, a significant fraction of which could be secondary in nature. The extent of contribution of each species depends on processes such as gas-phase chemistry and production of condensable vapours and strength of the condensation sink. Even though it is very difficult/challenging to determine the coating material on the BC particles that exist in a multi-component organic, inorganic aerosols, gaseous vapours system, the above discussion suggests two contrasting possibilities of coating material on BC: (a) concurrent peaks in RCT (as seen in Figure 8) and sulphate during the diurnal cycles indicates that the most probable material for the coating is sulphate, whereas (b) possibility of organic matter acting as coating material cannot be ruled out because observed minima in the mass fraction of organics during RCT peaks (during dawn and afternoon hours) suggested a possible loss of organic vapours through condensation on a large number of pre-existing BC particles, thereby contributing to their coating. Boundary layer dynamics and source processes play an important/essential role not only on particle loading but also in determining the coating (Liu et al., 2014; Gong et al., 2016; Thampan et al., 2017; Wang et al., 2018). Increased ventilation during day time due to enhanced boundary layer heights dilutes aerosol concentrations, thereby reduces competition among particles for adsorption of condensable vapours. The concentrations of freshly produced particles with little or no coating arising from primary as well as secondary sources are, in general, greater during day. It enables more efficient adsorption of condensable species on these particles, compared to relatively aged particles during the night which are already coated or internally mixed due to aging. A greater fractional change can occur more quickly on fresh BC particles compared to particles which are already thickly coated since a much smaller amount of condensable material is required. Further, freshly produced particles (with less or no coating) from primary as well as secondary sources are greater/higher during the day in general, and this enables more efficient adsorption condensable species on these particles, compared to relatively aged particles during the night which already more internally mixed. Further, the distinct nature of sources of various species is also an important/key factor. Majority of the BC and organic aerosol are produced in locations away from the sulphate sources. The sampling station sees local sources At-at night in a collapsed ABL with stable conditions and the sampling station sees local sources which are predominately consists of with BC and organics, but with reduced sulphate, whereas But during the day in a well-developed ABL, both near field and far-far-field source contributions mix/algalam well-together. This It results in dilution of the contribution of species from near-closefield-by sources to coating, but will introduce increased contribution-participation from species from far-far-field sources. This process changes the balance of sulphate to organics mass concentrations and also the RCT of the BC.

Formatted: Not Highlight

Formatted: Not Highlight

Formatted: Not Highlight

Formatted: Not Highlight

Our observations indicate enhanced sulphate occurs due to photochemistry. ~~In addition~~ Besides, the possibility of organic matter acting as a coating material is not ruled out since secondary organic aerosol is known to have a photochemical origin (Chakraborty et al., 2018). Thamban et al., (2017) have reported an increase in oxygenated organic species during the day time with a diurnal trend similar to the fraction of thickly coated BC.

3.7 Seasonality of the association between rBC relative coating thickness and NR-PM1 chemical species

Further, we examined the seasonal variation in the association between the mass fractions (MF) of different species with simultaneous RCT values by considering hourly mean values of both the parameters. The association between hourly mean RCT and MF of organics and sulphate (the dominant NR-PM1 species) for different seasons is shown in Figure 11-9 (other species did not show any perceptible association). The colour bar indicates the percentage of occurrence of a particular value of RCT for a corresponding MF value of the species considering the entire data set for that season. During SMS (Figure 11-9a & Figure 11-9e), since there are very few available simultaneous observations of RCT and MF no conclusion about their association can be drawn, and also the extent of coating is very much reduced during this season. During PoMS (when the IGP outflow airmasses prevailed), as seen from the Figure 11-9b & Figure 11-9f, instances of higher RCT decreased with increasing MF of organics, whereas the association is vice versa between RCT and MF of sulphates. This It suggests that sulphates may be the possible preferential coating substance, as increasing fractions of sulphates in the total mass concentrations contributed to the enhanced coating on BC particles.

During winter (Figure 11-9c & Figure 11-9g) similar to the PoMS increasing MF of organics has a negative correlation with RCT, whereas the MF of sulphate did not show any clear association. As the season changes to PMS, the association between RCT and MF is reversed to what it was during PoMS, with the population of highly coated particles decreasing with increasing MF of sulphate, while RCT increased with increasing MF of organics. It is known that the nature of the initial coating and mixing state of BC particles is dependent on the type of BC sources (Liu et al., 2013) and also on the nature of prevalent semi-volatile vapours and heterogeneous interactions with gas-phase species that act as condensable material. The observed association of organics and sulphate with RCT suggests possible preferential coating, which is not dependent on the mass loading of the dominant species in the PM1.0, but rather dependent on the nature of dominant sources (gaseous precursors from the similar sources that produce BC are important). Extent The extent of coating depends more on the strength of the sources, number/surface area size distribution of the particles and concentration of condensable vapours coupled with atmospheric dynamical processes.

As discussed in the previous sections, BC in the highly polluted IGP outflow is characterized by higher mass loadings and mixed sources (MMD ~0.180-0.190 μm) which include vehicular, industrial emissions (fossil fuel sources) and wide-spread thermal power plants over the IGP (Thamban et al., 2017; Brooks et al., 2018, 2019a,b) that co-emit gaseous SO₂ along with BC. Enhanced RCT with increased MF of sulphates indicates the possibility that sulphate resulting from the vapour phase chemistry of SO₂ emissions may be ~~an a key important~~ condensable species on BC particles during their

Formatted: Indent: First line: 1.27 cm

extended atmospheric transit in the outflow (Takami et al., 2013; Miyakawa et al., 2017). Larger BC cores (MMD ~ 0.200-0.220 μm) during the pre-monsoon indicate that solid fuel sources (including biomass/coal burning processes) which also emit organic material (vapours as well as particulates) along with BC, and sulphate in primary particulate form (Pandey et al., 2014; Fleming et al., 2018). As seen from the supplementary figure S1, increased fire counts during the PMS indicate sources of significant amounts of organic material apart from BC. This, combined with the enhanced dilution of the species due to ABL dynamics modulating both particle and condensable species concentrations during the atmospheric transit, contribute to a positive association between RCT and MF of organics. Such positive association suggest that organic vapours possibly ~~contributed~~ added to the enhanced coating on BC during the PMS.

It may be noted that it is difficult to decipher the exact coating on BC with the present approach, since the SP2 retrieves black carbon mass and provides a measure of co-existing material within the same particles (as measured by RCT) whereas the ACSM measures the mass of refractory material in the total submicron population. An examination of coating material can only be directly achieved by employing the instruments such as the soot particle aerosol mass spectrometer (Aerodyne SP-AMS) (Liu et al., 2018). However, the SP2 can determine both the rBC content of single particles and the optical size by light scattering for diameters between 200 and 400 nm. The coating thickness estimated within this range represents most of the particles which contribute significantly to the light extinction. A comparison of the proportion of rBC containing particles within the total population as a function of season sheds some light on interpreting variation throughout the year. In our study, the fraction of particles containing BC, i.e., the ratio of BC number concentration and total number concentration (BC number concentration + scattering number concentration) showed a clear seasonal variation. The fraction of BC containing particles was highest during the SMS (mean ~ 0.69 \pm 0.11) and decreased through winter (~0.44 \pm 0.16), PoMS (~0.36 \pm 0.11) to reach the lowest value (~0.25 \pm 0.10) during the PMS. This shows a gradual decrease in the overlap between the particle population detected with the ACSM and the population detected with the SP2 with changing seasons from SMS to PMS. This should be borne in mind while examining the association between the ACSM detected particle mass concentrations and the SP2 derived coating parameters.

While the present work highlighted the microphysical properties of the refractive BC aerosols and brought out the difference between the IGP outflow and other air mass regimes, further investigations (both experimental and theoretical) are needed to ascertain the possible radiative (including absorption enhancement) and climatic implications due to the observed microphysical properties, extent of coating and changes in the mixing state of the BC due to various host coating materials. This will form the focus of future work.

4 Summary and Conclusions

The present study has determined the mass concentration, size distributions and mixing state of refractive BC particles from the single particle soot photometer observations carried out over Bhubaneswar located in the eastern coast of India. ~~Our~~ important ~~Major~~ findings from our study are as follows.

Formatted: Not Highlight

Formatted: Font: (Default) +Headings (Times New Roman), 10 pt, Not Bold

- (1) The rBC mass concentration ~~are-is~~ higher during winter ($\sim 1.935\text{--}94 \pm 1.578 \mu\text{g m}^{-3}$), followed by post-monsoon ($\sim 1.3384 \pm 1.40396 \mu\text{g m}^{-3}$). Reduced rainfall, calm wind conditions, coupled with decreased ventilation due to the shallow boundary layer resulted in such build-up of aerosols. Lowest rBC mass loading ($\sim 0.82816 \pm 0.8354 \mu\text{g m}^{-3}$) is seen during the pre-monsoon, possibly due to enhanced convective mixing leading to significant dispersion of the ~~near-near~~-surface aerosols.
- (2) BC size distributions indicated seasonally changing nature of sources with smaller BC cores (MMD $\sim 0.150\text{--}0.170 \mu\text{m}$) in the summer monsoon highlighting fossil fuel sources to larger BC cores (MMD $> 0.210 \mu\text{m}$) in the pre-monsoon suggesting the prominence of solid fuel sources. rBC that originated from mixed sources (both fossil fuel and solid fuel) (MMD $\sim 0.190\text{--}0.195 \mu\text{m}$) prevailed when the air mass pathways originated from the highly polluted IGP region.
- (3) Further, the IGP outflow is ~~characterized-characterised~~ by the highly coated BC particles with bulk relative coating thickness (RCT) in the range $\sim 1.3\text{--}1.8$ and absolute coatings of $50\text{--}70 \text{ nm}$ on the BC cores. ~~Abundance-The abundance~~ of condensable species, combined with prevailing calm weather conditions and absence of precipitation resulted in ~~an~~ extended life-time, and thus thickly coated BC particles. During the SMS efficient wet scavenging restricts the life-time of aerosols and results in the lowest coatings observed throughout the year (median ACT $\sim 12.35 \text{ nm}$ and RCT ~ 1.15), indicating relatively nascent BC aerosols. During the PMS, significantly coated (RCT $\sim 1.2\text{--}1.3$) and larger core BC particles prevailed which may have ~~important-significant~~ regional climatic implications.
- (4) BC particles with relatively thicker coating are noticed during ~~the~~ day time in all the seasons, which is due to the abundance of photo-chemically produced condensable species; and thus gas-phase photochemical processing. The diurnal amplitude is highest in winter and lowest in the SMS, and this highlighted the role played by ABL dynamics in modulating rBC microphysical properties.
- (5) Diurnal variation of sulphate resembled that of the RCT of rBC with a clear day time dominance in the PoMS, winter and SMS, indicating strong photo-chemical production of sulphate from gas-phase chemistry. During the PMS, the day time peak in sulphate is weak which may be attributed to enhanced dispersion resulting in lower ~~near near~~-surface concentrations which overcomes photochemical production. Diurnal variation of the organics resembled that of BC mass concentrations with typical double maxima.
- (6) Examination of diurnal variations presented two contrasting possibilities of coating material on BC: (a) sulphate acting as the most probable material coating the BC core due to its abundance during the day time, and (b) organics ~~acting-serving~~ as condensable species; ~~as indicated by the observed minima in mass fraction of organics during RCT peaks suggesting during late evenings, where~~ a possibility ~~of~~ loss of organic vapours through condensation on large number of pre-existing BC particles; ~~thereby contributing to their coating can contribute to coating on BC.~~
- (7) Examination of NR-PM₁ mass fractions in conjunction with BC coating thickness suggests ~~t~~ that the coating on BC is positively associated with sulphates during the IGP outflow (March to September) while the association is ~~more~~

stronger with organics during PMS when coastal airmasses prevailed; thereby highlighting preferential coating in different seasons with conducive species availability through advection.

Our study provides insight into the seasonally varying source processes and changes in the microphysical properties of BC over Bhubaneswar and highlights the delineation between the IGP outflow and the non-IGP airmasses. Further investigations are needed to understand the sensitivity of the optical and hygroscopic properties of BC to such seasonally varying microphysical properties and atmospheric processing of BC over the Indian region.

Data availability

Data are available upon request from the contact author, S. Suresh Babu (s_sureshabu@vssc.gov.in).

Competing interests

The authors declare that they have no conflict of interest.

Author contributions

SSB, SKS, KKM and HC ~~conceptualized~~~~conceptualised~~ the experiment and ~~finalized~~~~finalised~~ the methodology. SKK, TD and RB are responsible for the maintenance and operation of the SP2 and the ACSM. SKK carried out the scientific analysis of the data supported by MF, DL, ED, JB and JA. SKK drafted the manuscript. SSB, KKM, SKS and HC carried out the review and editing of the manuscript.

Acknowledgements

This study was carried out as part of collaborative “South West Asian Aerosol Monsoon Interactions (SWAAMI)” experiment under a joint Indo-UK (NERC) project namely “Drivers of variability in the South Asian Monsoon” under the “National Monsoon Mission (NMM)” of the Ministry of Earth Sciences (MoES), Government of India, in which the ISRO, the Indian Institute of Science (IISc), Bengaluru and the University of Manchester, UK are partners. Bhubaneswar station is a supersite set-up under SWAAMI, for long term ~~characterization~~~~characterisation~~ of the IGP outflow. It also is a part of the network under the Aerosol Radiative Forcing over India (ARFI) project of the Indian Space Research Organisation-Geosphere Biosphere Program. The authors are thankful to the Director, Institute of Minerals and Materials Technology (CSIR-IMMT) for the support. We acknowledge NOAA Air Resources Laboratory for the provision of the HYSPLIT transport and dispersion model and READY website (<http://www.arl.noaa.gov/ready.html>) used in this study. We acknowledge the use of data and imagery from LANCE FIRMS operated by NASA's Earth Science Data and Information System (ESDIS) with funding provided by NASA Headquarters (<http://earthdata.nasa.gov/firms>).

Formatted: Not Highlight

References

- Adachi, K., ~~Y.~~Zaizen, ~~Y.~~, ~~M.~~Kajino, ~~M.~~ and ~~Y.~~Igarashi, ~~Y.~~: Mixing state of regionally transported soot particles and the coating effect on their size and shape at a mountain site in Japan, *J. Geophys. Res. Atmos.*, 119, 2014, 5386–5396, doi:10.1002/2013JD020880.
- Adachi, K., Chung, S. H., and Buseck, P. R.: Shapes of soot aerosol particles and implications for their effects on climate, *J. Geophys. Res.-Atmos.*, 115, D15206, doi:10.1029/2009JD012868, 2010
- Asnani, G.C., *Tropical Meteorology*, Vol.1 and Vol.2, 1012 pp, 1993. Indian Institute of Tropical Meteorology, Pashan, Pune.
- Babu, S.S., Kompalli, S.K. Moorthy, K.K.: Aerosol number size distributions over a coastal semi urban location: Seasonal changes and ultrafine particle bursts. *Sci.Total Environ.*, 563-564, pp 351–365,2016. <http://dx.doi.org/10.1016/j.scitotenv.2016.03.246>.
- Babu, S.S., Manoj, M.R., Moorthy, K.K., Gogoi, M.M., Nair V.S., Kompalli, S.K., Satheesh, S.K., Niranjana, K., Ramagopal, K., Bhuyan, P.K. and Singh, D.: Trends in aerosol optical depth over Indian region: Potential causes and impact indicators. *J. Geophys. Res.*, 118, 11: 794-11,806, 2013.
- Beegum, S.N., Moorthy, K.K., Babu, S.S., Satheesh, S.K., Vinoj, V., Badarinath, K.V.S., Safai, P.D., Devara, P.C.S., Singh, S.N., Vinod, Dumka, U.C., Pant, P.: Spatial distribution of aerosol black carbon over India during premonsoon season. *Atmos. Environ.*, 43: 1071–1078, 2009.
- [Bhandari, J., China, S., Onasch, T., Wolff, L., Lambe, A., Davidovits, P., Cross, E., Ahern, A., Olfert, J., Dubey, M., and Mazzoleni, C.: Effect of thermodenuding on the structure of nascent flame soot aggregates, *Atmos. Meas. Tech. Discuss.*, <https://doi.org/10.5194/amt-2016-270>, 2016.](https://doi.org/10.5194/amt-2016-270)
- Bond, T. C., Doherty, S. J., Fahey, D. W., Forster, P. M., Berntsen, T., DeAngelo, B. J., Flanner, M. G., Ghan, S., Karcher, B., Koch, D., Kinne, S., Kondo, Y., Quinn, P. K., Sarofim, M. C., Schultz, M. G., Schulz, M., Venkataraman, C., Zhang, H., Zhang, S., Bellouin, N., Guttikunda, S. K., Hopke, P. K., Jacobson, M. Z., Kaiser, J. W., Klimont, Z., Lohmann, U., Schwarz, J. P., Shindell, D., Storelvmo, T., Warren, S. G., and Zender, C. S.: Bounding the role of black carbon in the climate system: A scientific assessment, *J. Geophys. Res. Atmos.*, 118, 5380–5552, doi:10.1002/jgrd.50171, 2013.
- Bond, T. C. and Bergstrom, R. W.: Light absorption by carbonaceous particles: An investigative review, *Aerosol Sci. Tech.*, 40, 27–67, doi:10.1080/02786820500421521, 2006.

Brooks, J., Liu, D., Allan, J. D., Williams, P. I., Haywood, J., Highwood, E. J., Kompalli, S. K., Babu, S. S., Satheesh, S. K., Turner, A. G., and Coe, H.: Black carbon physical and optical properties across northern India during pre-monsoon and monsoon seasons, *Atmos. Chem. Phys.*, 19, 13079–13096, <https://doi.org/10.5194/acp-19-13079-2019>, 2019a.

Brooks, J., Allan, J. D., Williams, P. I., Liu, D., Fox, C., Haywood, J., Langridge, J. M., Highwood, E. J., Kompalli, S. K., O'Sullivan, D., Babu, S. S., Satheesh, S. K., Turner, A. G., and Coe, H.: Vertical and horizontal distribution of submicron aerosol chemical composition and physical characteristics across northern India during pre-monsoon and monsoon seasons, *Atmos. Chem. Phys.*, 19, 5615–5634, <https://doi.org/10.5194/acp-19-5615-2019>, 2019.

Cappa, C. D., Onasch, T. B., Massoli, P., Worsnop, D. R., Bates, T. S., Cross, E. S., Davidovits, P., Hakala, J., Hayden, K. L., Jobson, B. T., Kolesar, K. R., Lack, D. A., Lerner, B. M., Li, S.-M., Mellon, D., Nuaaman, I., Olfert, J. S., Petäjä, T., Quinn, P. K., Song, C., Subramanian, R., Williams, E. J., and Zaveri, R. A.: Radiative Absorption Enhancements Due to the Mixing State of Atmospheric Black Carbon, *Science*, 337, 1078–1081, doi:10.1126/science.1223447, 2012.

Chakraborty, A., Mandariya, A.K., Chakraborti, R., Gupta, T., Tripathi, S.N.: Realtime chemical characterization of post monsoon organic aerosols in a polluted urban city: sources, composition, and comparison with other seasons, *Environ. Pollu.*, 232, 310–321, 2018. <https://doi.org/10.1016/j.envpol.2017.09.079>.

Cheng, Y., Li, S.M., Gordon, M., and Liu, P.: Size distribution and coating thickness of black carbon from the Canadian oil sands operations. *Atmos. Chem. Phys.*, 18, 2653–2667, 2018.

China, S., Mazzoleni, C., Gorkowski, K., Aiken, A. C., and Dubey, M. K.: Morphology and mixing state of individual freshly emitted wildfire carbonaceous particles, *Nat. Commun.*, 4, 2122, doi:10.1038/ncomms3122, 2013.

Dey, S., S. N. Tripathi, and S. K. Mishra: Probable mixing state of aerosols in the Indo-Gangetic Basin, northern India, *Geophys. Res. Lett.*, 35, L03808, 2008.

Fleming, L.T., Lin, P., Laskin, A., Laskin, J., Weltman, R., Edwards, R.D., Arora, N.K., Yadav, A., Meinardi, S., Blake, D.R. & Pillarisetti, A.: Molecular composition of particulate matter emissions from dung and brushwood burning household cookstoves in Haryana, India. *Atmos. Chem. Phys.*, 18(4), pp.2461–2480, 2018.

Gautam, R., Hsu, N.C., Lau, K.M., Tsay, S.C., and Kafatos, M., Enhanced premonsoon warming over the Himalayan-Gangetic region from 1979 to 2007. *Geophys. Res. Lett.*, 36, L07704, 2009.

Gong, X. D., Zhang, C., Chen, H., Nizkorodov, S. A., Chen, J. M., and Yang, X.: Size distribution and mixing state of black carbon particles during a heavy air pollution episode in Shanghai, *Atmos. Chem. Phys.*, 16, 5399–5411, 2016.

Huang, X. F., Gao, R. S., Schwarz, J. P., He, L. Y., Fahey, D. W., Watts, L. A., McComiskey, A., Cooper, O. R., Sun, T. L., Zeng, L. W., Hu, M., and Zhang, Y. H.: Black carbon measurements in the Pearl River Delta region of China, *J. Geophys. Res.-Atmos.*, 116, D12208, doi:10.1029/2010jd014933, 2011.

Huang, X. F., Sun, T. L., Zeng, L. W., Yu, G. H., and Luan, S. J.: Black carbon aerosol characterization in a coastal city in South China using a single particle soot photometer, *Atmos. Environ.*, 51, 21–28, doi:10.1016/j.atmosenv.2012.01.056, 2012.

IPCC, 2013: Climate Change., The Physical Science Basis. Contribution of Working Group I to the Fifth Assessment Report of the Intergovernmental Panel on Climate Change (Stocker, T.F., D. Qin, G.-K. Plattner, M. Tignor, S.K. Allen, J. Boschung, A. Nauels, Y. Xia, V. Bex and P.M. Midgley (eds.)). Cambridge University Press, Cambridge, United Kingdom and New York, NY, USA, 2013, 1535 pp.

5 Jacobson, M. Z.: Strong Radiative Heating Due to the Mixing State of Black Carbon in Atmospheric Aerosols. *Nature*, 409:695–697, 2001.

Kompalli, S.K., Babu, S.S., Moorthy, K.K., Manoj, M.R., Kirankumar, N.V.P., Shaeb, K.H.B., Joshi, A.K.: Aerosol black carbon characteristics over central India: temporal variation and its dependence on mixed layer height. *Atmos. Res.* 147–148, 27–37. <http://dx.doi.org/10.1016/j.atmosres.2014.04.015>, 2014.

10 Kondo, Y., Matsui, H., Moteki, N., Sahu, L., Takegawa, N., Kajino, M., Zhao, Y., Cubison, M. J., Jimenez, J. L., Vay, S., Diskin, G. S., Anderson, B., Wisthaler, A., Mikoviny, T., Fuelberg, H. E., Blake, D. R., Huey, G., Weinheimer, A. J., Knapp, D. J., and Brune, W. H.: Emissions of black carbon, organic, and inorganic aerosols from biomass burning in North America and Asia in 2008, *J. Geophys. Res.*, 116, D08204, doi:10.1029/2010JD015152, 2011.

[Köylü, Ü.Ö., Faeth,G.M., Farias,T.L., Carvalho.M.G.: Fractal and projected structure properties of soot aggregates, Combustion and Flame,100, 621-633, 1995, ISSN 0010-2180, https://doi.org/10.1016/0010-2180\(94\)00147-K.](#)

15 Kumar, B., Chakraborty, A., Tripathi, S. N., & Bhattu, D.: Highly time resolved chemical characterization of submicron organic aerosols at a polluted urban location, *Environ. Sci.: Process. Imp.*, 18(10), 1285-1296, 2016.

Laborde, M., Crippa, M., Tritscher, T., Jurányi, Z., Decarlo, P. F., Temime-Roussel, B., Marchand, N., Eckhardt, S., Stohl, A., Baltensperger, U., Prévôt, A. S. H., Weingartner, E., and Gysel, M.: Black carbon physical properties and mixing state in the European megacity Paris, *Atmos. Chem. Phys.*, 13, 5831–5856, 2013.

20 Laborde, M., Mertes, P., Zieger, P., Dommen, J., Baltensperger, U., and Gysel, M.: Sensitivity of the Single Particle Soot Photometer to different black carbon types, *Atmos. Meas. Tech.*, 5, 1031–1043, doi:10.5194/amt-5-1031-2012, 2012.

Lambe, A. T., Cappa, C. D., Massoli, P., Onasch, T. B., Forestieri, S. D., Martin, A. T., Cummings, M. J., Croasdale, D. R., Brune, W. H., Worsnop, D. R., and Davidovits, P.: Relationship between oxidation level and optical properties of secondary organic aerosol, *Environ. Sci. Technol.*, 47, 6349–6357, 2013.

25 Lawrence, M. G., and Lelieveld, J.: Atmospheric pollutant outflow from southern Asia: A review. *Atmos. Chem. Phys.*, 10, 11,017 – 11,096, 2010.

Lee, S. H., Murphy, D. M., Thomson, D. S., Middlebrook, A.M.: Chemical components of single particles measured with Particle Analysis by Laser Mass Spectrometry (PALMS) during the Atlanta SuperSite Project: Focus on organic/sulfate, lead, soot, and mineral particles, *J. Geophys. Res.*, 107(D1–D2), 4003,2002 doi:10.1029/2000JD000011.

30 [Liu, D., Joshi, R., Wang, J., Yu, C., Allan, J. D., Coe, H., Flynn, M. J., Xie, C., Lee, J., Squires, F., Kotthaus, S., Grimmond, S., Ge, X., Sun, Y., and Fu, P.: Contrasting physical properties of black carbon in urban Beijing between winter and summer. *Atmos. Chem. Phys.*, 19, 6749-6769, https://doi.org/10.5194/acp-19-6749-2019, 2019.](#)

Liu, D., Taylor, J. W., Crosier, J., Marsden, N., Bower, K. N., Lloyd, G., Ryder, C. L., Brooke, J. K., Cotton, R., Marengo, F., Blyth, A., Cui, Z., Estelles, V., Gallagher, M., Coe, H., and Choulaton, T. W.: Aircraft and ground measurements of dust aerosols over the west African coast in summer 2015 during ICE-D and AER-D. *Atmos. Chem. Phys.*, 18, 3817–3838, <https://doi.org/10.5194/acp-18-3817-2018>, 2018.

5 Liu, D., Whitehead, J., Alfarra, M. R., Reyes-Villegas, E., Spracklen, Dominick V., Reddington, Carly L., Kong, S., Williams, Paul I., Ting, Y.-C., Haslett, S., Taylor, Jonathan W., Flynn, Michael J., Morgan, William T., McFiggans, G., Coe, H., and Allan, James D.: Black-carbon absorption enhancement in the atmosphere determined by particle mixing state. *Nat. Geosci.*, 10, 184–188, [10.1038/ngeo2901](https://doi.org/10.1038/ngeo2901), 2017.

10 Liu, D., Allan, J. D., Young, D. E., Coe, H., Beddows, D., Fleming, Z. L., Flynn, M. J., Gallagher, M. W., Harrison, R. M., Lee, J., Prevot, A. S. H., Taylor, J. W., Yin, J., Williams, P. I., and Zotter, P.: Size distribution, mixing state and source apportionment of black carbon aerosol in London during wintertime, *Atmos. Chem. Phys.*, 14, 10061–10084, <https://doi.org/10.5194/acp-14-10061-2014>, 2014.

15 Liu, D., Allan, J., Whitehead, J., Young, D., Flynn, M., Coe, H., McFiggans, G., Fleming, Z. L., and Bandy, B.: Ambient black carbon particle hygroscopic properties controlled by mixing state and composition, *Atmos. Chem. Phys.*, 13, 2015–2029, [doi:10.5194/acp-13-2015-2013](https://doi.org/10.5194/acp-13-2015-2013), 2013.

Liu, D., Flynn, M., Gysel, M., Targino, A., Crawford, I., Bower, K., Choulaton, T., Jurányi, Z., Steinbacher, M., Hüglin, C., Curtius, J., Kampus, M., Petzold, A., Weingartner, E., Baltensperger, U., and Coe, H.: Single particle characterization of black carbon aerosols at a tropospheric alpine site in Switzerland, *Atmos. Chem. Phys.*, 10, 7389–7407, [doi:10.5194/acp-10-7389-2010](https://doi.org/10.5194/acp-10-7389-2010), 2010.

20 Mahapatra, P.S., Panda, S., Das, N., Rath, S., Das T.: Variation in black carbon mass concentration over an urban site in the eastern coastal plains of the Indian sub-continent, *Theor. Appl. Climatol.*, 2013a, DOI 10.1007/s00704-013-0984-z.

Mahapatra, P.S., Ray, S., Das, N., Mohanty, A., Ramulu, T.S., Das, T., Chaudhury, G.R., Das, S. N.: Urban air-quality assessment and source apportionment studies for Bhubaneswar, Odisha, *Theor. Appl. Clim.*, 112, 243–25, 2013b.

25 McMeeking, G. R., Morgan, W. T., Flynn, M., Highwood, E. J., Turnbull, K., Haywood, J., and Coe, H.: Black carbon aerosol mixing state, organic aerosols and aerosol optical properties over the United Kingdom, *Atmos. Chem. Phys.*, 11, 9037–9052, 2011.

McMeeking, G. R., Hamburger, T., Liu, D., Flynn, M., Morgan, W. T., Northway, M., Highwood, E. J., Krejci, R., Allan, J. D., Minikin, A., and Coe, H.: Black carbon measurements in the boundary layer over western and northern Europe, *Atmos. Chem. Phys.*, 10, 9393–9414, 2010.

30 Middlebrook, A. M., Bahreini, R., Jimenez, J. L., and Canagaratna, M. R.: Evaluation of Composition-Dependent Collection Efficiencies for the Aerodyne Aerosol Mass Spectrometer using Field Data, *Aerosol Sci. Tech.*, 46, 258–271, [doi:10.1080/02786826.2011.620041](https://doi.org/10.1080/02786826.2011.620041), 2012.

Moffet, R.C. and Prather, K.A.: In-situ measurements of the mixing state and optical properties of soot with implications for radiative forcing estimates, *PNAS*, 106, 11872–11877, 2009.

Moorthy, K.K., Satheesh, S. K., Kotamarthi, V.R.: Evolution of aerosol research in India and the RAWEX–GVAX: an overview, *Curr. Sci.*, 111,1,53-75, 2016,DOI: 10.18520/cs/v111/i1/53-75.

Moorthy, K.K.: South Asian aerosols in perspective: Preface to the special issue, *Atmos. Environ.*, 125,307–311,2016, <http://dx.doi.org/10.1016/j.atmosenv.2015.10.073>.

- 5 Moorthy, K. K., Babu, S.S., Satheesh, S.K., Srinivasan, J., and Dutt, C.B.S.: Dust absorption over the “Great Indian Desert” inferred using ground-based and satellite remote sensing, *J. Geophys. Res.*, 112, D09206,2007 doi:10.1029/2006JD007690.

Moteki, N. and Kondo, Y.: Effects of mixing state on black carbon measurements by laser-induced incandescence, *Aerosol Sci. Technol.*, 41, 398–417, 2007.

- 10 Moteki, N., Kondo, Y., Miyazaki, Y., Takegawa, N., Komazaki, Y., Kurata, G., Shirai, T., Blake, D.R., Miyakawa, T., Koike, M.: Evolution of mixing state of black carbon particles: Aircraft measurements over the western Pacific in March 2004, *Geophys. Res. Lett.*, 34, L11803,2007, doi:10.1029/2006GL028943.

Moteki, N. and Kondo, Y.: Dependence of laser-induced incandescence on physical properties of black carbon aerosols: Measurements and theoretical interpretation, *Aerosol Sci. Tech.*, 44, 663-675, 2010.

- 15 [Moteki, N., Kondo, Y., and Nakamura, S.-i.: Method to measure refractive indices of small nonspherical particles: Application to black carbon particles, *J. Aerosol Sci.*, 41, 513-521, 2010.](#)

Miyakawa, T., Oshima, N., Taketani, F., Komazaki, Y., Yoshino, A., Takami, A., Kondo, Y., Kanaya, Y.: Alteration of the size distributions and mixing states of black carbon through transport in the boundary layer in east Asia, *Atmos. Chem. Phys.*, 17, 5851–5864, 2017.

- 20 Ng, N. L., Herndon, S. C., Trimborn, A., Canagaratna, M. R., Croteau, P. L., Onasch, T. B., Sueper, D., Worsnop, D.R., Zhang, Q., Sun, Y. L., Jayne, J. T., 2011. An Aerosol Chemical Speciation Monitor (ACSM) for Routine Monitoring of the Composition and Mass Concentrations of Ambient Aerosol, *Aerosol Science and Technology*, 45:7, 780-794, doi:10.1080/02786826.2011.560211.

Pandey, A., Sadavarte, P., Rao, A. B., Venkataraman, C.: Trends in multi-pollutant emissions from a technology-linked inventory for India: II. Residential, agricultural and informal industry sectors. *Atmos. Environ.*, 99, 341-352, 2014.

- 25 Peng, J., Hu, M., Guo, S., Du, Z., Zheng, J., Shang, D., Levy Zamora, M., Zeng, L., Shao, M., Wu, Y.-S., Zheng, J., Wang, Y., Glen, C. R., Collins, D. R., Molina, M. J., and Zhang, R.: Markedly enhanced absorption and direct radiative forcing of black carbon under polluted urban environments, *P. Natl. Acad. Sci. USA*, 113, 4266–4271, doi:10.1073/pnas.1602310113, 2016.

- 30 Petzold, A., Ogren, J. A., Fiebig, M., Laj, P., Li, S.-M., Baltensperger, U., Holzer-Popp, T., Kinne, S., Pappalardo, G., Sugimoto, N., Wehrli, C., Wiedensohler, A., and Zhang, X.-Y.: Recommendations for reporting “black carbon” measurements, *Atmos. Chem. Phys.*, 13, 8365–8379, doi:10.5194/acp-13-8365-2013, 2013.

Formatted: Font: (Default) +Headings (Times New Roman), 10 pt, Not Bold, English (India), Check spelling and grammar

Formatted: EndNote Bibliography, Indent: Left: 0 cm, Hanging: 1.27 cm, Right: 0 cm, Adjust space between Latin and Asian text, Adjust space between Asian text and numbers

- Prasad, P., Ramana, R., Venkat Ratnam, M., Chen, W., Vijaya Bhaskara Rao, S., Gogoi, M.M., Kompalli, S.K., Kumar, K.S., Babu, S.S.; Characterization of atmospheric Black Carbon over a semi-urban site of Southeast India: Local sources and long-range transport, *Atmos. Res.*, 213, 411–421, DOI:10.1016/j.atmosres.2018.06.024, 2018.
- Raatikainen, T., Brus, D., Hooda, R.K., Hyvärinen, A.P., Asmi, E., Sharma, V.P., Arola, A., Lihavainen, H., Size-selected black carbon mass distributions and mixing state in polluted and clean environments of northern India, *Atmos. Chem. Phys.*, 17, 371–383, doi:10.5194/acp-17-371-2017, 2017.
- Raatikainen, T., Brus, D., Hyvärinen, A.-P., Svensson, J., Asmi, E., and Lihavainen, H.: Black carbon concentrations and mixing state in the Finnish Arctic, *Atmos. Chem. Phys.*, 15, 10057–10070, doi:10.5194/acp-15-10057-2015, 2015.
- Reddington, C.L., McMeeking, G., Mann, G.W., Coe, H., Frontoso, M.G., Liu, D., Flynn, M., Spracklen, D.V., Carslaw, K.S.: The mass and number size distributions of black carbon aerosol over Europe. *Atmos. Chem. Phys.* 13, 4917–4939, 2013.
- Scarnato, B.V., China, S., Nielsen, K., and Mazzoleni, C.: Perturbations of the optical properties of mineral dust particles by mixing with black carbon: a numerical simulation study, *Atmos. Chem. Phys.*, 15, 6913–6928, 2015, www.atmos-chem-phys.net/15/6913/2015/ doi:10.5194/acp-15-6913-2015.
- Schwarz, J. P., Gao, R. S., Perring, A. E., Spackman, J. R., and Fahey, D. W.: Black carbon aerosol size in snow, *Sci. Rep.*, 3, 1356, <https://doi.org/10.1038/srep01356>, 2013.
- Schwarz, J. P., Gao, R. S., Spackman, J. R., Watts, L. A., Thomson, D. S., Fahey, D. W., Ryerson, T. B., Peischl, J., Holloway, J. S., Trainer, M., Frost, G. J., Baynard, T., Lack, D. A., de Gouw, J. A., Warneke, C., and Del Negro, L. A.: Measurement of the mixing state, mass, and optical size of individual black carbon particles in urban and biomass burning emissions, *Geophys. Res. Lett.*, 35, L13810, doi:10.1029/2008GL033968, 2008.
- Schnaiter, M., Linke, C., Möhler, O., Naumann, K. H., Saathoff, H., Wagner, R., Schurath, U., and Wehner, B.: Absorption amplification of black carbon internally mixed with secondary organic aerosol, *J. Geophys. Res.*, 110, D19204, <https://doi.org/10.1029/2005JD006046>, 2005.
- [Sedlacek, A. J., III, Lewis, E. R., Kleinman, L., Xu, J., and Zhang, Q.: Determination of and evidence for noncore-shell structure of particles containing black carbon using the Single-Particle Soot Photometer \(SP2\), *Geophys. Res. Lett.*, 39, L06802, 2012, doi:10.1029/2012GL050905.](#)
- [Sedlacek, A. J., III, Onasch, T.B., Nichman, L., Lewis, E.R., Davidovits, P., Freedman, A., and Williams, L.: Formation of refractory black carbon by SP2-induced charring of organic aerosol, *Aerosol Sci. and Technol.*, 52:12, 1345-1350, 2018, DOI:10.1080/02786826.2018.1531107.](#)
- Shiraiwa, M., Kondo, Y., Moteki, N., Takegawa, N., Miyazaki, Y., and Blake, D. R.: Evolution of mixing state of black carbon in polluted air from Tokyo, *Geophys. Res. Lett.*, 34, L16803, <https://doi.org/10.1029/2007GL029819>, 2007.
- Shiraiwa, M., Kondo, Y., Iwamoto, T., and Kita, K.: Amplification of light absorption of black carbon by organic coating, *Aerosol Sci. Technol.*, 44, 46–54, 2010.

- Srinivas, B., and Sarin, M.M.: PM_{2.5}, EC and OC in atmospheric outflow from the Indo-Gangetic Plain: Temporal variability and aerosol organic carbon-to-organic mass conversion factor, *Sci. of the Tot. Environ.* 487,196–205,2014, <http://dx.doi.org/10.1016/j.scitotenv.2014.04.002>.
- Srivastava, R. and Ramachandran, S.: The mixing state of aerosols over the Indo-Gangetic Plain and its impact on radiative forcing. *Q. J. R. Meteorol. Soc.* 139, 137–151. DOI:10.1002/qj.1958, 2013.
- Takami, A., Mayama, N., Sakamoto, T., Ohishi, K., Iri, S., Yoshino, A., Hatakeyama, S., Murano, K., Sadanaga, Y., Bandow, H., Misawa, K., and Fujii, M.: Structural analysis of aerosol particles by microscopic observation using a time of flight secondary ion mass spectrometer, *J. Geophys. Res. - Atmos.*, 118, 6726–6737, doi:10.1002/jgrd.50477, 2013.
- Thamban, N.M., Tripathi, S.N., Shamjad P. M., Kuntamukkala, P., Kanawade, V.P.: Internally mixed black carbon in the Indo-Gangetic Plain and its effect on absorption enhancement. *Atmos. Res.*, 197, 211–223, <http://dx.doi.org/10.1016/j.atmosres.2017.07.007>, 2017.
- Taylor, J. W., Allan, J. D., Liu, D., Flynn, M., Weber, R., Zhang, X., Lefer, B.L., Grossberg, N., Flynn, J., Coe, H.: Assessment of the sensitivity of core/shell parameters derived using the single particle soot photometer to density and refractive index. *Atmos. Meas. Tech. Discuss.*, 7, 5491–5532, 2014.
- Ueda, S., Nakayama, T., Taketani, F., Adachi, K., Matsuki, A., Iwamoto, Y., Sadanaga, Y., and Matsumi, Y.: Light absorption and morphological properties of soot-containing aerosols observed at an East Asian outflow site, Noto Peninsula, Japan. *Atmos. Chem. Phys.*, 16, 2525–2541, 2016.
- Venkatraman, C., Habib, G., Eiguren-Fernandez, A., Mignel, A.H., Friedlander, S.K.: Residential biofuels in South Asia: carbonaceous aerosol emissions and climate impacts. *Science* 307:1454–1456, 2005.
- Verma, S., Pani, S.K., Bhanja, S.N.: Sources and radiative effects of wintertime black carbon aerosols in an urban atmosphere in east India. *Chemosphere*, 2012. doi:10.1016/j.chemosphere.2012.06.063.
- Wang, Q. Y., Cao, J., Han, Y., Tian, J., Zhu, C., Zhang, Y., Zhang, N., Shen, Z., Ni, H., Zhao, S., and Wu, J.: Sources and physicochemical characteristics of black carbon aerosol from the southeastern Tibetan Plateau: internal mixing enhances light absorption. *Atmos. Chem. Phys.*, 18, 4639–4656, 2018.
- Wang, Q. Y., Huang, R. J., Zhao, Z. Z., Cao, J. J., Ni, H. Y., Tie, X. X., Zhao, S. Y., Su, X. L., Han, Y. M., Shen, Z. X., Wang, Y. C., Zhang, N. N., Zhou, Y. Q., and Corbin, J. C.: Physicochemical characteristics of black carbon aerosol and its radiative impact in a polluted urban area of China, *J. Geophys. Res.-Atmos.*, 121,12505–12519, <https://doi.org/10.1002/2016JD024748>, 2016.
- Wang, Q. Y., Huang, R.-J., Cao, J. J., Tie, X. X., Ni, H. Y., Zhou, Y. Q., Han, Y. M., Hu, T. F., Zhu, C. S., Feng, T., Li, N., and Li, J. D.: Black carbon aerosol in winter north-eastern Qinghai-Tibetan Plateau, China: the source, mixing state and optical property, *Atmos. Chem. Phys.*, 15, 13059–13069, <https://doi.org/10.5194/acp-15-13059-2015>, 2015.
- Weingartner, E., Burtscher, H., and Baltensperger, U.: Hygroscopic properties of carbon and diesel soot particles, *Atmos. Environ.*, 31, 2311–2327, 1997.

Wu, Y., Zhang, R., Tian, P., Tao, J., Hsu, S.-C., Yan, P., Wang, Q., Cao, J., Zhang, X., Xia, X.: Effect of ambient humidity on the light absorption amplification of black carbon in Beijing during January 2013. *Atmos. Environ.* 124, 217–223, 2016.

5 Zhang, J., Liu, J., Tao, S., and Ban-Weiss, G. A.: Long-range transport of black carbon to the Pacific Ocean and its dependence on aging timescale, *Atmos. Chem. Phys.*, 15, 11521–11535, <https://doi.org/10.5194/acp-15-11521-2015>, 2015.

Zuberi, B., Johnson, K. S., Aleks, G. K., Molina, L. T., and Molina, M. J.: Hydrophilic properties of aged soot, *Geophys. Res. Lett.*, 32, L01807, <https://doi.org/10.1029/2004GL021496>, 2005.

Figures and Tables

Figure 1: Geographic location of Bhubaneswar marked by a star symbol on the topographic map; the boundary of the Indo-Gangetic Plains (IGP) region is indicated with dotted lines. Experimental location Bhubaneswar (star symbol); In the background, time-time-averaged values of the aerosol optical depth at the wavelength 550 nm (colour map) for the period 2009-2017 obtained using Moderate Moderate-resolution Imaging Spectrometer (MODIS) (MODIS Terra MOD08_M3 v6; combined dark target and deep blue product) are shown.

Figure 2: Isentropic five-five-day air mass back trajectories arriving at 100 meters above the surface over the observational location (identified with star symbol) in different seasons.

Figure 3: Temporal variation of daily mean (a) r_{BC} mass concentration; and (b) number concentration of BC (bars) and non-BC scattering particles (filled circle). The vertical line passing through them is the standard deviation. The shaded portions demarcate the seasons.

Figure 4: (a) Typical mass (number) size distributions along with least-squares fitting to mono-modal log-normal distribution (in dotted lines) used to derive MMD and CM_{DNMD} . (b) Temporal variation of daily mean mass median diameter (triangle filled circle) and (b) Temporal variation of daily mean count-number median diameter (star) of BC; The symbols present the mean value for the day and the vertical line passing through them is the standard deviation. The solid continuous line shows the 30 day smoothed variation. Dotted vertical lines highlight demarcate different seasons.

Figure 5: Seasonal mean black carbon (a) mass size distributions and (b) number size distributions. Corresponding mode diameter values are also seen in brackets.

Figure 6: Temporal variation of daily mean relative coating thickness (half filled circle) and absolute coating thickness (star). The symbols present the mean value for the day and the vertical line passing through them is the standard deviation. The solid continuous line shows the 30 day smoothed variation. Dotted vertical lines highlight different seasons. Due to the failure of the scattering detector between 31-July-2016 to 20-September-2016 mixing state parameters could not be estimated.

Figure 7: Frequency of occurrence of (a) relative coating thickness and (b) absolute coating thickness in different seasons.

Figure 8: Diurnal variation of (a-d) r_{BC} mass concentrations and relative coating thickness (RCT) in different seasons. The vertical lines denote the Sunrise and Sunset. The vertical bars through solids points are the standard errors from the mean.

Figure 9: Seasonal variation of (a) mass concentrations and (b) percentage contributions to the total mass concentration of different species (organics, sulphates, nitrates, ammonium and chlorides)

Figure 10: Diurnal variation of mass fraction of different species (organics, sulphates, nitrates, ammonium and chlorides) of NR-PM1 in different seasons.

Figure 119: Association between mass-fraction of organics (top panels; a-d) and sulphates (bottom panels e-h) with relative coating thickness during different seasons. The colour bar indicates the percentage of occurrence of RCT for corresponding MF values of the species.

Supplementary Figures and Tables

Figure S1: Spatial distribution of Moderate Resolution Imaging Spectroradiometer (MODIS) fire radiative power (MODIS Thermal Anomalies / Fire locations Collection 6 product obtained from <https://earthdata.nasa.gov/firms>) for the representative months of different seasons; (a) August -2016 (SMS), (b) October -2016 (PoMS), (c) January -2017 (winter) and (d) May -2017 (PMS). A significant amount of fire events during PMS are seen over the Indian region. During the PoMS (fire events to confined to northwest IGP) and winter (fire events to confined to western, northeastern regions of India) less intense regional fire events are noticeable. During SMS (and PoMS as well), a considerable amount of fire events are noticeable below south of India (over Srilankan region).

Figure S2: Seasonal mean black carbon (a) mass size distributions and (b) number size distributions. Corresponding mode diameter values are also seen in brackets

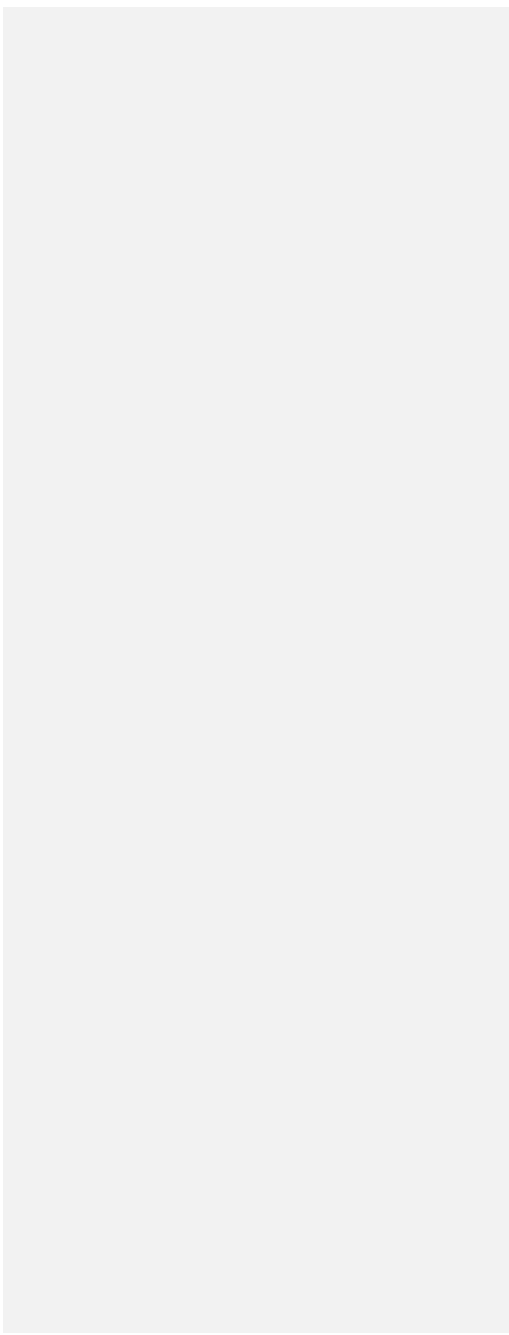
Figure S3: Frequency of occurrence of (a) relative coating thickness and (b) absolute coating thickness in different seasons.

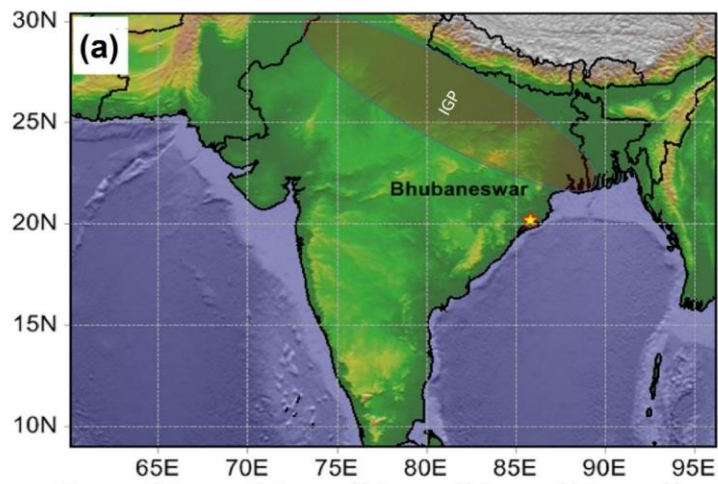
Figure S4: Diurnal variation of (a-d) rBC mass median diameter and absolute coating thickness (ACT) in different seasons. The vertical lines denote the Sunrise and Sunset. The vertical bars through solids points are the standard errors from the mean.

Formatted: Centered

Formatted: Font: Bold

|





Formatted: Font: (Default) Times New Roman, 10 pt,
Bold

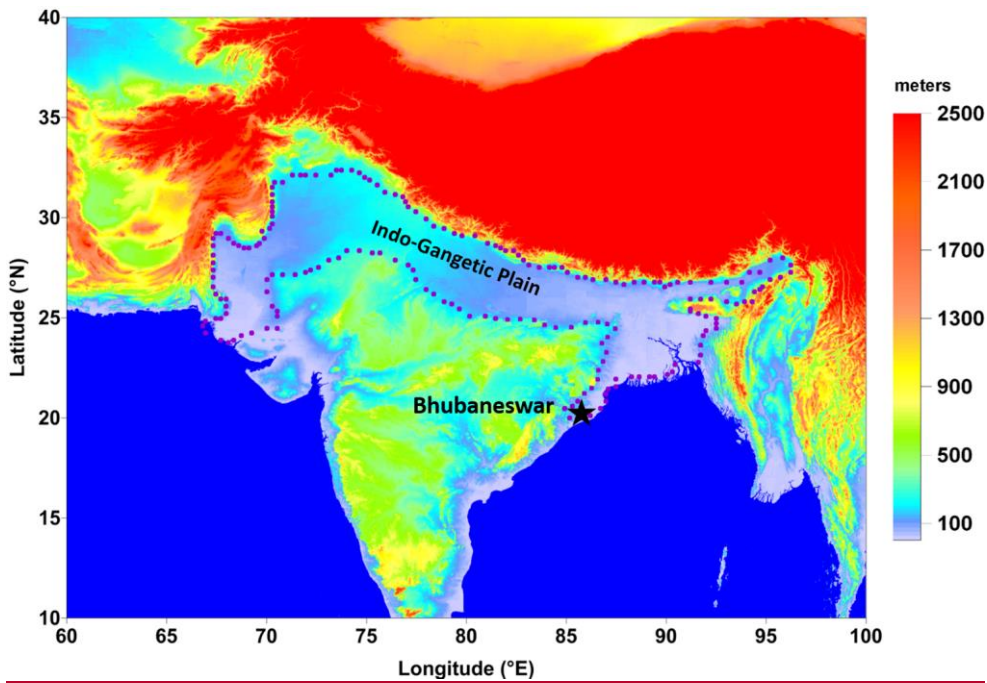
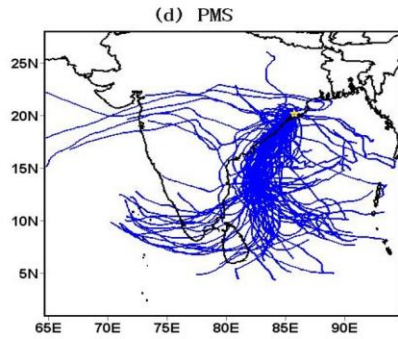
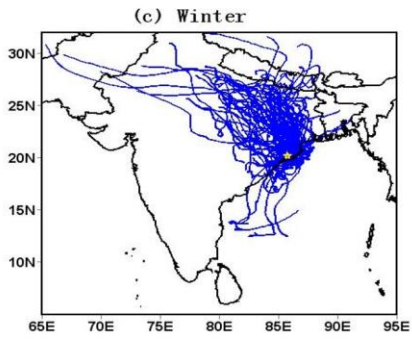
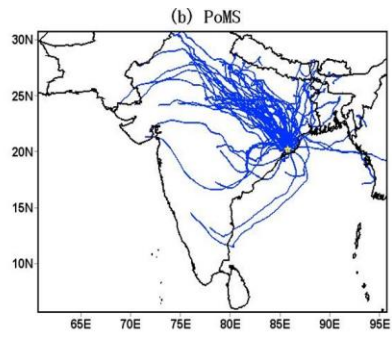
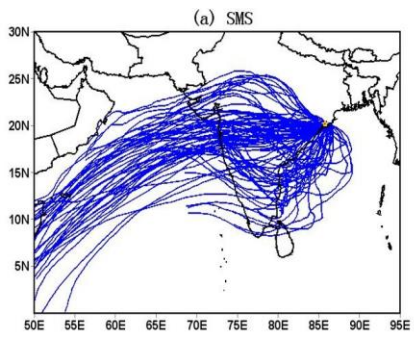
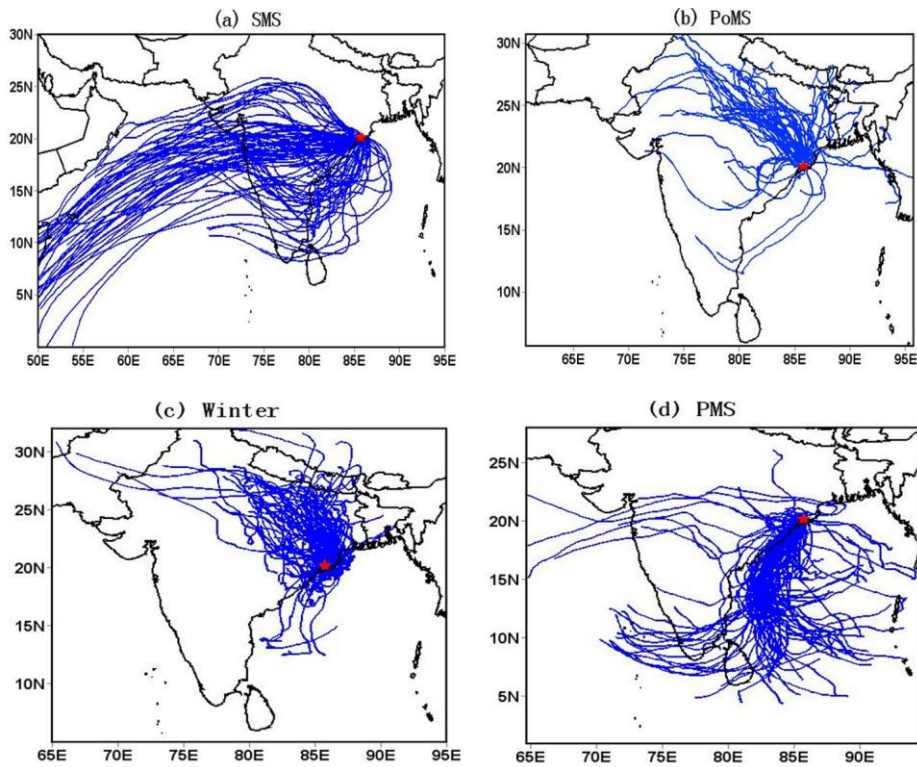


Figure 1: Geographic location of Bhubaneswar marked by a star symbol on the topographic map; the boundary of the Indo-Gangetic Plains (IGP) region is indicated with dotted lines. (a) Experimental location Bhubaneswar (star symbol); the Indo-Gangetic Plains (IGP) region is indicated with an oval symbol; (b) mobile container hosting the measurement setup at the experimental site.

5

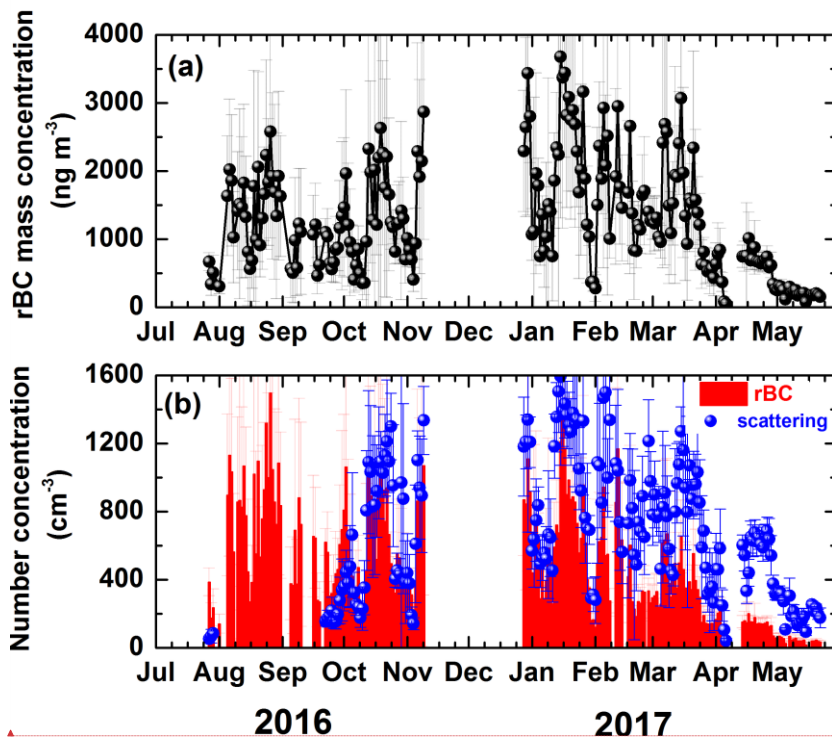


Formatted: Font: (Default) Times New Roman, 10 pt



Formatted: Font: (Default) Times New Roman, 10 pt, Bold

Figure 2: Isentropic five-five-day airmass back trajectories arriving at 100 meters above the surface over the observational location (identified with star symbol) in different seasons.



Formatted: Font: (Default) Times New Roman, 10 pt

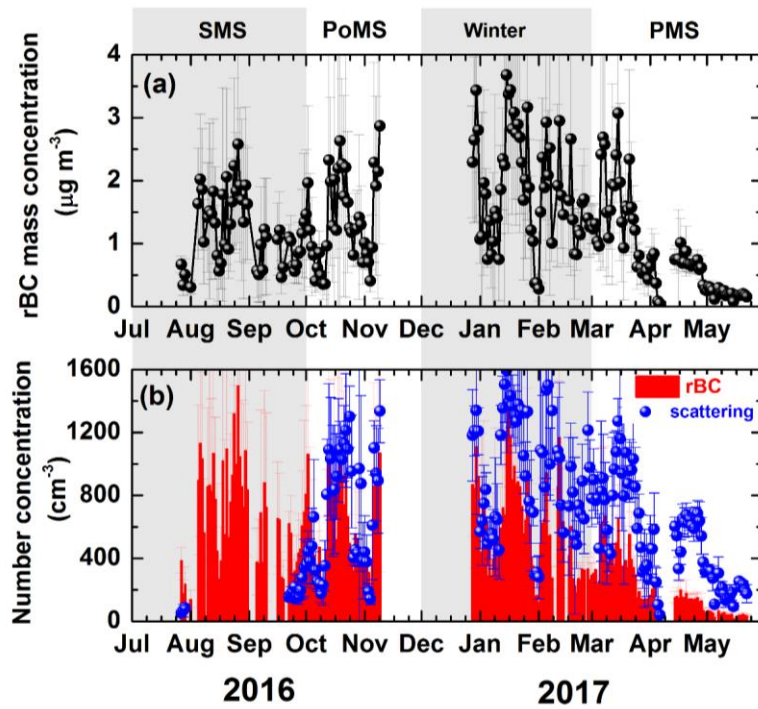
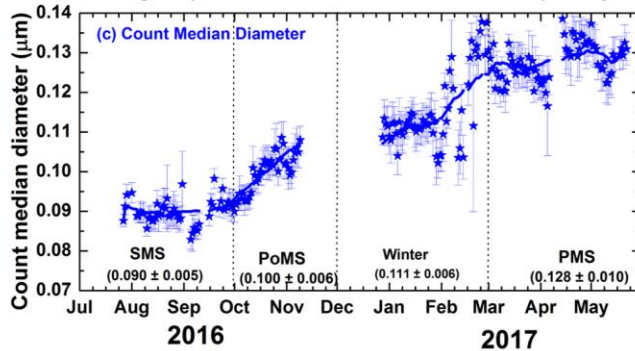
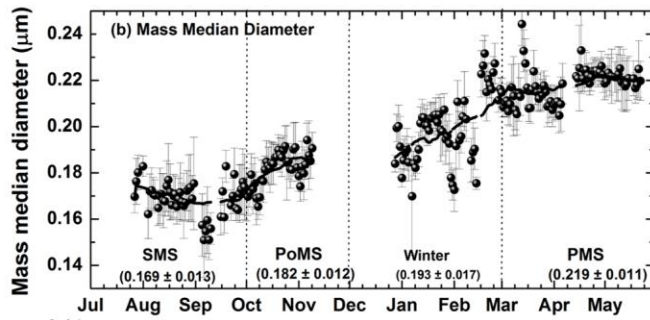
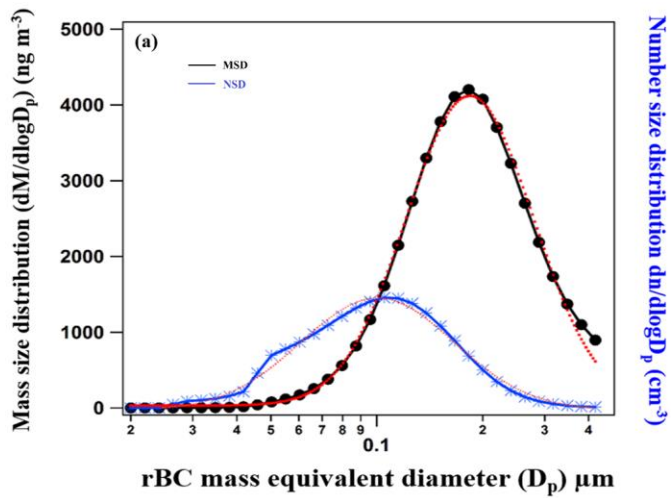


Figure 3: Temporal variation of daily mean (a) rBC mass concentration; and (b) number concentration of BC (bars) and non-BC scattering particles (filled circle). The vertical line passing through them is the standard deviation. The shaded portions demarcate the seasons. Temporal variation of daily mean (a) rBC mass concentration; and (b) number concentration of BC (bars) and non-BC scattering particles (filled circle). The vertical line passing through them is the standard deviation.



Formatted: Font: (Default) Times New Roman, 10 pt, Bold

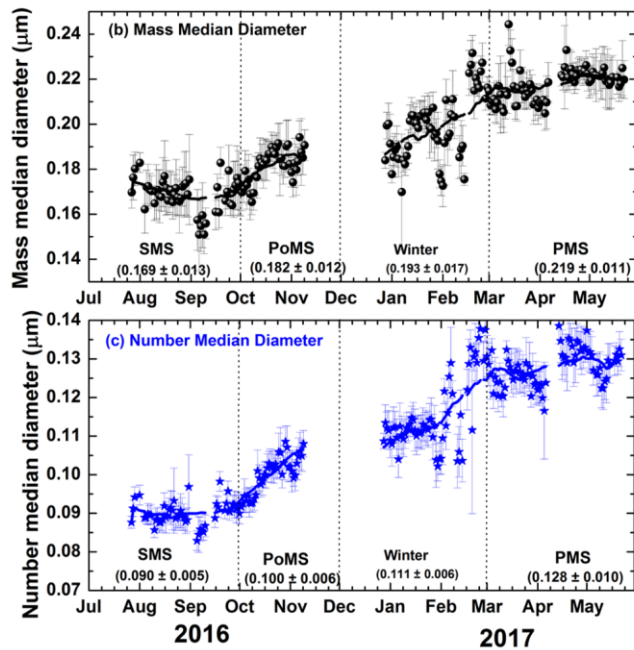
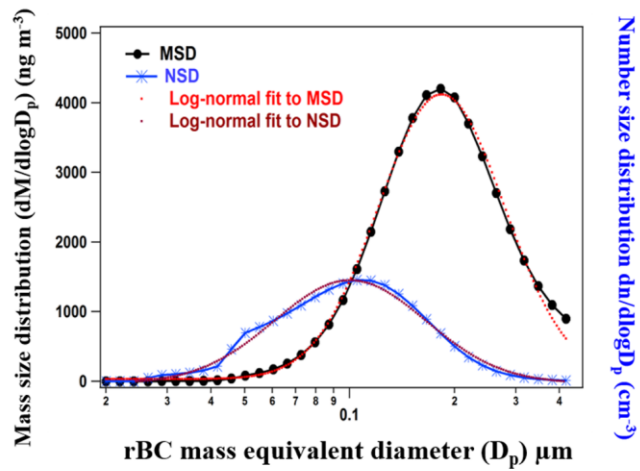


Figure 4: (a) Typical mass (number) size distributions along with least-squares fitting to mono-modal log-normal distribution (in dotted lines) used to derive MMD and \overline{MWD} . (b) Temporal variation of daily mean mass median diameter (\triangle) and (b) Temporal variation of daily mean \overline{MWD} median diameter (star) of BC; The symbols present the mean value for the day and the vertical line passing through them is the standard deviation. The solid continuous line shows the 30 day smoothed variation. Dotted vertical lines demarcate different seasons.

5

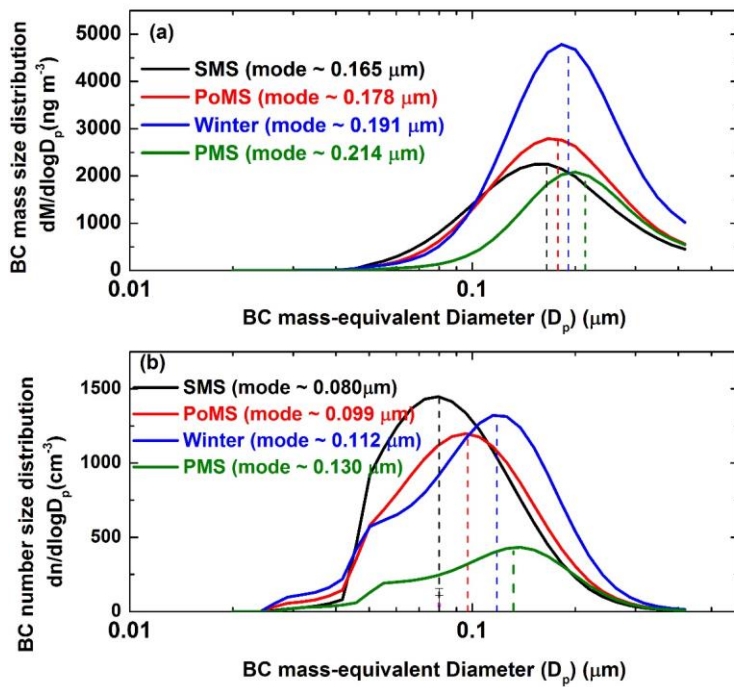


Figure 5: Seasonal mean black carbon (a) mass size distributions and (b) number size distributions. Corresponding mode diameter values are also seen in brackets.

Formatted: Font: (Default) Times New Roman, 10 pt, Bold

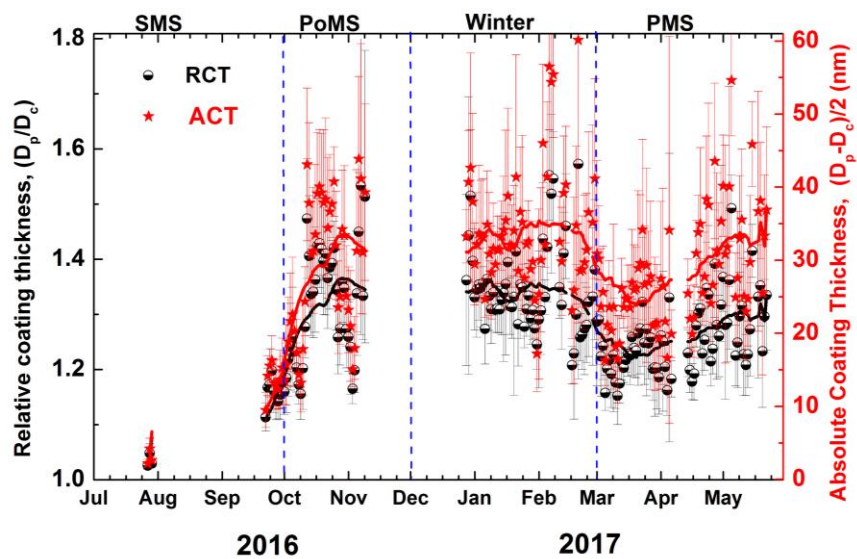
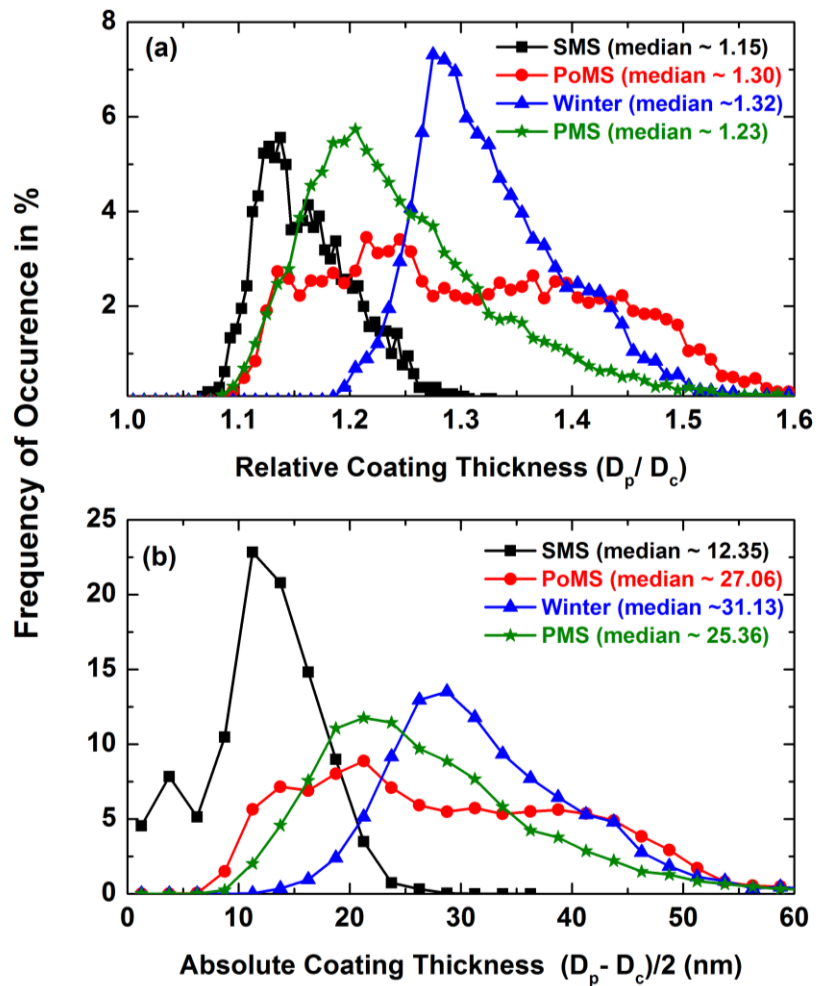


Figure 65: Temporal variation of daily mean relative coating thickness (half filled- circle) and absolute coating thickness (star). The symbols present the mean value for the day and the vertical line passing through them is the standard deviation. The solid continuous line shows the 30 day smoothed variation. Dotted vertical lines highlight different seasons. Due to the failure of the scattering detector between 31-July-2016 to 20-September-2016 mixing state parameters could not be estimated.

5



Formatted: Font: (Default) Times New Roman, 10 pt, Bold

Figure 7: Frequency of occurrence of (a) relative coating thickness and (b) absolute coating thickness in different seasons.

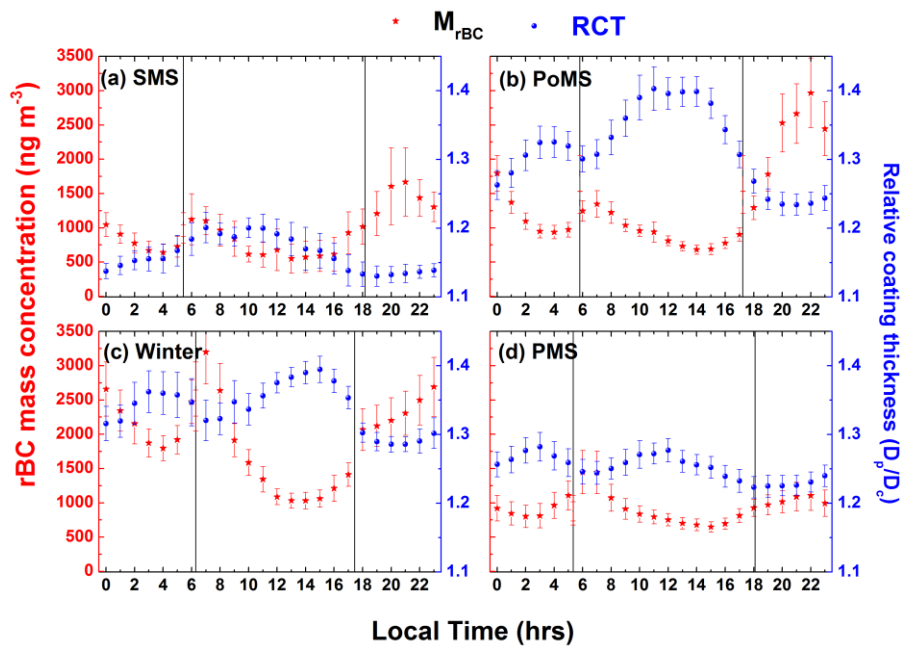


Figure 86: Diurnal variation of (a-d) rBC mass concentrations and relative coating thickness (RCT) in different seasons. The vertical lines denote the Sunrise and Sunset. The vertical bars through solids points are the standard errors from the mean.

5

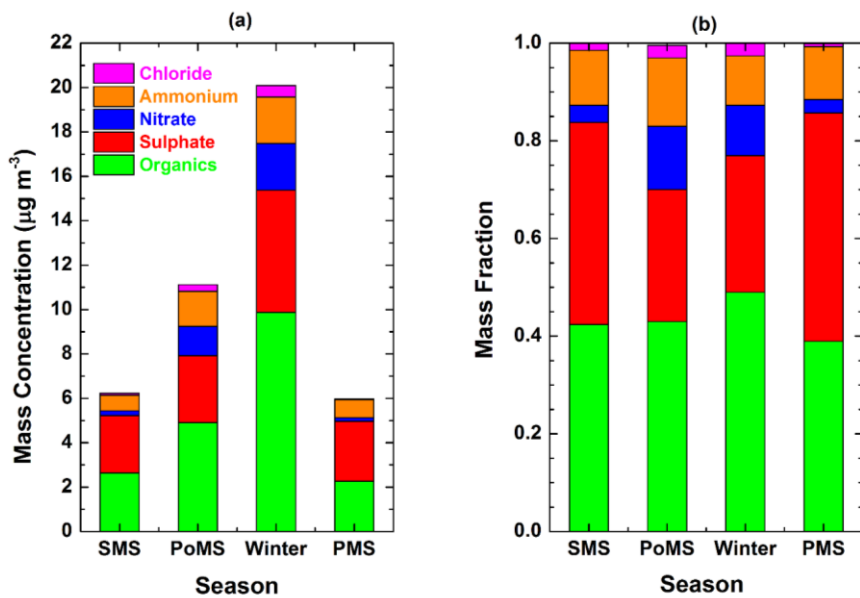


Figure 97: Seasonal variation of (a) mass concentrations and (b) percentage contributions to the total mass concentration of different species (organics, sulphate, nitrate, ammonium and chloride).

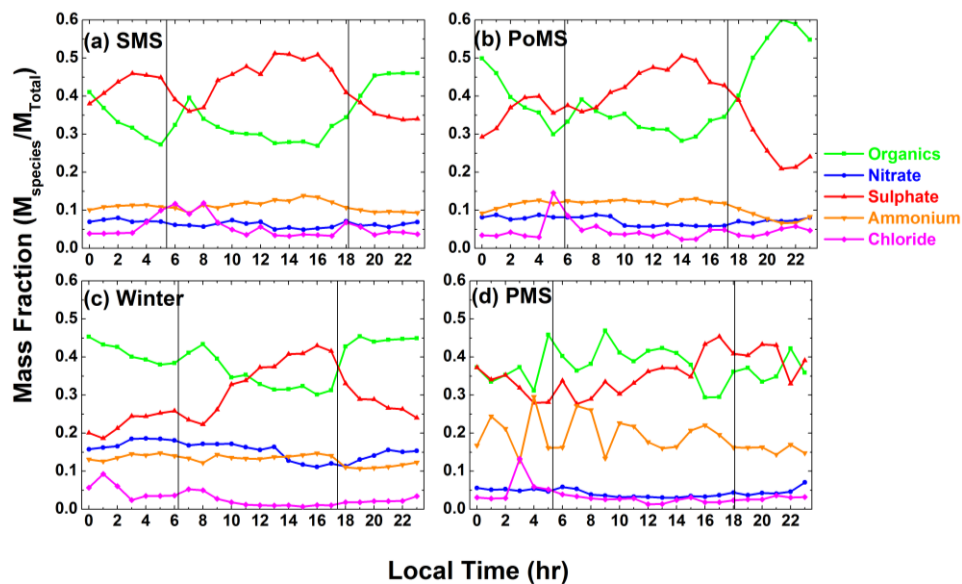


Figure 108: Diurnal variation of mass fraction of different species (organics, sulphate, nitrate, ammonium and chloride) of NR-PM1 in different seasons. The vertical lines denote the Sunrise and Sunset.

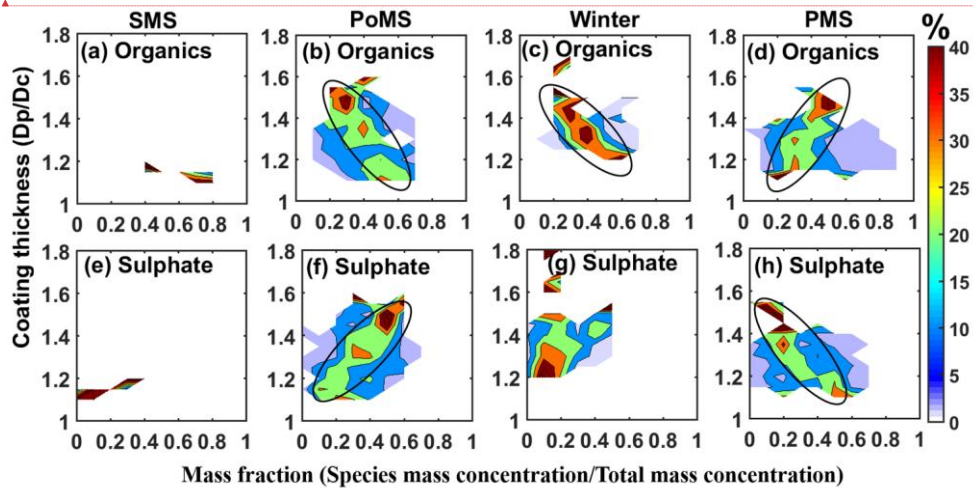
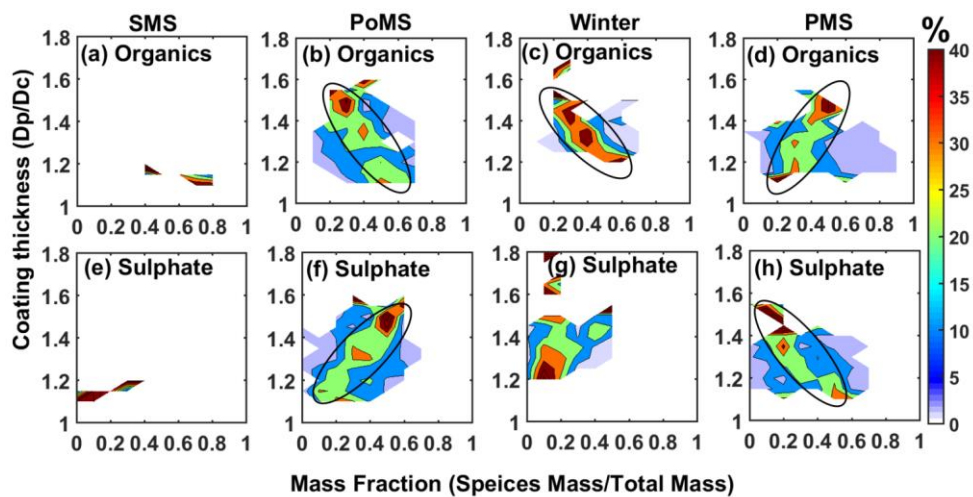


Figure 119: Association between mass-fraction of organics (top panels; a-d) and sulphate (bottom panels e-h) with relative coating thickness during different seasons. The colour bar indicates the percentage of occurrence of RCT for corresponding MF values of the species.

Formatted: Font: (Default) Times New Roman, 10 pt, Bold

Table 1: Seasonal average of ~~metreological~~meteorological parameters, temperature (T), Relative humidity (RH), Pressure (P) and Wind speed (WS). Maximum and minimum values recorded in that season are also listed.

Seasons		T (°C)	P (hPa)	WS (m s ⁻¹)	RH (%)
SMS	Mean	30.12 ± 3.76	995 ± 3.6	1.23 ± 0.62	77.1 ± 17.5
	Minimum	23.9	986.2	0	31
	Maximum	35	1001.7	5.2	99
PoMS	Mean	28.3 ± 6.3	1002 ± 4.4	1.07 ± 0.67	71.0 ± 21.2
	Minimum	21	993.9	0	17
	Maximum	34	1010	4.8	99
Winter	Mean	25.5 ± 8.2	1006 ± 2.6	0.95 ± 0.53	57.4 ± 22.9
	Minimum	18	998.1	0	8
	Maximum	36	1001	3.4	99
PMS	Mean	33 ± 7.5	999.8 ± 3.6	1.97 ± 0.92	67.1 ± 28.2
	Minimum	18.9	987.7	0	7
	Maximum	41	1008.3	8	98.5

Table 2: Mean modal parameters (peak concentrations, mode and geometric standard deviation) of the BC mass and number size distributions considering the log-normal distribution in different seasons: summer monsoon (SMS), post monsoon (PoMS), winter and pre-monsoon (PMS).

(a) Mass size distribution			
Season	M ₀ (µg m ⁻³)	Mode (µm)	Geometric standard deviation (σ)
SMS	2225	0.165	1.99
PoMS	2752	0.178	1.90
Winter	4679	0.194	1.77
PMS	2034	0.214	1.72
(b) Number size distribution			
Season	N ₀ (cm ⁻³)	Mode (µm)	Geometric standard deviation (σ)
SMS	1502	0.080	1.80
PoMS	1219	0.099	1.92
Winter	1270	0.112	2.01
PMS	407	0.130	2.01

Table 32. A Summary of BC mass median diameter from a few selected studies representing different sources in distinct environments.

S.No.	Location	Type of location	MSD mode/ MMD (μm)	Reference
Urban/suburban locations				
1.	<i>Bhubaneswar, India</i>	<i>Urban/fresh urban emissions continental outflow</i>	<i>0.165 (July-Sept)</i>	<i>Present study</i>
		<i>Urban/continental outflow, aged BC</i>	<i>0.178-0.191 (Oct-Feb)</i>	
		<i>Urban/with high solid fuel emissions</i>	<i>0.214 (Mar-May)</i>	
2.	Canadian oil sand mining (Aircraft studies), Canada	Urban/fresh urban emissions	0.135-0.145	Cheng et al. (2018)
3.	Gual Pahari, India	Urban polluted/ fresh biofuel, crop residue	0.221 ± 0.014	Raatikainen et al. (2017)
4.	Shanghai Shanghai, China	Urban/pollution episode with high biomass burning	0.230	Gong et al. (2016)
5.	Suzu, Japan	Urban/east Asian out flow site	0.200	Ueda et al. (2016)
6.	An urban site in London, UK	Urban/traffic emissions	0.119-0.124	Liu et al. (2014)
7.	Suburban site in Paris, France	Urban/traffic emissions	0.100-0.140	Laborde et al. (2013)
8.	Sacramento, USA	Urban/fossil fuel emissions	~ 0.145	Cappa et al. (2012)
9.	Tokyo, Japan	Urban outflow	0.130-0.170	Kondo et al. (2011)
10.	Cranfield airport in UK	Aircraft emissions near source	0.126	McMeeking et al. (2010)
11.	Regionally-averaged over flight segments over Europe	Near source to free troposphere	0.170-0.210 (a) continental pollution (0.18–0.21); (b) urban outflow (0.170 \pm 0.010)	McMeeking et al. (2010)
Remote locations				
12.	Lulang, Tibetan Plateau, China	High-altitude background	0.160 ± 0.023	Wang et al. (2018)
13.	Mukteshwar, The Himalayas, India	High-altitude background / biofuel, crop residue outflow	0.205 ± 0.016	Raatikainen et al. (2017)

Formatted: Font: Italic

Formatted: Font: Not Bold, Not Italic

Formatted: Font: Not Bold

Formatted: Font: Italic

Formatted: Font: Not Bold

Formatted: Font: Not Bold, Not Italic

Formatted: Font: Not Bold

14.	Northeastern Qinghai-Tibetan Plateau, China	Background site/biomass burning, aged BC	0.187	Wang et al. (2015)
15.	Jungfrauoch, Switzerland	High-altitude background / biomass burning, aged BC	0.220-0.240	Liu et al. (2010)

Table 43: A summary of the properties of the rBC concentrations, size distributions and its mixing state and scattering particle concentrations in different seasons: summer monsoon (SMS), post-monsoon (PoMS), winter and pre-monsoon (PMS). The values after \pm symbol are standard deviations.

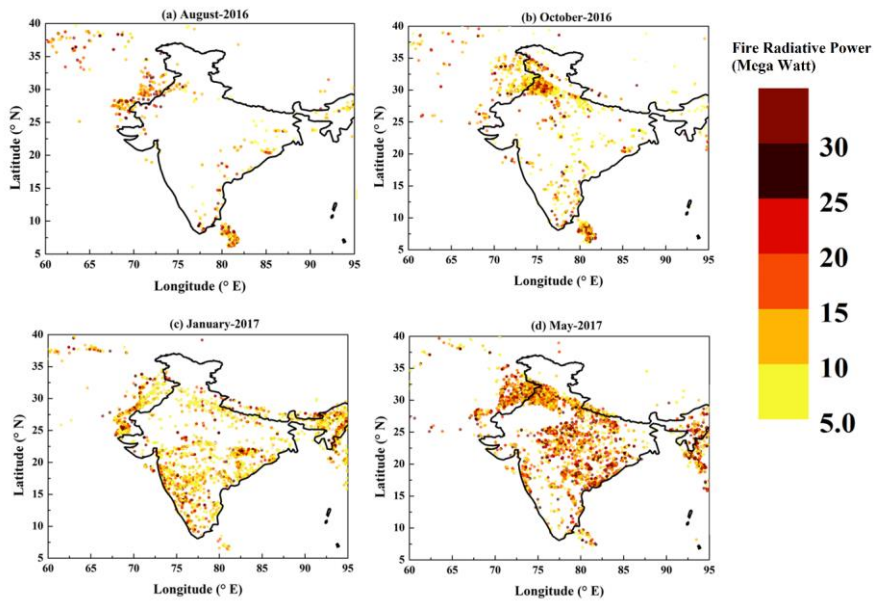
5

Parameter	SMS	PoMS	Winter	PMS
BC mass concentration ($\mu\text{g m}^{-3}$)	1.22 \pm 1.03	1.34 \pm 1.40	1.94 \pm 1.58	0.93 \pm 0.99
BC number concentration (cm^{-3})	500-695 \pm 322582	583 \pm 616	621 \pm 557	188-218 \pm 196239
Scattering particle concentration (cm^{-3})	211 \pm 114	690 \pm 471	950 \pm 464	548 \pm 349
Mass median diameter (μm)	0.169 \pm 0.013	0.182 \pm 0.012	0.193 \pm 0.017	0.219 \pm 0.011
count-number median diameter (μm)	0.090 \pm 0.005	0.100 \pm 0.006	0.111 \pm 0.006	0.128 \pm 0.010
Relative coating thickness	1.16 \pm 0.04	1.32 \pm 0.14	1.34 \pm 0.12	1.26 \pm 0.10
Absolute coating thickness (nm)	24.24 \pm 9.9	56.94 \pm 23.76	65.01 \pm 15.80	55.02 \pm 19.25

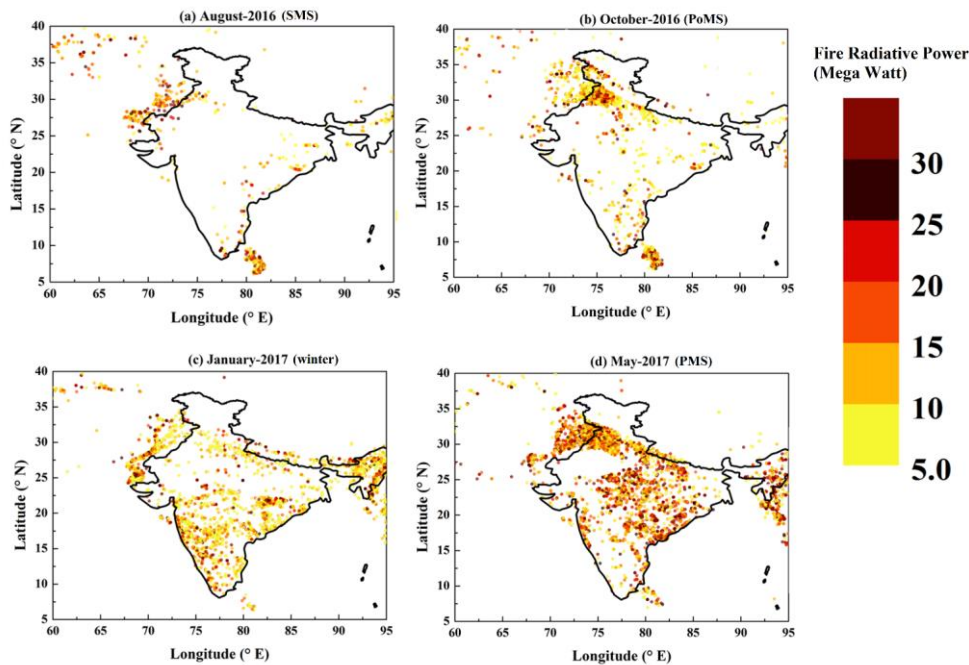
Formatted: Not Highlight

Formatted: Not Highlight

Supplementary Figures and Tables



Formatted: Font: (Default) + Headings (Times New Roman), 10 pt, Bold



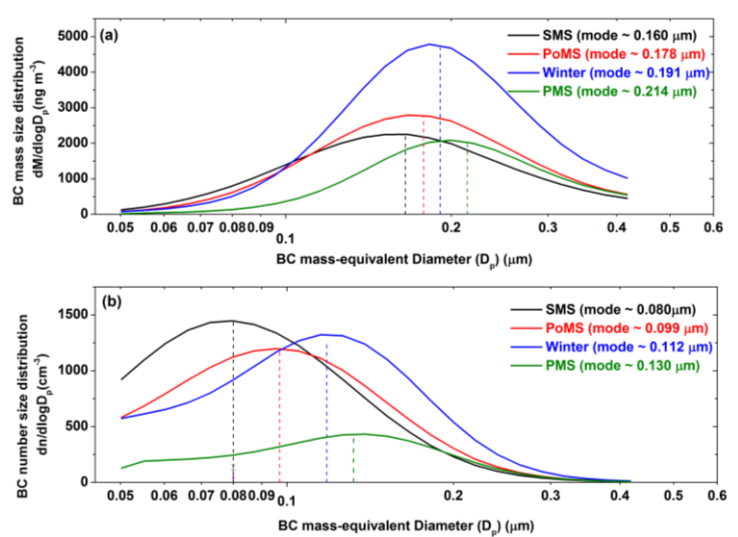
Formatted: Font: (Default) +Headings (Times New Roman), 10 pt, Bold

Figure S1: Spatial distribution of Moderate Resolution Imaging Spectroradiometer (MODIS) fire radiative power (MODIS Thermal Anomalies / Fire locations Collection 6 product obtained from <https://earthdata.nasa.gov/firms>) for the representative months of different seasons; (a) August -2016 (SMS), (b) October -2016 (PoMS), (c) January -2017 (winter) and (d) May -2017 (PMS). Significant-A significant amount of fire events during PMS are clearly seen over the Indian region. During the PoMS (fire events to confined to northwest IGP) and winter (fire events to confined to western, north-eastern regions of India) less intense regional fire events are noticeable. During SMS (and PoMS as well), a considerable amount of fire events are noticeable below south of India (over Srilankan region).

Formatted: Not Highlight

5

10



Formatted: Font: (Default) +Headings (Times New Roman), 12 pt, Bold, Font color: Text 1

Figure S2: Seasonal mean black carbon (a) mass size distributions and (b) number size distributions. Corresponding mode diameter values are also seen in brackets.

Supplementary table-1 and Figure S2 highlight the seasonal changes in BC microphysical properties. The modal diameters changed from lowest values ($\sim 0.165 \mu\text{m}$) during SMS to the highest value ($\sim 0.214 \mu\text{m}$) in the PMS through the seasons PoMS ($\sim 0.178 \mu\text{m}$) and winter ($\sim 0.191 \mu\text{m}$), signifying the changing source and atmospheric dynamical processes and that size distributions progressively developed towards larger sized BC particle dominance from SMS to PMS. The peak concentrations suggested the highest mass loading in winter ($M_0 \sim 4679 \text{ ng m}^{-3}$), followed by PoMS ($M_0 \sim 2752 \text{ ng m}^{-3}$) and SMS ($M_0 \sim 2225 \text{ ng m}^{-3}$), whereas the lowest loading was seen PMS ($M_0 \sim 2031 \text{ ng m}^{-3}$).

The size distribution during SMS is slightly skewed towards lower size regime and resulted in a broad width (standard deviation (σ_m) ~ 1.99). As the season progress towards PMS such skewness (or lack of it as indicated by decreased σ_m values) progressively shifted towards larger size ranges, in addition to drop in smaller sized particle concentrations due to the changes in the nature of sources. These values also indicate the other atmospheric dynamical processes that control the BC life cycle apart from the source and sink as described above. Extended rainfall reduces the overall mass loading due to wet scavenging in SMS and partly in PoMS, smaller BC particles prevailed while larger particles are more prone to being scavenged. Lack of wet removal mechanism in dry seasons (winter and PMS) resulted in an extended lifetime of BC.

resulting in a higher atmospheric lifetime. Also, seasonally varying boundary layer dynamics determine the extent of the near-surface aerosol loading (this aspect is discussed in a later section).

5 Similar to the mass size distributions, examination of the modes of the number size distribution in different seasons suggested smaller size particles (mode $\sim 0.080 \mu\text{m}$) during SMS which progressively increased towards larger core BC particles with season from PMS ($\sim 0.130 \mu\text{m}$) through PoMS ($\sim 0.099 \mu\text{m}$) and winter ($\sim 0.112 \mu\text{m}$) with broader widths, highlighting seasonal changes in the nature of dominant sources. But mean BC number size distributions showed a slightly different picture when mode peak values were considered. The largest modal number concentration is seen during SMS ($N_0 \sim 1502 \text{ cm}^{-3}$) (albeit lower mode diameter suggesting the smaller particle dominance possibly of regional origin due to the extended precipitation causing below-cloud scavenging restricting the abundance and lifetime of larger particles), followed

10 by winter ($N_0 \sim 1270 \text{ cm}^{-3}$) and PoMS ($N_0 \sim 1219 \text{ cm}^{-3}$). PMS showed the lowest peak number abundance ($N_0 \sim 407 \text{ cm}^{-3}$).

15

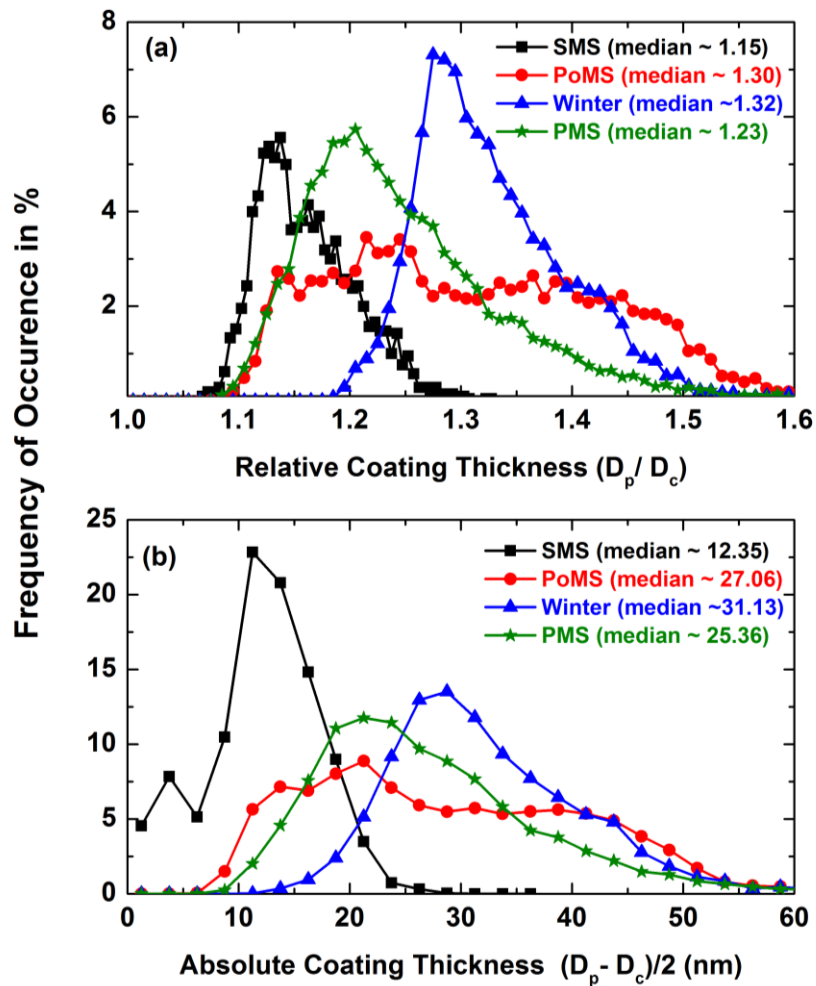


Figure 7S3: Frequency of occurrence of (a) relative coating thickness and (b) absolute coating thickness in different seasons.

Formatted: Font: (Default) Times New Roman, 10 pt, Bold

Formatted: Justified

5 The supplementary Figure S3, which shows the frequency distribution of the RCT and ACT values for each season (median values for each season are also shown in the figure) demonstrates the seasonality of the coating characteristics. The monsoon season was characterised by a narrow distribution, with the lowest median values for both RCT and ACT. Such thin coatings were seen due to the reduced life-time and absence of multiple processes which include: (a) decreased atmospheric life-time, leading to not having enough time to get thickly coated (as coating thickness depends on the particle life time also), (b) lowered concentration of advected anthropogenic precursor species, making lesser availability of coating material, and (c) fast wet-removal (of the core and the coating material) by extensive rainfall. South-westerly/westerly air masses prevailed during this period which advect cleaner marine air to the site, while wash-out due to large-scale precipitation removed aged aerosols. During the other seasons, the distributions are quite broad, and showed multiple maxima (especially during PoMS and winter). During the winter and PoMS, BC particles in the IGP outflow are characterised by extensive coating resulting from the enormous shift in the air mass from marine to continental at the end of the monsoon season bringing air from the most polluted central IGP, added with the associated change in the size distribution and residence time.

Formatted: Not Highlight

Formatted: Font: Not Bold

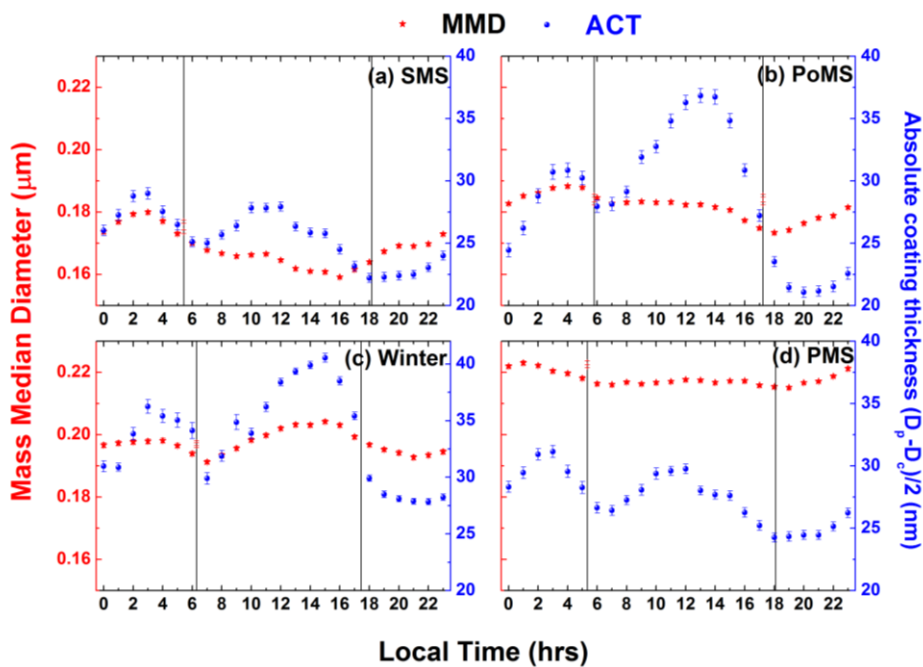


Figure S2S4: Diurnal variation of (a-d) rBC mass median diameter and absolute coating thickness (ACT) in different seasons. The vertical lines denote the Sunrise and Sunset. The vertical bars through solids points are the standard errors from the mean.

Formatted: Not Highlight

Supplementary Table 1: Mean modal parameters (peak concentrations, mode and geometric standard deviation) of the BC mass and number size distributions considering the log-normal distribution in different seasons: summer monsoon (SMS), post-monsoon (PoMS), winter and pre-monsoon (PMS).

<u>(a) Mass size distribution</u>			
<u>Season</u>	<u>M₀ (μg m⁻³)</u>	<u>Mode (μm)</u>	<u>Geometric standard deviation (σ)</u>
<u>SMS</u>	<u>2225</u>	<u>0.165</u>	<u>1.99</u>
<u>PoMS</u>	<u>2752</u>	<u>0.178</u>	<u>1.90</u>

<u>Winter</u>	<u>4679</u>	<u>0.191</u>	<u>1.77</u>
<u>PMS</u>	<u>2031</u>	<u>0.214</u>	<u>1.72</u>
<u>(b) Number size distribution</u>			
<u>Season</u>	<u>N_0 (cm⁻³)</u>	<u>Mode (μm)</u>	<u>Geometric standard deviation (σ)</u>
<u>SMS</u>	<u>1502</u>	<u>0.080</u>	<u>1.80</u>
<u>PoMS</u>	<u>1219</u>	<u>0.099</u>	<u>1.92</u>
<u>Winter</u>	<u>1270</u>	<u>0.112</u>	<u>2.01</u>
<u>PMS</u>	<u>407</u>	<u>0.130</u>	<u>2.01</u>

5

